2016

Mechanisms of communication in the filarial worm, Brugia malayi, at the mosquito vector-mammalian host interface

Lisa Marie Fraser
Iowa State University

Mechanisms of communication in the filarial worm, *Brugia malayi*, at the mosquito vector-mammalian host interface

by

Lisa M. Fraser

A dissertation submitted to the graduate faculty

in partial fulfillment of the requirements for the degree of

DOCTOR OF PHILOSOPHY

Major: Molecular, Cellular and Developmental Biology

Program of Study Committee:
Michael J. Kimber, Co-Major Professor
Lyric C. Bartholomay, Co-Major Professor
Bryony C. Bonning
Timothy Day
Thomas Baum

Iowa State University

Ames, Iowa

2016

TABLE OF CONTENTS

Page

ABSTRACT

Lymphatic Filariasis (LF) is a Neglected Tropical Disease, caused by mosquito-borne filarial nematodes including *Brugia malayi*, which infects over 120 million people. Mass drug administration is used for LF control but limited efficacy of the drugs combined with the threat of resistance drives the need for novel control strategies. Chemosensation is an essential behavior used by nematodes, including parasitic species, has roles in development, avoidance of noxious stimuli and finding food/mates/hosts, making genes involved in this system attractive targets for parasite control. Little, however, is known about the chemosensory system in parasitic nematodes. Here we address this knowledge gap and describe the structural, behavioral and genetic basis for chemosensation in filarial nematodes. Sensory structures and their innervation are identified in larval and adult stages of *B. malayi* using scanning electron and fluorescent microscopy. In addition, behavioral responses of *B. malayi* L3 stage parasites to host-derived stimuli were profiled and specific tactic behaviors that may be important in host-seeking and host-invasion identified. To further characterize the genetic basis for chemosensation in *B. malayi*, we surveyed heterotrimeric G-proteins (known mediators of nematode chemosensation) on a pan-phylum level using bioinformatic and phylogenetic approaches. This analysis revealed highly conserved and novel patterns of gene expression that may be exploited for novel LF control strategies. While the characterization of chemosensation in *B. malayi* has revealed one mechanism by which the nematode interacts with its environment, interactions between the nematode and host (both mosquito and human) are far more complex. Here we also present results, which demonstrate for the first time that parasitic nematodes of humans use exosomes, a

specific type of extracellular vesicle, to deliver bioactive molecules capable of manipulating the host-parasite interface. We show L3 stage *B. malayi* release extracellular vesicles of the size and shape of exosomes in prodigious quantities. The cargo of these vesicles includes exosomal markers and putative effector proteins as well as an abundant microRNA complement suggesting a role in host manipulation. The parasite vesicles are rapidly internalized by host macrophages where they stimulate a classically activated phenotype. These results suggest a novel mechanism by which human parasitic nematodes may actively direct the host responses to infection and could seed new therapeutic strategies for LF control.

CHAPTER 1

INTRODUCTION

Nematodes are one of the most diverse groups of organisms with over 23,000 species having been described to date [1]. Diverse species of nematode occupy terrestrial, freshwater and marine environments and display both free-living and parasitic life styles [1]. Parasitic nematodes infect both plants (plant-parasitic nematodes, PPN) and animals (animal-parasitic nematodes, APN) and can be transmitted through a number of different mechanisms, including insect vectors such as mosquitoes and black flies. The impact that parasitic nematodes have is enormous. For example, it is estimated that PPNs cause $125 billion USD in damage every year, although this is likely a gross underestimate of the real impact of these parasites [2, 3]. The outlook with APNs is equally grim with more than two billion people thought to be currently infected by parasitic nematodes [4]. The global burden of APNs is compounded by the fact that the number of effective drugs currently available to treat them is extremely limited [4, 5]. These factors, combined with the chronic nature of APN infection, underscore the need for the development of novel strategies for treatment and control. In pursuit of novel control targets, the work described in this dissertation has focused on elucidating those behaviors that are essential for successful transmission and establishment of infection of the filarial parasite *Brugia malayi*.

Three parasites are etiologic agents of Lymphatic Filariasis (LF): *Wuchereria bancrofti, B. malayi,* and *B. timori*, listed here in descending order of disease incidence. It is estimated that over 120 million people currently suffer from this disfiguring disease

while more than one billion people are at risk of contracting LF in 73 endemic countries worldwide [6]. While most cases of LF remain asymptomatic, clinical manifestations of the disease are debilitating and disfiguring. Symptoms including lymphedema, elephantiasis, hydrocele (in males) and hypereosinophilia often lead to permanent, long-term incapacity [6]. In addition to overt symptoms, damage to the lymphatic vasculature reduces the ability of the immune system to combat opportunistic pathogens and as a result secondary bacterial infections are common. LF is a disease that not only impacts those afflicted but also has a significant impact on their caregivers. Disfigurement as a result of LF leads to stigmatization within the community and chronic disability negatively impacts economic output and increases poverty making LF a leading cause of disability worldwide with at least 2.8 million disability-adjusted life years (DALYs) associated with this disease [6].

Both mosquito vectors and mammalian hosts are required for *B. malayi* to complete its life cycle. Microfilariae (mf) are ingested by the mosquito during a blood meal from a parasitemic host [7]. Once inside the mosquito, mf migrate to the indirect thoracic musculature where they undergo two molts to become infectious L3 stage parasites [7]. At this stage, the parasite migrates to the head and proboscis of the mosquito where they can be transmitted to an uninfected human host when the mosquito feeds again [7]. L3 stage parasites are deposited on the skin while the mosquito is taking a blood meal. In order to establish infection the parasite must identify and invade the human host using the wound made by the mosquito. Once inside the human host, the parasites migrate to the lymphatic vasculature where they undergo an additional two molts to become sexually mature adults [8].

In 2000, the World Health Organization launched the Global Program to Eliminate Lymphatic Filariasis (GPELF) with the ambitious goal of eliminating LF as a public health concern by 2020 [9]. The strategy for success incorporates two components: stopping the spread of infection by disrupting transmission and alleviation of suffering for those affected by LF [9]. To disrupt transmission, mass drug administration (MDA) and vector control have been implemented and while great strides have been made using these strategies, they are not without their limitations. Currently, only three drugs (diethylcarbamazine citrate, ivermectin and albendazole) are available to treat LF, none of which are effective against the adult stage of the parasite, which can live in the body for up to 10 years. This inefficiency against critical life stages along with the growing threat of resistance highlights the need for novel methods of treatment and control.

Disruption of transmission of this parasite can be achieved by targeting critical life stages such as L3 or adult stages using novel strategies to manipulate interactions between the parasite and the mosquito vector or human host. The first part of this chapter provides an overview of research related to the means by which nematodes communicate with, and take cues from, the environment, and how these interactions facilitate parasitism. All of the work described in this thesis emphasizes the parasitic nematode, *B. malayi* because, of the parasites that cause LF, *B. malayi* is the only species that is experimentally tractable by virtue of available laboratory animal and susceptible mosquito hosts. Various physical and genetic aspects of chemosensation in free-living, plant- and animal-parasitic nematodes will be addressed. In the second part of this chapter, extracellular vesicles will be described, with a focus on how parasites use them to navigate and manipulate their surroundings.

Chemosensation in nematodes

All nematodes likely respond to gustatory and olfactory cues (chemosensation) to elicit a variety of behaviors including finding food and mates, avoiding noxious conditions and entry/exit into arrested developmental stages [10-12]. In addition, chemosensation is critical in host-seeking and host-invasion behavior in parasitic nematodes of both plants and animals [12-14]. Not only must all parasitic species be able to locate a suitable host but they also have to adapt to rapidly changing environments, which often includes the switch from a free-living to a parasitic lifestyle or, in the case of vector-borne parasites, a drastic change in host environment. For instance, mosquitoes transmit the filarial worms that cause LF. For the parasite to be successful it must be able to rapidly adapt to both the physical and biochemical environments within the mosquito vector and the human host, identify and invade the appropriate host cells and tissues, and suppress or avoid host immune responses. Much of this is directly impacted by the parasite's ability to sense and respond to environmental cues, making chemosensation critical for successful infection by most, if not all, parasitic nematodes.

Numerous studies using the free-living nematode *Caenorhabditis elegans* have shown that this organism has a robust chemosensory response with the ability to sense hundreds of compounds and respond to many of them in a concentration-dependent manner [15]. Several studies have demonstrated that plant- and animal-parasitic nematodes also exhibit chemosensory responses. PPNs such as *Globodera pallida* and *Meloidogyne incognita* are attracted to compounds that are characteristic of preferred hosts and even facilitate parasite orientation towards ideal invasion sites, indicative of both long- and short-range chemosensory capabilities [16-18]. APNs including

Strongyloides stercoralis, *Brugia pahangi* and *Haemonchus contortus* use chemosensation to identify and invade preferred hosts [19-22]. Chemosensory perception varies depending on host preference to such a degree that these preferences reflect host specificity rather than phylogeny, implying that chemosensation is crucial for host selection [19, 22]. These studies demonstrate that chemosensory behavior is not unique to free-living nematodes like *C. elegans,* but a behavior that is central to species across the phylum.

Neuroanatomy

Nematodes, like other animals, have specialized organs to process chemosensory stimuli from their surroundings. These organs, called amphids and phasmids, contain numerous neurons dedicated to processing sensory information. The primary chemosensory organs in nematodes are the amphids and to a lesser extent, the phasmids [11, 23-28]. Various studies have demonstrated the presence of amphids and phasmids in free-living, plant- and animal-parasitic nematodes, strongly suggesting that these structures are a basal characteristic of the Phylum [12, 25, 27, 29-39]. Through these organs, nematodes have the ability to detect and respond to numerous chemical stimuli from the environment [15, 17, 24, 40].

In *C. elegans*, traditional nomenclature for amphid neurons and their associated cilia use a three letter scheme [28]. The first letter "A" stands for amphid, while the second letter is used to designate the type of dendritic processes present (S = single, D = double, W = wing and F = finger) [23, 28]. Each neuron pair identified in *C. elegans* was assigned a third letter A-L to differentiate between the neurons [23]. Thus, ASE neurons

are amphid neurons with a single process, ADL neurons have double processes, AWC neurons have wing cells and AFD neurons have a finger cell. In both APNs and PPNs, arrangement of amphidial neurons is similar to that in *C. elegans* and therefore, names of neurons in these species were assigned based on positional homology with *C. elegans* [41].

Amphids are a pair of lateral sensory organs located anteriorly with cephalic or cervical external openings while phasmids are located in the tail (Fig. 1) [11, 17, 23, 24, 26, 27]. Each amphid contains two glia cells called socket and sheath cells, which contribute to the formation of the amphid channel, as well as multiple specialized sensory receptive endings called cilia, the number of which varies among taxa (Fig. 1) [12, 17, 23, 24, 26, 40, 42]. Phasmids are a specialized pair of sense organs similar in structure to amphids but located posteriorly with caudal external openings [17, 27]. Phasmids, like amphids, have sheath and socket cells surrounding the channel, however, they are smaller and contain fewer neurons [26, 27, 42]. In addition to cilia, both amphid and phasmid channels contain a gelatinous material called a matrix that is secreted (amphid/phasmid secretions) to the environment (Fig. 1) [26, 40, 42]. The matrix composition, which varies between species, may have protective as well as sensory functions [17].

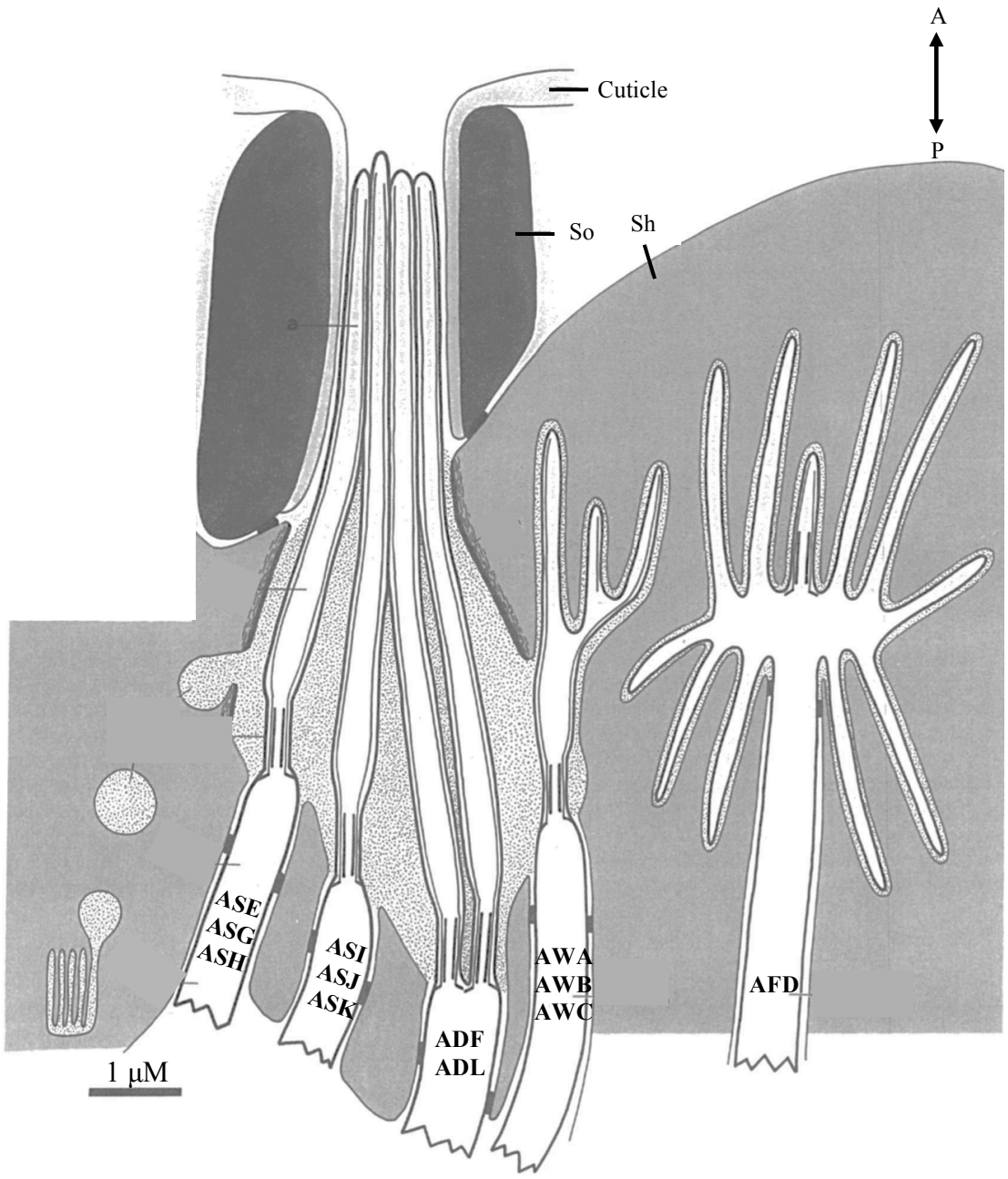

Figure 1. Schematic of *C. elegans* amphid. Detailed structure of amphid pocket showing cuticle, socket (So) and sheath (Sh) cells as well as ciliated nerve ending of the 12 neurons present in the amphid. Arrows indicate anterior (A) and posterior (P) direction. Image modified with permission from [26].

Amphid and phasmid channels are formed by both the socket and sheath cells, each portion of the channel however appears to arise through different mechanisms [26].

The socket cell forms the anterior portion surrounding the distal tips of the cilia and secretes cuticle, which lines the opening of the amphid and phasmid channels [14, 26]. The sheath cell, which is deeply folded or otherwise modified to provide a large surface area, forms the posterior portion of the amphid channel, is unlined with cuticle and is completely penetrated by all amphid neurons except the AFD neuron [14, 17, 26]. The sheath and socket cells surround the channel sealing to themselves and each other via tight junctions [14, 23, 26, 37].

A key function of sheath glia cells, which is broadly conserved in the sensory organs of both invertebrates and vertebrates, is the formation of an isolated extracellular compartment to house and protect neuronal sensory receptive endings [23, 40, 42, 43]. In addition to this function, sheath glia are required for the proper function of amphid sensory neurons as demonstrated by numerous profound defects elicited when these cells are ablated [24]. In *C. elegans*, ablation of sheath glia cells resulted in severe chemotaxis defects as well as aberrant ciliary morphology in several amphid neurons [24].

The sheath cell is the source of matrix-filled vesicles that deposit their contents around the cilia within the amphid and phasmid channels and that is secreted to the outside environment (amphid or phasmid secretions) [26, 35]. Amphid secretions have been found to play a role in ion/water regulation and through this provide an appropriate environment for the transmission of receptor potentials from the receptor site, thereby, facilitating signal transduction in chemosensation [14]. In addition, compounds that have direct roles in chemotaxis have been identified in amphid secretions, further implicating the matrix in chemosensation [44].

Although amphid secretions have been observed in numerous nematodes, the composition of these secretions appears to be dictated in part by the life style of the nematode, as demonstrated by the variety of behaviors that are affected by these secretions [45]. For example, anticoagulants have been identified in amphid secretions from the APNs *Ancylostoma caninum*, *Necator americanus* and *Syngamus trachea* which arose presumably as an adaptation to facilitate blood-feeding [14, 46]. In addition, acetylcholinesterase has been identified as a component of the matrix in several APNs and PPNs [45]. In APNs, the release of acetylcholinesterase has been linked with attachment to host gut, and to host membrane permeabilization and host immune modulation [46]. Components found in amphid secretions may also facilitate feeding in PPNs such as *H. glycines* by contributing material to the formation of a plug around the stylet of the nematode during feeding [35]. MAP-1 is a protein found in the amphid secretions of the PPN *M. incognita* during both migrating (infective pre-parasitic J2) and sedentary stages. It has also been detected along the cell wall of the adjacent giant cells within the plant apoplasm suggesting that this protein could be involved in both nematode-plant recognition and interactions [18].

Chemosensory neurons have to interact either directly or indirectly with the environment in order to elicit a chemosensory response [23, 42]. Many chemosensory neurons are exposed to the environment via specialized sensory receptive endings called cilia, which either terminates in the amphid channel or sheath cell (Fig. 1). These cilia are sites for receptors, ion channels and other signal transduction molecules that recognize environmental stimuli [40, 43]. Although the amphid structure is conserved across nematode species, cilia number, location and morphology appear to be highly variable

[14, 47]. For example, while *C. elegans* have eight chemosensory neurons that have cilia present in the amphid channels, only seven have been observed in the soybean cyst nematode, *Heterodera glycines,* and in the root-knot nematode, *Meloidogyne incognita* [35, 37]. In addition to the seven cilia, three to five cilia terminate within the sheath cell [35, 37, 47]. Furthermore, *Haemonchus contortus,* a parasite of ruminants, has seven single-cilia and three double-cilia located in the amphid channel [41]. In addition, there is one wing cell and one finger cell type cells in which cilia terminate within the sheath cell [41]. Cilia composition appears to be highly variable among nematodes. However, the reason for this is unknown. Studies done to characterize chemosensory structures in parasitic nematodes are extremely limited and none have been focused on identifying any relationship cilia structure has with amphid neuron function in these animals.

In *C. elegans*, eight neurons (ASE, ASG, ASH, ASI, ASJ, ASK, ADF and ADL) have microtubule-based sensory cilia that extend the length and terminate within the amphid channel [23, 24, 26, 40, 43]. These cilia are directly exposed to the outside environment through the amphid pore while the cilia of three neurons (AWA, AWB, AWC) initially enter the amphid channel but then divert and invaginate into the sheath cell [10, 23, 24, 26, 40, 43]. Although the distal segments of these neurons terminate in the amphid sheath, a large portion of the cilia including the neuron/sheath junction and the transition zone are exposed to the matrix-filled lumen and thus are in contact with the environment [48].

Cilia of both phasmid neurons (PHA and PHB) resemble the cilia of amphid channel neurons in that these neurons have a single microtubule-based dendritic process

that terminates within the phasmid channel thus allowing direct exposure to the environment through the phasmid pore [26].

Cilia structure is unique in each neuron pair, which allows the identification of the sensory neuron based upon cilia morphology [23, 24, 40]. ASE, ASG, ASH, ASI, ASJ and ASK neurons all have dendrites that end in a single cilium, while ADF and ADL dendrites end in a pair of cilia (Table 1) [26]. AWA, AWB and AWC neurons each have unique branched cilia, called wing cells (Table 1) [26]. AWA and AWB neurons have cilia similar in size to channel cilia, however, while the AWA dendrites split in multiple small cilia, AWB dendrites are branched and flattened [10, 26]. AWC neurons have branched cilia that flattened into large sheets resembling wings [26]. The remaining amphid neuron (AFD) has a single microtubule-based cilium, called the finger cell, which is surrounded by an array of actin-supported microvilli-like protrusions and is entirely embedded within the sheath cell (Table 1) [23, 24, 26, 40, 43].

Much of what is known about sensory neurons in nematodes is a result of studies on the free-living nematode *C. elegans,* which has a fixed number of neurons that have been mapped using electron microscopy [28]. Having a complete map of the neuronal arrangement, combined with the development of techniques such as laser ablation and RNA interference, has provided a unique opportunity to identify neuron function to a very high resolution. In *C. elegans*, more than 10% of all neurons are dedicated to sensory behavior, highlighting the importance and complexity of this physiology to this organism [49]. In contrast, although much work has been done to characterize neuronal function in chemosensation in *C. elegans,* very few studies have been dedicated to understanding these neurons in parasitic nematodes.

A list of chemosensory neurons present in *C. elegans* and their functions is provided in Table 1. In *C. elegans*, chemosensory neurons are used to discriminate between a wide variety of odors by not only segregating the detection of odors into distinct olfactory neurons but also by utilizing unique combinations of olfactory neurons [50]. Twelve pairs of sensory neurons are present in *C. elegans*, eleven of which are involved in chemosensory responses and one that mediates thermosensory behavior [49, 51]. Table 1 summarizes the amphid and phasmid neurons and functions present in *C. elegans.* ASE, ASG, ASH, ASI, ASJ, ASK, ADF, ADL, AWA, AWB and AWC amphid neuron pairs all have some involvement in chemosensation while the AFD neuron pair is involved in thermosensation in *C. elegans* [49, 51]. ASE neurons are required for responses to water-soluble attractants [51]. ASG, ASI and ADF neurons not only function in water-soluble chemotaxis but are also involved in dauer formation, which is an arrested life stage that is induced during harsh environmental conditions [10, 51, 52]. The ASH and ADL neuron pairs mediate avoidance to noxious water-soluble and volatile compounds [10, 53-55]. The function of ASJ neurons is primarily in dauer recovery, however, they also have a minor role in chemosensation [51, 52, 56]. ASK neurons are required for chemotaxis towards L-lysine and have a role in dauer development [51, 56-58]. AWA neurons sense attractive volatile compounds such diacetyl and pyrazine [10, 50, 59]. *C. elegans* uses the AWC neuron to sense and distinguish between numerous attractive volatile odors while AWB neurons mediate avoidance responses not only to repellent volatile odors but also to some pathogenic bacteria [10, 50, 59, 60]. Both neurons allow *C. elegans* to discriminate between food sources [60]. There are only two

pairs of phasmid neurons (PHA and PHB) involved in chemosensory behavior in *C. elegans*, both of which mediate avoidance behavior [51, 58].

Table 1: Amphid and phasmid neurons in *Caenorhabditis elegans*.			
Neuron	**Cilia**	**Function**	**References**
ASE	Single	Water-soluble chemotaxis	[51]
ASG	Single	Water-soluble chemotaxis, dauer formation	[51]
ASH	Single	Volatile chemotaxis (avoidance)	[53, 54, 58]
ASI	Single	Water-soluble chemotaxis, dauer formation	[51]
ASJ	Single	Chemotaxis, dauer recovery	[49, 52]
ASK	Single	Chemotaxis towards L-lysine, dauer recovery	[51, 57]
ADF	Double	Water-soluble chemotaxis, dauer formation	[51]
ADL	Double	Water-soluble and volatile chemotaxis (avoidance)	[54, 58]
AWA	Wing	Volatile chemotaxis (attractive)	[50, 54, 60]
AWB	Wing	Volatile chemotaxis (avoidance)	[50, 54, 60]
AWC	Wing	Volatile chemotaxis (attractive)	[50, 54, 60]
AFD	Finger	Thermosensation	[49, 51]
PHA	Single	Chemotaxis (avoidance)	[58]
PHB	Single	Chemotaxis (avoidance)	[58]

Amphid and phasmid neurons in *C. elegans*, most of which are involved in chemosensation. Neurons, associated cilia type and primary functions are listed. Relevant references are listed. Amphid neuron naming convention follows a three-letter scheme: first letter refers to amphid (A), second letter refers to cilia type (S = single, D = double, W = wing and F = finger) and third letter (A – L) was assigned to differentiate between neurons. Phasmid neuron naming convention follows in a similar format except that cilia type is not noted (PH = phasmid while last letter (A – B) was assigned to distinguish between neurons).

The lion's share of research to identify sensory neurons and their function has been done in *C. elegans* but pan-phylum positional homology has allowed the identification of sensory neurons in some parasitic nematodes. While there is significant morphological and positional conservation between sensory neurons in *C. elegans* and other nematodes, there are some differences [14, 23]. This is illustrated, in the number of

amphid neurons present in nematodes. In general, there are 12 pairs of sensory neurons in the amphids of nematodes [10, 41]. However in the case of *Strongyloides stercoralis*, a skin-penetrating parasite of mammals, there are 13 pairs of sensory neurons found within the amphids illustrating the variability that may arise as a result of adaptation to specialized life styles such as parasitism [14, 41].

While much is known about the function of amphid neurons in *C. elegans*, little is known about how these neurons work in parasitic nematodes. What is known in parasitic nematodes is restricted to a few studies involving the APNs, *Ancylostoma caninum* and *S. stercoralis*. Similar to *C. elegans*, *A. caninum* is repelled by sodium dodecyl sulphate (SDS) [61]. In *C. elegans*, ASH and ASK amphid neurons mediate this avoidance. However, laser ablation studies in *A. caninum* revealed that SDS avoidance is facilitated through the amphid neurons ASH and ADL [61]. Like *C. elegans*, the amphid neurons ASE and ASH mediate attraction and repulsion to sodium chloride in *S. stercoralis* [62]. Of particular note, ASF (analogous to ADF neurons in *C. elegans*), ASI and ASJ neurons, which all function in dauer development and recovery in *C. elegans*, may have similar functions in the analogous arrested development stage in *S. stercoralis* [14, 63, 64]. A unique pair of neurons in *S. stercoralis* is the ALD neurons [14, 65]. In contrast to *C. elegans*, the amphids of *S. stercoralis* do not contain finger cells, instead each amphid contains a pair of neurons whose dendrites end in a multi-layered complex of lamellae [65]. Preservation of established naming conventions led these neurons being named ALD neurons (A = amphid, L = lamellar cells, D = likely functional homology with AFD neurons in *C. elegans*) [28]. The ALD neuron differs from the AFD neuron as this neuron enters the amphid channel but terminates in the sheath cell similar to wing cell neurons

(AWA, AWB and AWC), while the AFD neuron resides completely within the sheath cell never entering the amphid channel [14, 65]. Similar to AFD neurons, which have numerous microvilli, the lamellae of ALD neurons greatly increase the surface area of these neurons suggesting that ALD neurons are involved in thermosensation in *S. stercoralis*, which was confirmed with laser ablation studies [14, 65]. To date, nothing is known about the role of phasmids in chemosensation in any parasitic nematodes. These studies demonstrate that while structural homology exists in sensory structure between *C. elegans* and parasitic nematodes, differences in function are present, underscoring the need for investigation into chemosensation in both plant- and animal-parasitic nematodes.

Very little is known about how sensory neurons, which detect environmental stimuli, are connected to the motor programs that execute behavioral responses. In the free-living nematode *C. elegans,* these circuits are thought to be shallow, using few interneuronal relays to move from detection of stimulus to action [66]. What little is known about the role of interneurons in chemosensation is restricted to studies done using *C. elegans*. However, sensory neuron conservation between this species and parasitic nematodes would dictate that APNs and PPNs are likely to possess interneurons that function in chemosensation [41].

There are four interneuron pairs that are considered sensory interneurons because they receive and process synaptic inputs from the amphids [16]. These are AIA, AIB, AIY and AIZ interneurons (first letter A = amphid, second letter I = interneuron and third letter used to distinguish between interneurons) [28]. AIA is a primary interneuron that is cholinergic and receives input from multiple amphid neurons including ASI and ASK amphid neurons [16, 67]. Both AIB and AIY are interneuron pairs that act downstream of

AWC sensory neurons, however activation of each leads to distinct behavioral responses. Activation of AIB leads to increased foraging behavior in *C. elegans*, while activation of AIY leads to a decrease in foraging behavior [68, 69]. AIZ interneurons are required for water-soluble sodium chemotaxis which is mediated through ASE amphid neurons [70].

Sensory transduction

Chemosensation is a complex and highly regulated process requiring input from a network of olfactory neurons that utilize a number of signaling pathways in a variety of ways in order to elicit behavioral responses [10, 43, 50, 60]. Although the anatomical components have been identified, the signaling cascades are not well defined. In *C. elegans*, G protein-coupled receptors (GPCRs), G-proteins, guanylyl cyclases and cGMP-gated channels are all required for chemosensation [50, 60]. Nothing is known about sensory signal transduction in parasitic nematodes and it remains to be seen how conserved sensory signaling cascades are across nematodes.

Nematodes only have a small number of chemosensory neurons compared to mammals, however several different receptor genes are expressed in each of these neurons, thereby providing a system in which nematodes can respond to an enormous number of different chemical stimuli [10, 11, 71]. Most chemoreceptors in animals, including nematodes, are G protein-coupled receptors (GPCRs) [10]. Over 1300 genes belong to putative chemoreceptor gene families in *C. elegans*, which comprises more than 5% of the genome [72]. Despite the large number of genes, direct evidence for a specific chemosensory function is limited to a single gene (*odr-10*). However, expression patterns and other indirect evidence implicate chemosensory roles for many GPCRs [10,

49, 72]. In *C. elegans*, genes encoding GPCRs fall into more than 20 families based on sequence homology [72, 73]. Of these, the *srh* family, a member of the seven transmembrane-domain (*str*) superfamily, is the largest encoding over 200 GPCRs, most of which are expressed predominately in sensory neurons [10, 72, 73]. This family includes *odr-10*, which is the only chemoreceptor for which a ligand has been identified in *C. elegans* [74]. *Odr-10*, which is expressed exclusively in AWA neurons, was found to have a high affinity for the volatile attractant diacetyl. However, responses to other odorants detected by AWA neurons were unaffected [74]. Parasitic nematodes appear to have fewer GPCRs than free-living nematodes. Although the *C. elegans* genome encodes over 1300 GPCRs, genome analysis of the APN, *H. contortus*, revealed 540 putative GPCRs, while the PPNs *M. hapla* and *M. incognita* are thought to encode fewer than 150 [75, 76]. It is not clear why such extreme variation in GPCR gene number exists but it may be related to life style differences. Whereas *C. elegans* is a free-living nematode, *H. contortus* is a parasite with both free-living and parasitic life stages. On the other hand *Meloidogyne spp*. are sedentary, obligate endoparasites of various plant roots [77].

Amphid neurons exist as structurally similar pairs; however receptor gene expression is often asymmetric [10, 50]. Asymmetric expression of specific receptors provides a mechanism in which nematodes are able to expand the repertoire of compounds they can assimilate from the external environment. For instance, high concentrations of butanone have been shown to block olfactory signaling to benzaldehyde [50]. Both compounds are detected by the AWC neurons but butanone is only detected by the AWC neuron that expresses *str-2*, which is a putative chemoreceptor that is also involved in AWC cell fate determination [50]. *Str-2* is expressed in either the

left or right AWC neuron but never in both AWC neurons [50]. Because butanone is able to block benzaldehyde signaling, the neuron expressing *str-2* does not detect it [50]. The remaining AWC neuron however is unaffected by butanone, therefore, this asymmetric expression pattern allows detection of benzaldehyde to proceed [50].

The type of response elicited could be specified by a receptor or by the sensory neuron in which the receptor is expressed [10]. In *C. elegans*, one model for the organization of olfactory information is that each chemosensory neuron pair is dedicated to a characteristic response (either attractive or repellent, not both) and all receptors expressed in that neuron pair drive the same behavior [10]. Evidence for this model was first demonstrated by expressing *odr-10* in AWB neurons [10]. When expressed in AWB neurons, *odr-10* drives a repellent behavior response to diacetyl, a volatile compound normally attractive to *C. elegans*, indicating that the cell type expressing the receptor is more important than the receptor itself in determining behavioral outcomes [10]. This model extends further in demonstrating that signal transduction pathways vary between cell types even if the same receptor is used [10]. For instance, ODR-10 mediated signaling in AWA sensory neurons occurs via ODR-3 and OSM-9, while ODR-10 signaling in AWB neurons occurs through ODR-3 and the cGMP-gated channel, TAX-4/TAX-2 [10]. This model explains that while some receptors may be expressed in only one neuron, others may be expressed in multiple neurons and mediate multiple behaviors [17].

The role of GPCRs in chemosensation is poorly understood even in the model organism, *C. elegans* and even less so in nematode parasites. Chemoreceptors are thought to couple with heterotrimeric guanine nucleotide binding proteins (G-proteins) in *C.*

elegans [49]. G-proteins serve to relay signals from GPCRs to downstream intracellular effectors [78]. Three peptides comprise G-proteins; G-protein α subunits which confer functional specificity to the G-protein, G-protein β subunits and G-protein γ subunits, which typically functions as a dimer [78]. In the inactive state, Gα bound to GDP (Gα-GDP) is associated with the Gβγ dimer and with its GPCR [79]. Ligand binding to the GPCR leads to activation of the G-protein [79]. Upon activation, GTP is exchanged for GDP on the Gα subunit which causes Gα-GTP to dissociate from the Gβγ dimer [79]. At this point both entities can interact with a variety of downstream effectors [79]. Signal termination occurs via hydrolysis of GTP to GDP by the intrinsic GTPase activity of Gα thereby allowing Gα-GDP to reassociate with Gβγ [79].

In *C. elegans* there are 22 G-protein α subunit (GPA) genes, *gpa 1-18*, *goa-1*, *gsa-1*, *egl-30* and *odr-3*; two Gβ subunit genes (GPB), *gpb-1* and *gpb-2*; and two Gγ subunit (GPC) genes, *gpc-1* and *gpc-2* [80]. The majority of these genes cluster on chromosomes I and V [80]. Of the 22 GPAs, only six have human homologues: *gpa*-4, *gpa*-16 & *goa-1*, $G\alpha_{i/o}$; *gsa-1*, $G\alpha_s$; *egl-30*, $G\alpha_q$; and *gpa*-16, $G\alpha_{12}$, while the remaining 16 are specific to Nematoda [80]. Of the 16 "nematode-specific" GPAs, 13 are exclusively expressed sensory neurons, including amphid and phasmid neurons suggesting a role for these GPAs in chemosensation [78, 80]. Studies using gain- and loss-of-function mutations demonstrated roles for GPA 1-7, 10-11 and ODR-3 in chemosensation [50, 60, 80]. Both gain- and loss-of-function mutants for ODR-3 demonstrate severe defects in food odor recognition and preference responses mediated by AWB and AWC sensory neurons [60]. In addition, animals defective for EAT-16, a negative regulator of neuronal G-protein signaling, also showed severe defects for food-odor mediated responses [60].

Gbp-1, *gbp-2* and *gpc-2* are widely expressed while *gpc-1* expression is restricted to amphid and phasmid neurons however due to the limited number of subunits available, the various Gα subunits likely associate with these in limited combinations to form heterotrimers [81-83]. All but GPC-2 have been found to function in chemosensation; GBP-1 is required for avoidance behaviors mediated by ASH neurons while GPB-2 and GPC-1 are required for NaCl adaptation [83-85].

While there is a clear role for heterotrimeric G-proteins in chemosensation in *C. elegans*, nothing is known about their function in parasitic nematodes. Genetic analysis has shown that GPAs are present in numerous parasitic species however there appear to be fewer when compared to *Caenorhabditis* spp. indicating this gene family has undergone significant gene expansion in *Caenorhabditis* although this has not been confirmed [78].

Once activated, Gα subunits can interact with guanylyl cyclases (GCY) to produce the secondary messenger cyclic guanosine monophasphate (cGMP), which opens a cyclic nucleotide-gated channel (CNG channel) leading to an influx of Ca^{2+} ions into the cell [49, 86]. GCYs are multi-domain proteins that occur in two forms; receptor guanylyl cyclases (rGCY) and soluble guanylyl cyclases (sGCY) [87]. Both forms contain a cyclase domain, however, rGCYs contain an additional protein kinase as well as a single transmembrane sequence domain and a signal sequence while sGCYs contain a heme nitric oxide-binding domain [88]. Both forms appear to have function in sensory behavior in *C. elegans*; rGCYs may function in chemosensation while sGCYs have roles in aerotaxis [49].

In *C. elegans*, there are 34 guanylyl cyclases of which 27 are rGCYs while seven are sGCYs [87]. Many GCYs are expressed exclusively in sensory neurons indicating they may have a function in chemosensation [60, 88]. In ASE neurons, *gcy* genes are expressed in a left/right asymmetric manner similar to GPCRs, further implicating them in chemosensation [88, 89]. As shown in *C. elegans*, the rGCYs, ODR-1 and DAF-11 are expressed in the cilia of AWB and AWC sensory neurons and are required for AWC mediated olfaction [60, 90]. In addition, GCY-14 is essential for ASE mediated chemotaxis in response to alkaline conditions [86]. While GCYs have been identified in several parasitic nematodes there are far less GCYs present in parasites when compared to *C. elegans*, similar to GPAs [87]. For example, only three GCYs have been identified in the PPN *H. glycines* and no function has yet been assigned any of them highlighting how little is known about GCY function in parasitic nematode chemosensation [91].

rGCYs function to produce cGMP which is thought to be the primary secondary messenger in chemosensation in *C. elegans* because activation of a CNG channel consisting of TAX-4 and TAX-2 subunits is resistant to cyclic adenosine monophosphate (cAMP) [49]. This channel has been shown to be essential for a number of chemosensory related behaviors including those involving ASE and AWC neurons [49, 92]. In *C. elegans*, *tax-4* genes encode for the α-subunit of the cGMP-gated channel while *tax-2* genes encode for the β-subunit [60]. This channel is essential for numerous sensory behaviors including responses to volatile attractants and repellents, chemotaxis to water-soluble compounds such as NaCl and reactions to preferential food odors [59, 60]. Mutants showing loss of expression for *tax-2* only in subset of neurons had several sensory response defects demonstrating the requirement for the TAX-4/TAX-2 cGMP-

channel in behaviors such as food foraging, CO_2 avoidance and thermotaxis [60]. Currently, nothing is known about CNG channels in parasitic nematodes and it remains to be seen if this channel is indeed important in chemosensation in these nematodes.

Transient receptor potential, or TRP, channels can mediate odorant chemotaxis by AWA neurons [49]. In *C. elegans*, *osm-9* and *ocr-2* encode a TRPV (TRP vanilloid) channel, a member of the TRP superfamily [60]. Like the TAX-4/TAX-2 cGMP-channel, the OSM-9/OCR-2 channel functions downstream of GPCRs and GCYs and mutants of osm-9 or ocr-2 exhibit severe defects to AWA mediated chemosensation [49, 58]. Similar to the above components of sensory transduction, nothing about this channel is known in parasitic nematodes.

Use in control of parasitic nematodes

While numerous studies have shed light on the molecular mechanisms involved in chemosensation, we have only begun to navigate the complexity of chemosensory behavior in *C. elegans*. The role of chemosensation in parasitic life styles is even less well understood. This behavior is clearly necessary in parasitic life styles, and manipulation of chemosensory behaviors in these parasites could disrupt transmission of the parasite either to animal or plant. In fact, studies have demonstrated that disruption of chemosensory behavior can prevent parasites from finding suitable hosts [93]. For example, the acetylcholinesterase inhibiting nematicide aldicarb led to 50% reduction in chemosensation in *H. glycines* at very low doses ($10^{\wedge 6}$ fold lower than required to affect locomotion) [93]. It is thought that aldicarb is taken up from the environment by chemoreceptive sensillae leading to retrograde dendritic transport to neuronal cell bodies

where it binds to and inhibits acetylcholinesterase [93]. This inhibition causes an accumulation of acetylcholinesterase at the synapse which results in an over-stimulation of the nerve cells leading to paralysis and death at high concentrations [94]. At low concentrations, aldicarb does not kill the nematode but instead impairs the nematode's ability to orient towards chemical stimuli from the environment [93]. In parasitic nematodes, this impairment may prevent the parasite from identifying and infecting a suitable host. That chemosensation is an attractive target for control has also been demonstrated in the potato cyst nematode *G. pallida* [16]. In this case, infectious J2 stage nematodes were not attracted to root exudate from transgenic potato plants expressing a synthetic peptide (nAChRbp) which binds to nicotinic acetylcholine receptors (nAChR) [16]. These studies illustrate that disruption of chemosensation in nematodes can be a useful mechanism for control and prevention. A strategy similar to this could be applied to vector-borne APNs. For instance, a transgenic mosquito, expressing peptides that disrupt chemosensation in a filarial worm such as *B. malayi* could prevent transmission of the parasite to the human host. In addition, this type of strategy could be targeted against any receptor that leads to the disruption of chemosensory behavior thus providing the means to allow this strategy to "evolve" with the parasite.

Entomopathogenic nematodes (EPN) are parasites of insects that are used for the control of many insect pests [22]. These parasites respond to chemical cues elicited by their insect hosts [13]. Manipulation of this behavior could be used to enhance the spread of the nematode to targeted insect pests providing a means of control. For example, plants secreting compounds that are attractive to EPNs like *Heterorhabditis bacteriophora*

would stimulate the EPN to migrate to the plant thereby bringing the EPN into contact with any potential insect pests that could serve as hosts for the EPN.

Chemosensation is one way in which nematode parasites interact with their environment. Through this, the animal receives information from their surroundings but this behavior does not explain how these organisms reciprocally provide information back to the environment. Parasites must be able to manipulate their environment, which requires methods to not only receive signals but to send them out as well. This requirement is visibly demonstrated in interactions involving the parasite and the host immune response, as well as parasite invasion of hosts. As noted above, worm secretions are one means by which parasites manipulate host biochemistry. Another, largely unexplored possibility is that parasites may communicate with their environment through the use of extracellular vesicles.

Extracellular vesicles

Extracellular vesicles (EVs) are small vesicles containing an intricate assortment of components including proteins, lipids, nucleic acids and glycans that are released into the extracellular environment by a wide variety of cell types. Numerous names have been given to EV subtypes including exosomes, microvesicles (MVs), microparticles, apoptotic bodies and nanoparticles in an attempt to identify extracellular vesicles based on characteristics such as originating cell, size, contents and isolation methods which has confounded the literature. To rectify this, the scientific community collectively agreed to categorize EVs based on their mode of origin [95].

Exosomes, originally identified in reticulocytes in 1983, have a diameter generally between 30-120 nm and are formed by inward budding or invagination of late endosomes to form multivesicular endosomes (MVEs) containing the nascent exosomes [96-99]. Release of exosomes occurs by fusion of the MVE with the plasma membrane [96, 98, 99]. MVs, first discovered in 1967, are generally larger than exosomes with sizes up to ~1,000 nm in diameter and are formed by direct budding of the plasma membrane [100]. Both exosomes and MVs exhibit a right-side-out membrane topology in which the cytosolic side of the lipid bilayer is inside the vesicle, and the luminal part of the membrane is exposed [98]. While the different biogenic and release pathways of exosomes and MVs would imply the cellular machinery responsible is divergent, the exact molecular mechanisms involved have yet to be elucidated, although both ESCRT-dependent and -independent mechanisms have been implicated [101, 102].

Biological systems contain diverse populations of EVs, and while function is often attributed to one specific type or another, extracellular vesicles in circulation are likely a heterogeneous mix of EVs because current purification methods, many of which are based on differential centrifugation, do not discriminate between these vesicle subtypes [101, 103]. Since their discovery, a broad range of cell types have been shown to release EVs including: B lymphocytes, dendritic cells, mast cells, stem cells, platelets, endothelial cells and breast cancer cells [98, 99, 104-108]. In addition EVs have been isolated from cell culture media and diverse body fluids such as blood, semen, urine, saliva, amniotic fluid, bile, cerebrospinal fluid, breast milk and ascites fluid [109-117].

EVs contain a variety of proteins, RNAs and other bioactive molecules making them potent vehicles for cell-to-cell communication. The composition of EV cargo

appears to be dependent on both source and target cell environments and has been shown to be enriched relative to the cell of origin suggesting that EV cargo is selectively incorporated although the exact method of vesicle-loading remains unknown [98, 99, 104, 105, 118]. Most RNAs identified in EVs are miRNAs. However, EVs also contain mRNAs and a large variety of other small noncoding RNA species, including structural RNAs, tRNA fragments, vault RNAs, Y RNAs and siRNAs [101, 103].

EVs selectively bind to target cells in order to deliver their cargo, and while the mechanisms of this selectivity remain to be resolved it appears that both target cell-dependent and -conditional aspects are involved [101]. After binding to recipient cells, EVs can remain bound, dissociate or fuse with the plasma membrane or they can be internalized thereby delivering their cargo to the target cell and affecting cell-to-cell communication [101].

EVs have been shown to have a significant impact on target cells in several ways, including altering RNA and protein expression as well as impacting the behavior of the recipient cell [101]. mRNAs packaged in EVs can be translated into functional proteins by the host cell demonstrating the ability of EV cargo to manipulate target cells [104]. Since EVs can transport proteins and nucleic acids between cells, it is not surprising that they have emerging fundamental roles in cell-to-cell communication [101, 119] but further, they also appear to have important roles in immunity and disease pathogenesis. For example, EVs have been shown to stimulate tumor progression in cancer metastasis while extracellular vesicles secreted by B-cells carry MHC class II molecules which are capable of inducing antigen-specific MHC class II-restricted T cell responses [99, 119, 120].

Extracellular vesicles in parasitism

EVs have generated significant renewed interest because of their involvement in immune responses, disease pathogenesis, and roles in cell-to-cell communication [99, 103, 105]. Although most examples have focused on EV release from mammalian cell types, it has been shown that many organisms such as bacteria, fungi, protists and nematodes also secrete EVs [121-124]. EVs are quickly becoming attractive candidates as mechanisms of gene transfer between parasites and hosts. Through this mechanism, parasites may be able to modulate the host environment to the benefit of the parasite.

A picture is emerging that parasites from widely divergent phyla actively release EVs into their environment, and whilst most reports have focused on protozoan parasites, this behavior has also been observed in helminth parasites including both platyhelminths and nematodes. As research in this field progresses, it is likely that EV release by parasites will appear the rule rather than the exception. EV secretion has been described thus far in the flukes, *Dicrocoelium dendriticum* and *Fasciola hepatica*, the cestode *Echinostoma caproni*, the kinetoplastid *Leishmania* spp. and the flagellate protozoan *Trichomonas vaginalis* [118, 125-127]. Parasites not only release EVs that interact with host cells, but they stimulate the release of EVs from host cells as well. Such parasites typically have an intracellular stage and include *Toxoplasma gondii*, *Trypanosoma cruzi*, *Plasmodium falciparum* and *Plasmodium yoelii* [124, 128-132].

Parasite-derived EVs play an important role in host-parasite communication in both helminth and protozoan infections [118]. These EVs are actively taken up by host cells, and contain an array of bioactive molecules, including RNAs and putative effector

proteins, that can be released in the host cell to affect the outcome of infection [125, 126]. In some species, the molecules contained within EVs constitute a significant portion of the parasite secretome, and several EV proteins identified, such as tetraspanins and peroxiredoxin, are involved in behaviors that may impact infection [118, 125, 126, 133].

EVs from parasites have immunomodulatory and other properties that may act to facilitate and promote host infection. *Leishmania* spp. EV secretions induce an alternative cytokine profile in infected macrophages and may also prime uninfected cells for infection, thus augmenting infection in the host [125]. *T. vaginalis*-derived EVs facilitate host-parasite interactions by increasing adherence to endothelial cells in the host, which is required for the establishment of infection [126]. The EVs secreted by *Plasmodium* spp. mediate a number of behaviors that enhance infection in the host [124]. *Plasmodium* derived EVs have significant roles in communication between parasites, for instance communication between parasites via EVs not only mediated the spread of drug resistance in the parasite but also promoted differentiation to sexual forms of the parasite [124]. In addition, EVs released by *Plasmodium* spp. stimulate innate immune responses through macrophage and neutrophil activation in humans [132].

Like protozoan parasites, nematode parasites also use EVs to modulate the host immune response [123]. Most recently, EVs secreted by the APN *Heligmosomoides polygyrus*, have been shown to suppress innate immune responses in mice [123]. Extracellular vesicles may also function in animal-to-animal communication; EVs identified in *C. elegans* induce mating behavior in male worms [134]. This is the first study to demonstrate the involvement of EVs in such behavior and highlights that in

addition to already identified roles, extracellular vesicles may play important as of yet unexplored roles in animal behavior and communication.

Applications and future prospects with extracellular vesicles

Infection with *Plasmodium* spp. has been shown to lead to the elevation of circulating host EVs [135]. In addition, elevated numbers correlated with severity of infection (i.e., the more severe the infection the more EVs found circulating) thus providing a useful diagnostic tool [136]. Since host-derived EVs carry cargo specific to the cell type from which they originate, the elevation of specific host-derived EVs in biofluids may serve as biomarkers of different disease states, and this has indeed been postulated for non-communicable diseases such as ovarian and prostate cancers [103]. Such an application may be of particular value for infections that are not readily detected through traditional means or which are asymptomatic.

The ability of extracellular vesicles to deliver bioactive molecules to specific cells or tissues is potentially exploitable as a means for targeted delivery of therapeutics. This is especially true with exosomes because their small size allows them to evade phagocytosis and rapid clearance [95]. In addition to their potential as vehicles for drug delivery, EVs have also shown a protective capacity and may have promise as vaccines against bacterial and other diseases [103]. While some pathogens release extracellular vesicles that modulate expression of immune related genes, others have been shown to induce enhanced immune responses and conferred some protective effects [130, 137]. For example, mice vaccinated with purified exosomes from *P. yoelii* elicited IgG antibodies capable of recognizing *P. yoelii* infected erythrocytes [128]. Upon subsequent challenge

with a lethal strain of *P. yoelii*, vaccinated mice not only survived but also cleared the infection, clearly demonstrating the protective effect of the exosome-derived vaccine [128].

Many proteins identified in parasite-derived EVs appear to contribute significantly to successful infection of the host making these proteins attractive targets for the development of novel chemotherapeutics [125]. Proteins identified in parasite-derived EVs include homologues of pathogen-associated molecular pattern (PAMP) molecules, such as peroxiredoxin [118]. Peroxiredoxin has been shown to have immunomodulatory properties and therefore is a promising target for chemotherapeutic interventions [133].

Dissertation organization

The focus of this dissertation is the nematode parasite and etiological agent of Lymphatic Filariasis (LF), *Brugia malayi,* and how this parasite utilizes chemosensation and extracellular vesicles to navigate and manipulate its environment to achieve successful infection. Chapter 2 presents an investigation of chemosensory structures and behavior in *B. malayi*. Using SEM, dye-filling assays and chemotaxis plate assays, I describe chemosensory anatomy and demonstrate that this nematode parasite has a functional chemosensory response that may facilitate host infection. Chapter 3 describes a bioinformatic and phylogenetic analysis of heterotrimeric G-proteins, which are known to be involved in chemosensation, across the phylum Nematoda. Chapter 4 demonstrates the presence of exosome-like vesicles (ELVs), a specific subtype of EV, in *B. malayi* and further characterizes these vesicles through the characterization of both protein and RNA cargo found within. In the final chapter, key findings from the research chapters are

summarized along with general conclusions and discussion of implications of the contained research including the development of novel therapeutics for prevention and treatment of LF.

References

1. Blaxter M, Koutsovoulos G. The evolution of parasitism in Nematoda. Parasitology. 2014:1-14. doi: 10.1017/S0031182014000791. PubMed PMID: 24963797.

2. Nicol P, Gill R, Fosu-Nyarko J, Jones MG. *de novo* analysis and functional classification of the transcriptome of the root lesion nematode, *Pratylenchus thornei*, after 454 GS FLX sequencing. Int J Parasitol. 2012;42(3):225-37. doi: 10.1016/j.ijpara.2011.11.010. PubMed PMID: 22309969.

3. Jones JT, Haegeman A, Danchin EG, Gaur HS, Helder J, Jones MG, et al. Top 10 plant-parasitic nematodes in molecular plant pathology. Mol Plant Pathol. 2013;14(9):946-61. doi: 10.1111/mpp.12057. PubMed PMID: 23809086.

4. Holden-Dye L, Walker RJ. Anthelmintic drugs and nematicides: studies in *Caenorhabditis elegans*. WormBook. 2014:1-29. doi: 10.1895/wormbook.1.143.2. PubMed PMID: 25517625.

5. Knopp S, Steinmann P, Hatz C, Keiser J, Utzinger J. Nematode infections: filariases. Infect Dis Clin North Am. 2012;26(2):359-81. doi: 10.1016/j.idc.2012.02.005. PubMed PMID: 22632644.

6. Global programme to eliminate lymphatic filariasis: progress report, 2014. Wkly Epidemiol Rec. 2015;90(38):489-504. PubMed PMID: 26387149.

7. Choi YJ, Aliota MT, Mayhew GF, Erickson SM, Christensen BM. Dual RNA-seq of parasite and host reveals gene expression dynamics during filarial worm-mosquito interactions. PLoS Negl Trop Dis. 2014;8(5):e2905. doi: 10.1371/journal.pntd.0002905. PubMed PMID: 24853112; PubMed Central PMCID: PMCPMC4031193.

8. Devaney E, Osborne J. The third-stage larva (L3) of *Brugia*: its role in immune modulation and protective immunity. Microbes Infect. 2000;2(11):1363-71. PubMed PMID: 11018453.

9. Global programme to eliminate lymphatic filariasis: progress report, 2011. Wkly Epidemiol Rec. 2012;87(37):346-56. PubMed PMID: 22977953.

10. Troemel ER, Kimmel BE, Bargmann CI. Reprogramming chemotaxis responses: sensory neurons define olfactory preferences in *C. elegans*. Cell. 1997;91(2):161-9. PubMed PMID: 9346234.

11. Ward S. Chemotaxis by the nematode *Caenorhabditis elegans*: identification of attractants and analysis of the response by use of mutants. Proc Natl Acad Sci U S A. 1973;70(3):817-21. PubMed PMID: 4351805; PubMed Central PMCID: PMCPMC433366.

12. Wright KA. Nematode chemosensilla: form and function. J Nematol. 1983;15(2):151-8. PubMed PMID: 19295785; PubMed Central PMCID: PMCPMC2618269.

13. Pye AE, Burman M. *Neoaplectana carpocapsae*: Nematode accumulations on chemical and bacterial gradients. Exp Parasitol. 1981;51(1):13-20. PubMed PMID: 6257537.

14. Ashton FT, Schad GA. Amphids in *Strongyloides stercoralis* and other parasitic nematodes. Parasitol Today. 1996;12(5):187-94. PubMed PMID: 15275212.

15. Culotti JG, Russell RL. Osmotic avoidance defective mutants of the nematode *Caenorhabditis elegans*. Genetics. 1978;90(2):243-56. PubMed PMID: 730048; PubMed Central PMCID: PMCPMC1213887.

16. Wang D, Jones LM, Urwin PE, Atkinson HJ. A synthetic peptide shows retro- and anterograde neuronal transport before disrupting the chemosensation of plant-pathogenic nematodes. PLoS One. 2011;6(3):e17475. doi: 10.1371/journal.pone.0017475. PubMed PMID: 21408216; PubMed Central PMCID: PMCPMC3049761.

17. Robinson AF, Perry RN. Behaviour and Sensory Perception. In: Perry RN, Moens M, editors. Plant Nematology. 2nd ed. Wallingford, Oxfordshire: CAB International; 2006. p. 210-33.

18. Vieira P, Danchin EG, Neveu C, Crozat C, Jaubert S, Hussey RS, et al. The plant apoplasm is an important recipient compartment for nematode secreted proteins. J Exp

Bot. 2011;62(3):1241-53. doi: 10.1093/jxb/erq352. PubMed PMID: 21115667; PubMed Central PMCID: PMCPMC3022405.

19. Castelletto ML, Gang SS, Okubo RP, Tselikova AA, Nolan TJ, Platzer EG, et al. Diverse host-seeking behaviors of skin-penetrating nematodes. PLoS Pathog. 2014;10(8):e1004305. doi: 10.1371/journal.ppat.1004305. PubMed PMID: 25121736; PubMed Central PMCID: PMCPMC4133384.

20. Gunawardena NK, Fujimaki Y, Aoki Y. Chemotactic response of *Brugia pahangi* infective larvae to jird serum in vitro. Parasitol Res. 2003;90(4):337-42. doi: 10.1007/s00436-003-0838-1. PubMed PMID: 12695907.

21. Kusaba T, Fujimaki Y, Vincent AL, Aoki Y. In vitro chemotaxis of *Brugia pahangi* infective larvae to the sera and hemolymph of mammals and lower animals. Parasitol Int. 2008;57(2):179-84. doi: 10.1016/j.parint.2007.12.006. PubMed PMID: 18243775.

22. Hallem EA, Dillman AR, Hong AV, Zhang Y, Yano JM, DeMarco SF, et al. A sensory code for host seeking in parasitic nematodes. Curr Biol. 2011;21(5):377-83. doi: 10.1016/j.cub.2011.01.048. PubMed PMID: 21353558; PubMed Central PMCID: PMCPMC3152378.

23. Ward S, Thomson N, White JG, Brenner S. Electron microscopical reconstruction of the anterior sensory anatomy of the nematode *Caenorhabditis elegans*. J Comp Neurol. 1975;160(3):313-37. doi: 10.1002/cne.901600305. PubMed PMID: 1112927.

24. Bacaj T, Tevlin M, Lu Y, Shaham S. Glia are essential for sensory organ function in *C. elegans*. Science. 2008;322(5902):744-7. doi: 10.1126/science.1163074. PubMed PMID: 18974354; PubMed Central PMCID: PMCPMC2735448.

25. Abdel-Ghaffar F, Bashtar AR, Abdel-Gaber R, Morsy K, Mehlhorn H, Al Quraishy S, et al. *Cucullanus egyptae* sp. nov. (Nematoda, Cucullanidae) infecting the European eel *Anguilla anguilla* in Egypt. Morphological and molecular phylogenetic studies. Parasitol Res. 2014;113(9):3457-65. doi: 10.1007/s00436-014-4016-4. PubMed PMID: 25030116.

26. Perkins LA, Hedgecock EM, Thomson JN, Culotti JG. Mutant sensory cilia in the nematode *Caenorhabditis elegans*. Dev Biol. 1986;117(2):456-87. PubMed PMID: 2428682.

27. Nguyen KB, Smart GC. Location of the Phasmids on Infective Juveniles of *Steinernema glaseri*. J Nematol. 1993;25(4):625-7. PubMed PMID: 19279819; PubMed Central PMCID: PMCPMC2619410.

28. White JG, Southgate E, Thomson JN, Brenner S. The structure of the nervous system of the nematode *Caenorhabditis elegans*. Philos Trans R Soc Lond B Biol Sci. 1986;314(1165):1-340. PubMed PMID: 22462104.

29. Schacher JF. Morphology of the microfilaria of *Brugia pahangi* and of the larval stages in the mosquito. J Parasitol. 1962;48:679-92. PubMed PMID: 13976565.

30. Schacher JF. Developmental stages of *Brugia pahangi* in the final host. J Parasitol. 1962;48:693-706. PubMed PMID: 13976564.

31. Tongu Y. Ultrastructural studies on the microfilaria of *Brugia malayi*. Acta Med Okayama. 1974;28(3):219-42. PubMed PMID: 4280233.

32. Poinar GO, Petersen JJ. *Drilomermis leioderma* n. gen., n. sp. (Mermithidae:Nematoda) parasitizing *Cybister fimbriolatus* (Say) (Dystiscidae-Coleoptera). J Nematol. 1978;10(1):20-3. PubMed PMID: 19305807; PubMed Central PMCID: PMCPMC2617855.

33. Poinar GO, Chang PM. *Hexamermis cathetospiculae* n. sp. (Mermithidae: Nematoda), a Parasite of the Rice Stemborer, *Tryporyza incertulas* (Wlk.) (Pyralidae: Lepidoptera) in Malaysia. J Nematol. 1985;17(3):360-3. PubMed PMID: 19294107; PubMed Central PMCID: PMCPMC2618465.

34. de Doucet MM, Poinar GO. *Gastromermis kolleonis* n. sp. (Nematoda: Mermithidae), a Parasite of Midges (*Chironomus* sp. *Chironomidae*) from Argentina. J Nematol. 1984;16(3):252-5. PubMed PMID: 19294020; PubMed Central PMCID: PMCPMC2618395.

35. Endo BY. Ultrastructure of the anterior neurosensory organs of the larvae of the soybean cyst nematode, *Heterodera glycines*. J Ultrastruct Res. 1980;72(3):349-66. PubMed PMID: 7191907.

36. Baldwin JG, Hirschmann H. Fine Structure of Cephalic Sense Organs in *Heterodera glycines* Males. J Nematol. 1975;7(1):40-53. PubMed PMID: 19308132; PubMed Central PMCID: PMCPMC2620085.

37. Wergin WP, Endo BY. Ultrastructure of a neurosensory organ in a root-knot nematode. J Ultrastruct Res. 1976;56(3):258-76. PubMed PMID: 957473.

38. Golden AM, Maqbool MA, Handoo ZA. Descriptions of Two New Species of *Tylenchorhynchus* Cobb, 1913 (Nematoda: Tylenchida), with Details on Morphology and Variation of *T. claytoni*. J Nematol. 1987;19(1):58-68. PubMed PMID: 19290107; PubMed Central PMCID: PMCPMC2618616.

39. Mutafchiev Y, Dantas-Torres F, Giannelli A, Abramo F, Papadopoulos E, Cardoso L, et al. Redescription of *Onchocerca lupi* (Spirurida: Onchocercidae) with histopathological observations. Parasit Vectors. 2013;6(1):309. doi: 10.1186/1756-3305-6-309. PubMed PMID: 24499611; PubMed Central PMCID: PMCPMC3818983.

40. Oikonomou G, Shaham S. The glia of *Caenorhabditis elegans*. Glia. 2011;59(9):1253-63. doi: 10.1002/glia.21084. PubMed PMID: 21732423; PubMed Central PMCID: PMCPMC3117073.

41. Li J, Zhu X, Ashton FT, Gamble HR, Schad GA. Sensory neuroanatomy of a passively ingested nematode parasite, *Haemonchus contortus*: amphidial neurons of the third-stage larva. J Parasitol. 2001;87(1):65-72. doi: 10.1645/0022-3395(2001)087[0065:SNOAPI]2.0.CO;2. PubMed PMID: 11227904.

42. Perens EA, Shaham S. *C. elegans* daf-6 encodes a patched-related protein required for lumen formation. Dev Cell. 2005;8(6):893-906. doi: 10.1016/j.devcel.2005.03.009. PubMed PMID: 15935778.

43. Shaham S. Chemosensory organs as models of neuronal synapses. Nat Rev Neurosci. 2010;11(3):212-7. doi: 10.1038/nrn2740. PubMed PMID: 20029439; PubMed Central PMCID: PMCPMC2860653.

44. Stewart GR, Perry RN, Alexander J, Wright DJ. A glycoprotein specific to the amphids of *Meloidogyne* species. Parasitology. 1993;106(4):405-12. Epub 06 April 2009.

45. Premachandran D, Von Mende N, Hussey RS, McClure MA. A method for staining nematode secretions and structures. J Nematol. 1988;20(1):70-8. PubMed PMID: 19290186; PubMed Central PMCID: PMCPMC2618786.

46. Maule AG, Curtis R. Parallels between plant and animal parasitic nematodes. In: Jones J, Gheysen G, Fenoll C, editors. Genomics and Molecular Genetics of Plant-Nematode Interactions. Dordrecht, Netherlands: Springer; 2011. p. 221-51.

47. Perry RN. Chemoreception in plant parasitic nematodes. Annu Rev Phytopathol. 1996;34:181-99. doi: 10.1146/annurev.phyto.34.1.181. PubMed PMID: 15012540.

48. Doroquez DB, Berciu C, Anderson JR, Sengupta P, Nicastro D. A high-resolution morphological and ultrastructural map of anterior sensory cilia and glia in *Caenorhabditis elegans*. Elife. 2014;3:e01948. doi: 10.7554/eLife.01948. PubMed PMID: 24668170; PubMed Central PMCID: PMCPMC3965213.

49. Bargmann CI. Chemosensation in *C. elegans*. WormBook. 2006:1-29. doi: 10.1895/wormbook.1.123.1. PubMed PMID: 18050433.

50. Wes PD, Bargmann CI. *C. elegans* odour discrimination requires asymmetric diversity in olfactory neurons. Nature. 2001;410(6829):698-701. doi: 10.1038/35070581. PubMed PMID: 11287957.

51. Bargmann CI, Horvitz HR. Chemosensory neurons with overlapping functions direct chemotaxis to multiple chemicals in *C. elegans*. Neuron. 1991;7(5):729-42. PubMed PMID: 1660283.

52. Bargmann CI, Horvitz HR. Control of larval development by chemosensory neurons in *Caenorhabditis elegans*. Science. 1991;251(4998):1243-6. PubMed PMID: 2006412.

53. Kaplan JM, Horvitz HR. A dual mechanosensory and chemosensory neuron in *Caenorhabditis elegans*. Proc Natl Acad Sci U S A. 1993;90(6):2227-31. PubMed PMID: 8460126; PubMed Central PMCID: PMCPMC46059.

54. Troemel ER, Chou JH, Dwyer ND, Colbert HA, Bargmann CI. Divergent seven transmembrane receptors are candidate chemosensory receptors in *C. elegans*. Cell. 1995;83(2):207-18. PubMed PMID: 7585938.

55. Hukema RK, Rademakers S, Dekkers MP, Burghoorn J, Jansen G. Antagonistic sensory cues generate gustatory plasticity in *Caenorhabditis elegans*. EMBO J. 2006;25(2):312-22. doi: 10.1038/sj.emboj.7600940. PubMed PMID: 16407969; PubMed Central PMCID: PMCPMC1383522.

56. Crook M. The dauer hypothesis and the evolution of parasitism: 20 years on and still going strong. Int J Parasitol. 2014;44(1):1-8. doi: 10.1016/j.ijpara.2013.08.004. PubMed PMID: 24095839; PubMed Central PMCID: PMCPMC3947200.

57. Wakabayashi T, Kimura Y, Ohba Y, Adachi R, Satoh Y, Shingai R. In vivo calcium imaging of OFF-responding ASK chemosensory neurons in *C. elegans*. Biochim Biophys Acta. 2009;1790(8):765-9. doi: 10.1016/j.bbagen.2009.03.032. PubMed PMID: 19362117.

58. Hilliard MA, Bargmann CI, Bazzicalupo P. *C. elegans* responds to chemical repellents by integrating sensory inputs from the head and the tail. Curr Biol. 2002;12(9):730-4. PubMed PMID: 12007416.

59. Hirotsu T, Saeki S, Yamamoto M, Iino Y. The Ras-MAPK pathway is important for olfaction in *Caenorhabditis elegans*. Nature. 2000;404(6775):289-93. doi: 10.1038/35005101. PubMed PMID: 10749212.

60. Harris G, Shen Y, Ha H, Donato A, Wallis S, Zhang X, et al. Dissecting the signaling mechanisms underlying recognition and preference of food odors. J Neurosci. 2014;34(28):9389-403. doi: 10.1523/JNEUROSCI.0012-14.2014. PubMed PMID: 25009271; PubMed Central PMCID: PMCPMC4087214.

61. Ketschek AR, Joseph R, Boston R, Ashton FT, Schad GA. Amphidial neurons ADL and ASH initiate sodium dodecyl sulphate avoidance responses in the infective larva of the dog hookworm *Anclyostoma caninum*. Int J Parasitol. 2004;34(12):1333-6. doi: 10.1016/j.ijpara.2004.08.008. PubMed PMID: 15542093.

62. Forbes WM, Ashton FT, Boston R, Zhu X, Schad GA. Chemoattraction and chemorepulsion of *Strongyloides stercoralis* infective larvae on a sodium chloride gradient is mediated by amphidial neuron pairs ASE and ASH, respectively. Vet Parasitol. 2004;120(3):189-98. doi: 10.1016/j.vetpar.2004.01.005. PubMed PMID: 15041094.

63. Ashton FT, Zhu X, Boston R, Lok JB, Schad GA. *Strongyloides stercoralis*: Amphidial neuron pair ASJ triggers significant resumption of development by infective larvae under host-mimicking in vitro conditions. Exp Parasitol. 2007;115(1):92-7. doi: 10.1016/j.exppara.2006.08.010. PubMed PMID: 17067579; PubMed Central PMCID: PMCPMC3091007.

64. Ashton FT, Bhopale VM, Holt D, Smith G, Schad GA. Developmental switching in the parasitic nematode *Strongyloides stercoralis* is controlled by the ASF and ASI amphidial neurons. J Parasitol. 1998;84(4):691-5. PubMed PMID: 9714195.

65. Lopez PM, Boston R, Ashton FT, Schad GA. The neurons of class ALD mediate thermotaxis in the parasitic nematode, *Strongyloides stercoralis*. Int J Parasitol. 2000;30(10):1115-21. PubMed PMID: 10996330.

66. Allen EN, Ren J, Zhang Y, Alcedo J. Sensory systems: their impact on *C. elegans* survival. Neuroscience. 2014. doi: 10.1016/j.neuroscience.2014.06.054. PubMed PMID: 24997267.

67. Macosko EZ, Pokala N, Feinberg EH, Chalasani SH, Butcher RA, Clardy J, et al. A hub-and-spoke circuit drives pheromone attraction and social behaviour in *C. elegans*. Nature. 2009;458(7242):1171-5. doi: 10.1038/nature07886. PubMed PMID: 19349961; PubMed Central PMCID: PMCPMC2760495.

68. Chalasani SH, Chronis N, Tsunozaki M, Gray JM, Ramot D, Goodman MB, et al. Dissecting a circuit for olfactory behaviour in *Caenorhabditis elegans*. Nature. 2007;450(7166):63-70. doi: 10.1038/nature06292. PubMed PMID: 17972877.

69. Kocabas A, Shen CH, Guo ZV, Ramanathan S. Controlling interneuron activity in *Caenorhabditis elegans* to evoke chemotactic behaviour. Nature. 2012;490(7419):273-7. doi: 10.1038/nature11431. PubMed PMID: 23000898; PubMed Central PMCID: PMCPMC4229948.

70. Iino Y, Yoshida K. Parallel use of two behavioral mechanisms for chemotaxis in *Caenorhabditis elegans*. J Neurosci. 2009;29(17):5370-80. doi: 10.1523/JNEUROSCI.3633-08.2009. PubMed PMID: 19403805.

71. Carey AF, Carlson JR. Insect olfaction from model systems to disease control. Proc Natl Acad Sci U S A. 2011;108(32):12987-95. doi: 10.1073/pnas.1103472108. PubMed PMID: 21746926; PubMed Central PMCID: PMCPMC3156210.

72. Thomas JH, Robertson HM. The *Caenorhabditis* chemoreceptor gene families. BMC Biol. 2008;6:42. doi: 10.1186/1741-7007-6-42. PubMed PMID: 18837995; PubMed Central PMCID: PMCPMC2576165.

73. Robertson HM, Thomas JH. The putative chemoreceptor families of *C. elegans*. WormBook. 2006:1-12. doi: 10.1895/wormbook.1.66.1. PubMed PMID: 18050473.

74. Sengupta P, Chou JH, Bargmann CI. *odr-10* encodes a seven transmembrane domain olfactory receptor required for responses to the odorant diacetyl. Cell. 1996;84(6):899-909. PubMed PMID: 8601313.

75. Bird DM, Williamson VM, Abad P, McCarter J, Danchin EG, Castagnone-Sereno P, et al. The genomes of root-knot nematodes. Annu Rev Phytopathol. 2009;47:333-51. doi: 10.1146/annurev-phyto-080508-081839. PubMed PMID: 19400640.

76. Schwarz EM, Korhonen PK, Campbell BE, Young ND, Jex AR, Jabbar A, et al. The genome and developmental transcriptome of the strongylid nematode *Haemonchus contortus*. Genome Biol. 2013;14(8):R89. doi: 10.1186/gb-2013-14-8-r89. PubMed PMID: 23985341; PubMed Central PMCID: PMCPMC4053716.

77. Castagnone-Sereno P, Danchin EG, Perfus-Barbeoch L, Abad P. Diversity and evolution of root-knot nematodes, genus *Meloidogyne*: new insights from the genomic era. Annu Rev Phytopathol. 2013;51:203-20. doi: 10.1146/annurev-phyto-082712-102300. PubMed PMID: 23682915.

78. O'Halloran DM, Fitzpatrick DA, McCormack GP, McInerney JO, Burnell AM. The molecular phylogeny of a nematode-specific clade of heterotrimeric G-protein alpha-subunit genes. J Mol Evol. 2006;63(1):87-94. doi: 10.1007/s00239-005-0215-z. PubMed PMID: 16786439.

79. Bastiani C, Mendel J. Heterotrimeric G proteins in *C. elegans*. WormBook. 2006:1-25. doi: 10.1895/wormbook.1.75.1. PubMed PMID: 18050432.

80. Jansen G, Thijssen KL, Werner P, van der Horst M, Hazendonk E, Plasterk RH. The complete family of genes encoding G proteins of *Caenorhabditis elegans*. Nat Genet. 1999;21(4):414-9. doi: 10.1038/7753. PubMed PMID: 10192394.

81. Zwaal RR, Ahringer J, van Luenen HG, Rushforth A, Anderson P, Plasterk RH. G proteins are required for spatial orientation of early cell cleavages in *C. elegans* embryos. Cell. 1996;86(4):619-29. PubMed PMID: 8752216.

82. van der Linden AM, Simmer F, Cuppen E, Plasterk RH. The G-protein beta-subunit GPB-2 in *Caenorhabditis elegans* regulates the G(o)alpha-G(q)alpha signaling network through interactions with the regulator of G-protein signaling proteins EGL-10 and EAT-16. Genetics. 2001;158(1):221-35. PubMed PMID: 11333232; PubMed Central PMCID: PMCPMC1461628.

83. Jansen G, Weinkove D, Plasterk RH. The G-protein gamma subunit gpc-1 of the nematode *C.elegans* is involved in taste adaptation. EMBO J. 2002;21(5):986-94. doi: 10.1093/emboj/21.5.986. PubMed PMID: 11867526; PubMed Central PMCID: PMCPMC125897.

84. Esposito G, Di Schiavi E, Bergamasco C, Bazzicalupo P. Efficient and cell specific knock-down of gene function in targeted *C. elegans* neurons. Gene. 2007;395(1-2):170-6. doi: 10.1016/j.gene.2007.03.002. PubMed PMID: 17459615.

85. Yamada K, Hirotsu T, Matsuki M, Kunitomo H, Iino Y. GPC-1, a G protein gamma-subunit, regulates olfactory adaptation in *Caenorhabditis elegans*. Genetics. 2009;181(4):1347-57. doi: 10.1534/genetics.108.099002. PubMed PMID: 19189947; PubMed Central PMCID: PMCPMC2666504.

86. Murayama T, Takayama J, Fujiwara M, Maruyama IN. Environmental alkalinity sensing mediated by the transmembrane guanylyl cyclase GCY-14 in *C. elegans*. Curr Biol. 2013;23(11):1007-12. doi: 10.1016/j.cub.2013.04.052. PubMed PMID: 23664973.

87. Fitzpatrick DA, O'Halloran DM, Burnell AM. Multiple lineage specific expansions within the guanylyl cyclase gene family. BMC Evol Biol. 2006;6:26. doi: 10.1186/1471-2148-6-26. PubMed PMID: 16549024; PubMed Central PMCID: PMCPMC1435932.

88. Ortiz CO, Etchberger JF, Posy SL, Frøkjaer-Jensen C, Lockery S, Honig B, et al. Searching for neuronal left/right asymmetry: genomewide analysis of nematode receptor-type guanylyl cyclases. Genetics. 2006;173(1):131-49. doi: 10.1534/genetics.106.055749. PubMed PMID: 16547101; PubMed Central PMCID: PMCPMC1461427.

89. Yu S, Avery L, Baude E, Garbers DL. Guanylyl cyclase expression in specific sensory neurons: a new family of chemosensory receptors. Proc Natl Acad Sci U S A. 1997;94(7):3384-7. PubMed PMID: 9096403; PubMed Central PMCID: PMCPMC20379.

90. L'Etoile ND, Bargmann CI. Olfaction and odor discrimination are mediated by the *C. elegans* guanylyl cyclase ODR-1. Neuron. 2000;25(3):575-86. PubMed PMID: 10774726.

91. Yan Y, Davis EL. Characterisation of guanylyl cyclase genes in the soybean cyst nematode, *Heterodera glycines*. Int J Parasitol. 2002;32(1):65-72. PubMed PMID: 11796123.

92. Smith HK, Luo L, O'Halloran D, Guo D, Huang XY, Samuel AD, et al. Defining specificity determinants of cGMP mediated gustatory sensory transduction in *Caenorhabditis elegans*. Genetics. 2013;194(4):885-901. doi: 10.1534/genetics.113.152660. PubMed PMID: 23695300; PubMed Central PMCID: PMCPMC3730918.

93. Winter MD, McPherson MJ, Atkinson HJ. Neuronal uptake of pesticides disrupts chemosensory cells of nematodes. Parasitology. 2002;125(Pt 6):561-5. PubMed PMID: 12553575.

94. Wren JF, Kille P, Spurgeon DJ, Swain S, Sturzenbaum SR, Jager T. Application of physiologically based modelling and transcriptomics to probe the systems toxicology of aldicarb for *Caenorhabditis elegans* (Maupas 1900). Ecotoxicology. 2011;20(2):397-408. doi: 10.1007/s10646-010-0591-z. PubMed PMID: 21253838; PubMed Central PMCID: PMCPMC3037492.

95. Momen-Heravi F, Balaj L, Alian S, Mantel PY, Halleck AE, Trachtenberg AJ, et al. Current methods for the isolation of extracellular vesicles. Biol Chem. 2013;394(10):1253-62. doi: 10.1515/hsz-2013-0141. PubMed PMID: 23770532.

96. Harding C, Heuser J, Stahl P. Receptor-mediated endocytosis of transferrin and recycling of the transferrin receptor in rat reticulocytes. J Cell Biol. 1983;97(2):329-39. PubMed PMID: 6309857; PubMed Central PMCID: PMCPMC2112509.

97. Pan BT, Johnstone RM. Fate of the transferrin receptor during maturation of sheep reticulocytes in vitro: selective externalization of the receptor. Cell. 1983;33(3):967-78. PubMed PMID: 6307529.

98. Théry C, Boussac M, Véron P, Ricciardi-Castagnoli P, Raposo G, Garin J, et al. Proteomic analysis of dendritic cell-derived exosomes: a secreted subcellular compartment distinct from apoptotic vesicles. J Immunol. 2001;166(12):7309-18. PubMed PMID: 11390481.

99. Raposo G, Nijman HW, Stoorvogel W, Liejendekker R, Harding CV, Melief CJ, et al. B lymphocytes secrete antigen-presenting vesicles. J Exp Med. 1996;183(3):1161-72. PubMed PMID: 8642258; PubMed Central PMCID: PMCPMC2192324.

100. Wolf P. The nature and significance of platelet products in human plasma. Br J Haematol. 1967;13(3):269-88. PubMed PMID: 6025241.

101. Raposo G, Stoorvogel W. Extracellular vesicles: exosomes, microvesicles, and friends. J Cell Biol. 2013;200(4):373-83. doi: 10.1083/jcb.201211138. PubMed PMID: 23420871; PubMed Central PMCID: PMCPMC3575529.

102. Colombo M, Moita C, van Niel G, Kowal J, Vigneron J, Benaroch P, et al. Analysis of ESCRT functions in exosome biogenesis, composition and secretion

highlights the heterogeneity of extracellular vesicles. J Cell Sci. 2013;126(Pt 24):5553-65. doi: 10.1242/jcs.128868. PubMed PMID: 24105262.

103. Witwer KW, Buzás EI, Bemis LT, Bora A, Lässer C, Lötvall J, et al. Standardization of sample collection, isolation and analysis methods in extracellular vesicle research. J Extracell Vesicles. 2013;2. doi: 10.3402/jev.v2i0.20360. PubMed PMID: 24009894; PubMed Central PMCID: PMCPMC3760646.

104. Valadi H, Ekström K, Bossios A, Sjöstrand M, Lee JJ, Lötvall JO. Exosome-mediated transfer of mRNAs and microRNAs is a novel mechanism of genetic exchange between cells. Nat Cell Biol. 2007;9(6):654-9. doi: 10.1038/ncb1596. PubMed PMID: 17486113.

105. Ratajczak J, Miekus K, Kucia M, Zhang J, Reca R, Dvorak P, et al. Embryonic stem cell-derived microvesicles reprogram hematopoietic progenitors: evidence for horizontal transfer of mRNA and protein delivery. Leukemia. 2006;20(5):847-56. doi: 10.1038/sj.leu.2404132. PubMed PMID: 16453000.

106. Heijnen HF, Schiel AE, Fijnheer R, Geuze HJ, Sixma JJ. Activated platelets release two types of membrane vesicles: microvesicles by surface shedding and exosomes derived from exocytosis of multivesicular bodies and alpha-granules. Blood. 1999;94(11):3791-9. PubMed PMID: 10572093.

107. Deregibus MC, Cantaluppi V, Calogero R, Lo Iacono M, Tetta C, Biancone L, et al. Endothelial progenitor cell derived microvesicles activate an angiogenic program in endothelial cells by a horizontal transfer of mRNA. Blood. 2007;110(7):2440-8. doi: 10.1182/blood-2007-03-078709. PubMed PMID: 17536014.

108. Muralidharan-Chari V, Clancy JW, Sedgwick A, D'Souza-Schorey C. Microvesicles: mediators of extracellular communication during cancer progression. J Cell Sci. 2010;123(Pt 10):1603-11. doi: 10.1242/jcs.064386. PubMed PMID: 20445011; PubMed Central PMCID: PMCPMC2864708.

109. Ronquist G, Brody I. The prostasome: its secretion and function in man. Biochim Biophys Acta. 1985;822(2):203-18. PubMed PMID: 2992593.

110. Caby MP, Lankar D, Vincendeau-Scherrer C, Raposo G, Bonnerot C. Exosomal-like vesicles are present in human blood plasma. Int Immunol. 2005;17(7):879-87. doi: 10.1093/intimm/dxh267. PubMed PMID: 15908444.

111. Pisitkun T, Shen RF, Knepper MA. Identification and proteomic profiling of exosomes in human urine. Proc Natl Acad Sci U S A. 2004;101(36):13368-73. doi: 10.1073/pnas.0403453101. PubMed PMID: 15326289; PubMed Central PMCID: PMCPMC516573.

112. Ogawa Y, Miura Y, Harazono A, Kanai-Azuma M, Akimoto Y, Kawakami H, et al. Proteomic analysis of two types of exosomes in human whole saliva. Biol Pharm Bull. 2011;34(1):13-23. PubMed PMID: 21212511.

113. Admyre C, Johansson SM, Qazi KR, Filén JJ, Lahesmaa R, Norman M, et al. Exosomes with immune modulatory features are present in human breast milk. J Immunol. 2007;179(3):1969-78. PubMed PMID: 17641064.

114. Asea A, Jean-Pierre C, Kaur P, Rao P, Linhares IM, Skupski D, et al. Heat shock protein-containing exosomes in mid-trimester amniotic fluids. J Reprod Immunol. 2008;79(1):12-7. doi: 10.1016/j.jri.2008.06.001. PubMed PMID: 18715652.

115. Andre F, Schartz NE, Movassagh M, Flament C, Pautier P, Morice P, et al. Malignant effusions and immunogenic tumour-derived exosomes. Lancet. 2002;360(9329):295-305. doi: 10.1016/S0140-6736(02)09552-1. PubMed PMID: 12147373.

116. Vella LJ, Sharples RA, Lawson VA, Masters CL, Cappai R, Hill AF. Packaging of prions into exosomes is associated with a novel pathway of PrP processing. J Pathol. 2007;211(5):582-90. doi: 10.1002/path.2145. PubMed PMID: 17334982.

117. Masyuk AI, Huang BQ, Ward CJ, Gradilone SA, Banales JM, Masyuk TV, et al. Biliary exosomes influence cholangiocyte regulatory mechanisms and proliferation through interaction with primary cilia. Am J Physiol Gastrointest Liver Physiol. 2010;299(4):G990-9. doi: 10.1152/ajpgi.00093.2010. PubMed PMID: 20634433; PubMed Central PMCID: PMCPMC2957333.

118. Marcilla A, Trelis M, Cortés A, Sotillo J, Cantalapiedra F, Minguez MT, et al. Extracellular vesicles from parasitic helminths contain specific excretory/secretory proteins and are internalized in intestinal host cells. PLoS One. 2012;7(9):e45974. doi: 10.1371/journal.pone.0045974. PubMed PMID: 23029346; PubMed Central PMCID: PMCPMC3454434.

119. Robbins PD, Morelli AE. Regulation of immune responses by extracellular vesicles. Nat Rev Immunol. 2014;14(3):195-208. doi: 10.1038/nri3622. PubMed PMID: 24566916.

120. EL Andaloussi S, Mäger I, Breakefield XO, Wood MJ. Extracellular vesicles: biology and emerging therapeutic opportunities. Nat Rev Drug Discov. 2013;12(5):347-57. doi: 10.1038/nrd3978. PubMed PMID: 23584393.

121. Kuehn MJ, Kesty NC. Bacterial outer membrane vesicles and the host-pathogen interaction. Genes Dev. 2005;19(22):2645-55. doi: 10.1101/gad.1299905. PubMed PMID: 16291643.

122. Rodrigues ML, Nakayasu ES, Almeida IC, Nimrichter L. The impact of proteomics on the understanding of functions and biogenesis of fungal extracellular vesicles. J Proteomics. 2014;97:177-86. doi: 10.1016/j.jprot.2013.04.001. PubMed PMID: 23583696; PubMed Central PMCID: PMCPMC3745587.

123. Buck AH, Coakley G, Simbari F, McSorley HJ, Quintana JF, Le Bihan T, et al. Exosomes secreted by nematode parasites transfer small RNAs to mammalian cells and modulate innate immunity. Nat Commun. 2014;5:5488. doi: 10.1038/ncomms6488. PubMed PMID: 25421927.

124. Regev-Rudzki N, Wilson DW, Carvalho TG, Sisquella X, Coleman BM, Rug M, et al. Cell-cell communication between malaria-infected red blood cells via exosome-like vesicles. Cell. 2013;153(5):1120-33. doi: 10.1016/j.cell.2013.04.029. PubMed PMID: 23683579.

125. Silverman JM, Clos J, de'Oliveira CC, Shirvani O, Fang Y, Wang C, et al. An exosome-based secretion pathway is responsible for protein export from Leishmania and communication with macrophages. J Cell Sci. 2010;123(Pt 6):842-52. doi: 10.1242/jcs.056465. PubMed PMID: 20159964.

126. Twu O, de Miguel N, Lustig G, Stevens GC, Vashisht AA, Wohlschlegel JA, et al. Trichomonas vaginalis exosomes deliver cargo to host cells and mediate host：parasite interactions. PLoS Pathog. 2013;9(7):e1003482. doi: 10.1371/journal.ppat.1003482. PubMed PMID: 23853596; PubMed Central PMCID: PMCPMC3708881.

127. Bernal D, Trelis M, Montaner S, Cantalapiedra F, Galiano A, Hackenberg M, et al. Surface analysis of *Dicrocoelium dendriticum*. The molecular characterization of exosomes reveals the presence of miRNAs. J Proteomics. 2014;105:232-41. doi: 10.1016/j.jprot.2014.02.012. PubMed PMID: 24561797.

128. Martin-Jaular L, Nakayasu ES, Ferrer M, Almeida IC, Del Portillo HA. Exosomes from *Plasmodium yoelii*-infected reticulocytes protect mice from lethal infections. PLoS One. 2011;6(10):e26588. doi: 10.1371/journal.pone.0026588. PubMed PMID: 22046311; PubMed Central PMCID: PMCPMC3202549.

129. Pope SM, Lässer C. *Toxoplasma gondii* infection of fibroblasts causes the production of exosome-like vesicles containing a unique array of mRNA and miRNA transcripts compared to serum starvation. J Extracell Vesicles. 2013;2. doi: 10.3402/jev.v2i0.22484. PubMed PMID: 24363837; PubMed Central PMCID: PMCPMC3862870.

130. Bhatnagar S, Shinagawa K, Castellino FJ, Schorey JS. Exosomes released from macrophages infected with intracellular pathogens stimulate a proinflammatory response in vitro and in vivo. Blood. 2007;110(9):3234-44. doi: 10.1182/blood-2007-03-079152. PubMed PMID: 17666571; PubMed Central PMCID: PMCPMC2200902.

131. Cestari I, Ansa-Addo E, Deolindo P, Inal JM, Ramirez MI. *Trypanosoma cruzi* immune evasion mediated by host cell-derived microvesicles. J Immunol. 2012;188(4):1942-52. doi: 10.4049/jimmunol.1102053. PubMed PMID: 22262654.

132. Mantel PY, Hoang AN, Goldowitz I, Potashnikova D, Hamza B, Vorobjev I, et al. Malaria-infected erythrocyte-derived microvesicles mediate cellular communication within the parasite population and with the host immune system. Cell Host Microbe. 2013;13(5):521-34. doi: 10.1016/j.chom.2013.04.009. PubMed PMID: 23684304; PubMed Central PMCID: PMCPMC3687518.

133. Robinson MW, Hutchinson AT, Donnelly S, Dalton JP. Worm secretory molecules are causing alarm. Trends Parasitol. 2010;26(8):371-2. doi: 10.1016/j.pt.2010.05.004. PubMed PMID: 20542734.

134. Wang J, Silva M, Haas LA, Morsci NS, Nguyen KC, Hall DH, et al. *C. elegans* ciliated sensory neurons release extracellular vesicles that function in animal communication. Curr Biol. 2014;24(5):519-25. doi: 10.1016/j.cub.2014.01.002. PubMed PMID: 24530063.

135. Combes V, Taylor TE, Juhan-Vague I, Mège JL, Mwenechanya J, Tembo M, et al. Circulating endothelial microparticles in malawian children with severe falciparum malaria complicated with coma. JAMA. 2004;291(21):2542-4. doi: 10.1001/jama.291.21.2542-b. PubMed PMID: 15173142.

136. Pankoui Mfonkeu JB, Gouado I, Fotso Kuaté H, Zambou O, Amvam Zollo PH, Grau GE, et al. Elevated cell-specific microparticles are a biological marker for cerebral dysfunctions in human severe malaria. PLoS One. 2010;5(10):e13415. doi: 10.1371/journal.pone.0013415. PubMed PMID: 20976232; PubMed Central PMCID: PMCPMC2954805.

137. Hassani K, Olivier M. Immunomodulatory impact of *leishmania*-induced macrophage exosomes: a comparative proteomic and functional analysis. PLoS Negl Trop Dis. 2013;7(5):e2185. doi: 10.1371/journal.pntd.0002185. PubMed PMID: 23658846; PubMed Central PMCID: PMCPMC3642089.

CHAPTER 2

CHEMOSENSORY BEHAVIOR IN THE FILARIAL WORM, *BRUGIA MALAYI*

Lisa M. Fraser[1,2], R. Isai Madriz[2], Lyric C. Bartholomay[2]* and Michael J. Kimber[1]

[1]Department of Biomedical Sciences, Iowa State University, Ames, Iowa, United States of America, [2]Department of Entomology, Iowa State University, Ames, Iowa, United States of America, *Current Address: Department of Pathobiological Sciences, University of Wisconsin-Madison, Madison, Wisconsin, United States of America

Abstract

Lymphatic Filariasis (LF) is a disease caused by mosquito-borne filarial nematodes including *Wuchereria bancrofti* and *Brugia malayi*. Over 120 million people suffer from this disfiguring disease yet chemotherapeutic options for LF are limited to three drugs: diethylcarbamazine citrate (DEC), albendazole and ivermectin, none of which cure an infected patient. The threat of drug resistance, combined with adverse side effects and inefficacy against critical life stages, drives the need for new anthelmintic drugs. Chemosensation is an essential behavior used by multi-cellular organisms to interact with the environment. In the model free-living nematode *Caenorhabditis elegans*, chemosensation plays a crucial role in development, avoiding noxious conditions and finding food and mates. In parasitic nematodes, chemosensation likely plays critical roles in host-seeking and host-invasion behaviors, making genes involved in this system attractive targets for drug or vaccine development. Little is known, however, about the

chemosensory system in filarial nematodes. In this study, we examined the chemosensory apparatus of *B. malayi* and elucidate chemosensory-induced behavior during the infectious L3 stage of the parasite. Scanning electron microscopy revealed that amphids, the major chemosensory organs of nematodes, are present and arranged in a conserved manner while internal sensory neuroanatomy was examined using fluorescent microscopy in both juvenile and adult stages of *B. malayi*. Finally, a cohort of chemical compounds tested using a plate-based chemotaxis assay, were shown to elicit specific tactic behaviors that may facilitate infection with *B. malayi* L3 stage parasites. Combined, these results are the first to demonstrate that *B. malayi* has a responsive chemosensory pathway and also indicate that the chemosensory response in *B. malayi* may have an important role in parasite transmission and host invasion.

Introduction

Chemosensation is essential for organisms to perceive the outside environment [1, 2]. This vital process begins with the detection of environmental compounds by chemoreceptors, which are most commonly G protein-coupled receptors (GPCRs) [2]. Receptor binding leads to the activation of chemosensory neurons and ultimately to the activation of motor neurons resulting in a physical response to the detected stimulus [2]. While the fundamental process of chemosensation is conserved across organisms, comparison of chemosensory systems in insects, nematodes and all higher animals has revealed some fundamental differences. In *Caenorhabditis elegans* adult hermaphrodites, only 32 neurons are presumed to be chemosensory neurons [3-5]. This is in stark contrast to *Drosophila melanogaster* which has ~2600 olfactory neurons and mammals which have millions of odorant sensory neurons [2, 6, 7]. Even though *C. elegans* is limited to a

small number of chemosensory neurons, this nematode encodes genes for more than 1000 putative chemoreceptors [2, 8]. Thus, the small number of chemosensory neurons in *C. elegans* has led to the employment of a different strategy in chemoreceptor expression. Unlike vertebrates and insects, which follow a functionally similar arrangement of one or few receptor genes per neuron, nematodes express many chemoreceptors in each chemosensory neuron, thus enabling the detection of a wide array of compounds with remarkable precision [2, 9].

Chemosensory behavior in nematodes has been characterized primarily through the study of the free-living model *C. elegans* [4, 10-12]. These studies have demonstrated that *C. elegans* has a robust chemosensory response with the ability to sense and respond to hundreds of compounds [13, 14]. Olfactory cues elicit a number of important behaviors in nematodes; in *C. elegans*, these cues have been shown to be involved in finding food and mates, avoiding noxious conditions and entry/exit into the dauer stage [1, 12]. In contrast, research investigating chemosensation in parasitic nematodes is very limited but there is evidence that chemosensation is critical for both host-seeking and host-invasion behaviors [15-17]. For example, the infective stages of skin penetrating parasitic nematodes such as *Strongyloides ratti* and *Ancylostoma caninum* exhibit positive chemotaxis to host serum, which may provide a positive stimulus for skin penetration and thereby facilitate transmission and infection [18-20]. In addition, studies in both plant- and animal-parasitic nematodes have shown that chemosensation in these animals is used to identify a suitable host, and this behavior varies depending on host preference [15, 16, 21, 22]. Collectively, these findings support the hypothesis that

chemosensation is important for the transmission and establishment of infection of parasitic nematodes in their hosts.

Successful infection of a host requires nematode parasites to rapidly adapt to diverse physical and biochemical environments. To establish infection, filarial worms such as *Brugia malayi* must be able to penetrate the host then identify and invade appropriate host cells and tissues, as well as avoid or suppress the immune response in both mosquito and human hosts. To date, very little is known about chemosensory behavior in filarial worms and how this facilitates establishment of infection. Research has been limited to the infectious L3 stage of the feline parasite *B. pahangi*, which is attracted to host serum and sodium ions in a concentration dependent manner [23-25].

Here we characterized chemosensory structures and behavior in the human filarial parasite *B. malayi*. Scanning electron microscopy was used to identify the presence of the anterior chemosensory organs, the amphids, across multiple life stages in *B. malayi*. In addition, we visualized internal sensory neuroanatomy through the use the lipophilic dye, 1,1'-dioctadecyl-3,3,3',3'-tetramethylindocarbocyanine perchlorate (DiI). Finally, we evaluated the response of infectious stage parasites to compounds present in both human and mosquito hosts using a modified agar plate assay. The results presented here demonstrate that *B. malayi* has a functional chemosensory response and displays tactic behaviors to specific stimuli such that transmission from the mosquito vector to the human host may be facilitated. A better understanding of chemosensation in filarial worms will not only provide insight into mechanisms of transmission and establishment of infection but may also lead to the development of novel strategies for disruption of parasite transmission from mosquito to human hosts.

Materials and Methods

Mosquito maintenance

Adult female *Aedes aegypti* (Black eyed Liverpool strain, LVP) that were previously selected for susceptibility to infection with *Brugia malayi* [26], were fed a diet of 10% sucrose and maintained in controlled conditions (27°C ± 1°C and 75% ± 5% relative humidity) with a 16:8 photoperiod.

Establishment of *Brugia malayi* infection and parasite collection

B. malayi - infected cat blood was obtained from the University of Georgia NIH/NIAID Filariasis Research Reagent Resource Center (FR3). Blood containing the parasites was diluted with defibrinated sheep blood (Hemostat Laboratories, CA, USA) to achieve a concentration of 150-250 mf per 20 µl. To establish infection, three- to five-day-old female *Ae. aegypti* (LVP) were allowed to feed for one hour on a glass membrane feeder. Mosquitoes were sucrose-starved for 24 hrs prior to blood feeding and those that did not take a blood meal were removed. Infected mosquitoes were maintained under the conditions described for 12-19 days post infection (dpi) to allow development of parasites to the L3 stage.

To collect L3 stage parasites, infected adult female *Ae. aegypti* were cold-anesthetized on ice and dissected into three sections (head and proboscis, thorax and abdomen) in separate drops of room temperature *Aedes* physiological saline, and parasites were allowed to migrate out of the mosquito into the saline solution [27]. In addition to L3 parasites harvested in-house, we also obtained supplementary L3, L4, adult male and adult female stages from FR3 for scanning electron microscopy,

fluorescence staining and chemotaxis plate assays. During L3 chemotaxis studies, no difference in movement or behavior was observed between L3s freshly collected from infected mosquitoes and those obtained from FR3.

Scanning electron microscopy

Samples were fixed in 1.5 mL microcentrifuge tubes with 2% paraformaldehyde and 2% glutaraldehyde (Sigma-Aldrich, St. Louis, MO, USA) in 0.1 M cacodylate buffer (Thermo Fisher Scientific, Waltham, MA, USA), pH 7.2, for 24 hrs at 4°C. Samples were rinsed four times with the same buffer and post-fixed in 2% aqueous osmium tetroxide (Sigma-Aldrich) for 24 hrs. Specimens were then rinsed four times with the same buffer followed by dehydration in a graded ethanol series (10, 30, 50, 70, 90, 95, 100, 100, 100%), each step for 15 min. Finally, samples were dried using an ultrapure ethanol and carbon dioxide in a critical point drying apparatus (Denton Vacuum DCP-1, Denton Vacuum, LLC, Moorestown, NJ USA). Dried samples were stored in a desiccator or adhered to aluminum stubs using double-stick tape and silver paint. The samples were sputter-coated (Denton Desk II sputter coater, Denton Vacuum) with 120 nm palladium-gold (60:40). Samples were viewed with a scanning electron microscope (JEOL 5800LV) at 10–13 kV in the Microscopy and NanoImaging Facility, Iowa State University. Images were captured using a SIS ADDA II (Olympus Soft Imaging Systems Inc., Lakewood, CO, USA).

Dye filling assays

Staining of live animals (L3, L4, adult male and adult female) was performed using 1,1'-dioctadecyl-3,3,3',3'-tetramethylindocarbocyanine perchlorate (DiI, Thermo

Fisher Scientific, Waltham, MA, USA). Worms were washed using RPMI 1640 (Thermo Fisher Scientific, Waltham, MA, USA) containing pen-strep (0.4 units penicillin/ml, 0.4 mcg streptomycin/ml). L3, L4, adult female and adult male *B. malayi* were then placed into clean RPMI containing DiI (10 µg/ml) and pen-strep (0.4 units penicillin/ml, 0.4 mcg streptomycin/ml) and incubated at 37°C for 16-24 hrs. After staining, animals were washed twice with RPMI 1640 containing pen-strep and visualized using a Nikon Eclipse 50i compound fluorescent microscope (Nikon, Japan).

Chemotaxis plate assays

Chemotaxis assays were prepared as described in Margie *et al.* [28] with minor modifications: 35 mm plates containing 0.8% agarose were divided into four equal quadrants. A circle with a diameter of 3 mm was marked around the origin to designate the center. A circle was placed in each quadrant 5mm away from the center. Each quadrant was designated with a T_1 or T_2 for test or a C_1 or C_2 for control (Figure 1). Assays were performed by placing 2 µl of the test compound into the circles in T1 and T2 quadrants and 2 µl of the control compound (water or paraffin oil) in the circles in C1 and C2 quadrants. Up to seven L3s were positioned in the center in 2 µl of water and the assay plates were placed uncovered at 35°C ± 3°C and left undisturbed on a vibration reducing platform for 30 minutes.

To constitute a full experiment (N), chemotaxis plate assays were run until at least 50 parasites had shown a response to the compound tested by moving either into the test or control quadrants. Three experiments were performed for each compound tested. Chemotaxis index (CI) for each experiment was calculated as: CI = [(total # of L3s at T_1

and T_2) - (total # of L3s at C_1 and C_2)]/[(total # of L3s at T_1 and T_2) + (total # of L3s at C_1 and C_2)]. L3s that did not move out of the center were not scored. Scoring ranged from -1.0 for maximal repulsion to +1.0 for maximal attraction. Liquid compounds were tested undiluted. Solid compounds were resuspended at a 1 M concentration with the exception of *Aedes* saline which was prepared as described in Hayes [27] and contained 154 mM NaCl, 1.36 mM $CaCl_2$, 2.68 mM KCl, 1.19 mM $NaHCO_3$.

Statistical analysis

For analysis of chemotaxis plate assays, unpaired two-tailed t-tests were used to compare C.I. of test compounds to C.I. of control compounds. All statistical analyses were performed using Prism 6 for Mac (GraphPad).

Results and Discussion

***B. malayi* possess conserved chemosensory structures.**

The primary chemosensory organs in nematodes are the amphids, which are a pair of lateral structures located anteriorly on either side of the mouth of the nematode [3, 22, 29-31]. Scanning electron microscopy (SEM) was used to determine if amphids are present in *B. malayi*. SEM revealed the presence of amphids in all life stages examined (L3, L4, adult male and adult female) (Figure 2). Amphid pores in *B. malayi* are narrow, crescent-shaped openings that are less prominent than those found in *C. elegans* but similar to what has been previously observed in both *Onchocerca lupi* and *O. eberhardi*, two species closely related to *B. malayi* [32, 33].

Amphid pore shape is highly variable among nematodes and while the significance of this is unknown, it may be that the more convoluted shapes are functional and enhance the sensitivity of these organs as chemoreceptors. *C. elegans,* which has a very sensitive chemosensory response, is capable of detecting and responding to hundreds of different chemical cues [13]. In fact, *C. elegans* chemosensation is so sensitive that these nematodes are able to distinguish between bacteria that are food sources and those that are pathogenic [34]. Furthermore, these worms also respond to environmental compounds in a concentration-dependent manner and exhibit adaptive behavior when pre-exposed to chemical compounds [35, 36]. Compared to *C. elegans*, *B. malayi* may be exposed to fewer chemical stimuli, which may not necessitate highly sensitive chemoreceptors. Indeed, it has been observed that amphids of animal-parasitic nematodes (APNs) are often less pronounced than those of free-living nematodes, thus providing support for this hypothesis [37].

While not the focus of this study, it was observed that *B. malayi* possess fewer cephalic papillae (four inner labial sensilla and four outer labial sensilla) (Figure 2) than *C. elegans* (six inner labial sensilla, six outer labial sensilla and four additional cephalic sensilla), which is considered to have the classical arrangement of cephalic papillae [3, 38]. Similar to *B. malayi*, *O. eberhardi* also exhibits a reduction in anterior papillae [33] indicating that this reduction may be a feature common to filarial worms. This disparity in structures that are thought to be primarily mechanosensory could indicate filarial nematodes have a reduced mechanosensory response.

To further characterize the sensory neuroanatomy present in *B. malayi*, dye-filling assays using the lipophilic dye DiI were performed. Dye-filling, which was originally

developed by Hedgecock *et al.* in 1985, is a common method used to visualize sensory neuroanatomy in nematodes [39]. While the mechanisms behind dye-filling have yet to be fully elucidated, defects are associated with abnormal ciliary ultrastructure [30]. Dye-filling patterns varied across life stages in *B. malayi*. Amphid channel staining was observed in all life stages tested and could be readily discriminated using light microscopy (Figure 3). In addition to the amphid channels, sheath cell bodies took up DiI in L3, adult male and adult females (Figure 3b, h, k), while socket cell bodies were detected in L3 stage parasites (Figure 3b). The nerve ring filled with DiI in all but adult male *B. malayi* (Figure 3b, e, k). Of note, no amphidial neurons were found to take up DiI in any life stage (Figure 3). This is a distinct departure from *C. elegans* in which six amphid neurons (ASH, ASI, ASJ, ASK, ADL and AWB) can be observed using DiI [40]. Although the neuroanatomy of nematodes is highly conserved, these differences in dye-filling patterns may indicate variation in neuroanatomy at the cellular level.

While our observations contrast to what has been observed for a number of free-living nematodes, they are comparable to what has been observed in other parasitic nematodes. Dye-filling assays in *Parastrongyloides trichosuri*, a parasite of Australian brush-tailed possums, detected only one amphid neuron (ASL) pair [41]. More recently, Han *et al.* (2015) investigated dye-filling patterns of several other parasitic nematode species [42]. The authors found that staining patterns in parasites were often reduced compared to their free-living counterparts [42]. This observation held true regardless of preferred host or invasion strategy, for example amphid neurons of the soybean cyst nematode, *Heterodera glycines*, and the root knot nematode *Meloidogyne hapla*, did not stain [42]. In addition, no dye-filling was observed in the amphid neurons of the

infectious juvenile (IJ) stage of the entomopathogenic nematode *Heterorhabditis bacteriophora*, and only periodic staining of these neurons was detected in non-IJ stages [42]. The reductions of sensitivity to dye-filling in parasitic nematodes suggest possible structural modifications to the sensory neurons of these nematodes. Notably, although dye-filling patterns are not representative of phylogeny, there appears to be some commonalities that are indicative of life style (parasite vs. free-living). This raises the possibility that underlying structural or biochemical differences in chemosensory structures may be required for a parasitic life strategy and could be exploited in the pursuit of novel methods of control.

Host-derived gustatory and olfactory compounds elicit specific tactic behaviors in L3 stage *B. malayi*

A number of sensory neurons are involved in nematode chemosensory responses such that each type of neuron recognizes different categories of molecules [43]. The primary taste receptor neurons in *C. elegans* are the ASE amphid neurons [10, 14, 43]. These neurons are required for responses to a number of gustatory cues such as salts, amino acids and other water soluble molecules [10]. Sodium chloride has been shown to elicit behavioral responses in *C. elegans* demonstrating that this is a gustatory compound [44]. In contrast to gustatory compounds, responses to odorants (volatile compounds) are mediated by the olfactory neurons, AWA, AWB and AWC, in *C. elegans* [11, 14]. Olfaction is crucial for a number of parasitic organisms, such as mosquitoes, which often identify hosts primarily through olfactory cues [45, 46]. The identification in *B. malayi* of both the ultrastructure and neuroanatomy required for chemosensation (Figures 2 and 3), led us to question whether or not environmental cues could elicit behavioral responses in

B. malayi and if these responses have a role in parasite invasion and, consequently, transmission. We therefore sought to interrogate responses to both gustatory and olfactory compounds in infectious *B. malayi* L3 stage parasites using chemotaxis plate assays (Figure 1). *B. malayi* L3s were strongly attracted to the gustatory compound sodium chloride (NaCl) (mean C. I. = 0.55, $p < 0.01$) when compared to water controls (Figure 4). It should be noted that the concentration of NaCl used here was high (1M), however the chemotaxis plate assays used allow for diffusion of water-soluble compounds, thereby, creating a gradient. It is likely that parasites were responding to an "ideal" concentration within the gradient. That said, previous studies have shown that when placed in a low NaCl concentration, the skin-penetrating parasite *Strongyloides stercoralis* will migrate up the gradient to NaCl concentrations as high as 1.1M [47].

Studies using parasitic nematodes such as *S. stercoralis* suggest that chemosensation plays an essential role in host-selection and invasion [15]. To determine if chemosensation plays a role in *B. malayi* host-invasion, we assayed responses of L3 stage worms to a number of host-derived compounds. Parasites were attracted to L-lactic acid (mean C. I. = 0.32, $p < 0.05$) (Figure 5), a compound produced in the muscles of humans. Interrogation with additional host-derived odorants revealed that both 3-methyl-1-butanol (mean C. I. = -0.21, $p < 0.01$) and 1-nonanol (mean C. I. = -0.21, $p < 0.05$) are repellent to *B. malayi* L3 stage parasites (Figure 6). In addition to host-derived volatiles, we also examined the response of L3 stage *B. malayi* to more complex host compounds such as human serum. L3 stage parasites were strongly attracted to *Aedes* saline (mean C. I. = 0.36, $p < 0.05$), fetal bovine serum (FBS) (mean C. I. = 0.49, $p < 0.01$) and human serum (mean C. I. = 0.4, $p < 0.01$) (Figure 7). No difference was found in the parasite

response to *Aedes* saline, FBS or human serum. Bovids are not hosts for *B. malayi* so although these compounds are attractive to this parasite, they are unlikely to dictate host specificity.

To our knowledge, this is the first report to demonstrate that filarial nematodes exhibit specific tactile behaviors in response to host-derived odorants and the first to demonstrate chemosensory responses to host-derived compounds in *B. malayi*. Of note, both 3-methyl-1-butanol and 1-nonanol, which are human skin and sweat odorants and are known mosquito attractants, repelled L3 stage parasites [46, 48-52]. In contrast, physiologic saline that mimics the internal environment of the mosquito (*Aedes* saline) and human host compounds (L-lactic acid and human serum) were attractive. Together, these results indicate chemosensation in this nematode that may be important in transmission of this parasite by providing both positive and negative stimuli to encourage host penetration. In contrast to *S. stercoralis*, which actively seeks out a suitable host, *B. malayi* L3s are transmitted to human hosts through the bite of an infected mosquito. When the mosquito takes a blood meal, these worms migrate out of the proboscis onto the skin and crawl into the wound track left by the blood-feeding mosquito. In contrast, *S. stercoralis* must actively seek out a suitable host, so these parasites are strongly attracted to 3-methyl-1-butanol, 2-methyl-1-butanol and 1-nonanol, all of which are compounds found in human sweat [15]. Unlike *B. malayi* L3s, IJ stage *S. stercoralis* are soil dwelling nematodes, and it is likely that these and other host-derived compounds direct this parasite to a suitable host, where *B. malayi* is delivered directly onto the host skin and has to rapidly enter before it desiccates and dies. The results presented here indicate that *B. malayi* either have no response to, or are repelled by compounds found in human sweat.

This negative response may facilitate transmission of the parasite by acting as a stimulant to move away from the host surface and drive skin penetration while the attractive response to serum and L-lactic acid may act as a "beacon" to direct the parasite to the wound track left by the mosquito vector. Additional research will reveal the molecular mechanisms involved in this behavior and characterize the precise role that chemosensation plays in transmission of this parasite. Elucidation of this behavior may lead to the development of novel methods of control for these parasites.

Author Contributions

Conceived and designed the experiments: LMF, LCB, MJK. Performed the experiments: LMF, RIM. Analyzed the data: LMF, LCB, MJK. Wrote the paper: LMF, RIM, LCB, MJK.

Acknowledgements

The authors would like to thank Brendan Dunphy, Michael Nazarchyk and Joel Bauer for technical assistance with mosquito rearing and maintenance. The authors would also like to acknowledge parasite materials provided by Dr. Andrew Moorhead, Erica Burkman, Molly Riggs and the NIH-NIAID Filariasis Research Reagent Resource Center (FR3).

References

1. Prasad BC, Reed RR. Chemosensation: molecular mechanisms in worms and mammals. Trends Genet. 1999;15(4):150-3. PubMed PMID: 10203825.

2. Bargmann CI. Comparative chemosensation from receptors to ecology. Nature. 2006;444(7117):295-301. doi: 10.1038/nature05402. PubMed PMID: 17108953.

3. Ward S, Thomson N, White JG, Brenner S. Electron microscopical reconstruction of the anterior sensory anatomy of the nematode *Caenorhabditis elegans*. J Comp Neurol. 1975;160(3):313-37. doi: 10.1002/cne.901600305. PubMed PMID: 1112927.

4. Troemel ER, Chou JH, Dwyer ND, Colbert HA, Bargmann CI. Divergent seven transmembrane receptors are candidate chemosensory receptors in *C. elegans*. Cell. 1995;83(2):207-18. PubMed PMID: 7585938.

5. Thomas JH, Robertson HM. The *Caenorhabditis* chemoreceptor gene families. BMC Biol. 2008;6:42. doi: 10.1186/1741-7007-6-42. PubMed PMID: 18837995; PubMed Central PMCID: PMCPMC2576165.

6. Li Q, Liberles SD. Aversion and attraction through olfaction. Curr Biol. 2015;25(3):R120-9. doi: 10.1016/j.cub.2014.11.044. PubMed PMID: 25649823; PubMed Central PMCID: PMCPMC4317791.

7. Liberles SD. Mammalian pheromones. Annu Rev Physiol. 2014;76:151-75. doi: 10.1146/annurev-physiol-021113-170334. PubMed PMID: 23988175; PubMed Central PMCID: PMCPMC4310675.

8. Robertson HM, Thomas JH. The putative chemoreceptor families of *C. elegans*. WormBook. 2006:1-12. doi: 10.1895/wormbook.1.66.1. PubMed PMID: 18050473.

9. von der Weid B, Rossier D, Lindup M, Tuberosa J, Widmer A, Col JD, et al. Large-scale transcriptional profiling of chemosensory neurons identifies receptor-ligand pairs *in vivo*. Nat Neurosci. 2015;18(10):1455-63. doi: 10.1038/nn.4100. PubMed PMID: 26322926.

10. Bargmann CI, Horvitz HR. Chemosensory neurons with overlapping functions direct chemotaxis to multiple chemicals in *C. elegans*. Neuron. 1991;7(5):729-42. PubMed PMID: 1660283.

11. Chalasani SH, Chronis N, Tsunozaki M, Gray JM, Ramot D, Goodman MB, et al. Dissecting a circuit for olfactory behaviour in *Caenorhabditis elegans*. Nature. 2007;450(7166):63-70. doi: 10.1038/nature06292. PubMed PMID: 17972877.

12. Troemel ER, Kimmel BE, Bargmann CI. Reprogramming chemotaxis responses: sensory neurons define olfactory preferences in *C. elegans*. Cell. 1997;91(2):161-9. PubMed PMID: 9346234.

13. Hart AC, Chao MY. From odors to behaviors in *Caenorhabditis elegans*. In: Menini A, editor. The neurobiology of olfaction. Frontiers in Neuroscience. Boca Raton, FL: CRC Press; 2010. p. 1-33.

14. Bargmann CI. Chemosensation in *C. elegans*. WormBook. 2006:1-29. doi: 10.1895/wormbook.1.123.1. PubMed PMID: 18050433.

15. Castelletto ML, Gang SS, Okubo RP, Tselikova AA, Nolan TJ, Platzer EG, et al. Diverse host-seeking behaviors of skin-penetrating nematodes. PLoS Pathog. 2014;10(8):e1004305. doi: 10.1371/journal.ppat.1004305. PubMed PMID: 25121736; PubMed Central PMCID: PMCPMC4133384.

16. Hallem EA, Dillman AR, Hong AV, Zhang Y, Yano JM, DeMarco SF, et al. A sensory code for host seeking in parasitic nematodes. Curr Biol. 2011;21(5):377-83. doi: 10.1016/j.cub.2011.01.048. PubMed PMID: 21353558; PubMed Central PMCID: PMCPMC3152378.

17. Chaisson KE, Hallem EA. Chemosensory behaviors of parasites. Trends Parasitol. 2012;28(10):427-36. doi: 10.1016/j.pt.2012.07.004. PubMed PMID: 22921895.

18. Granzer M, Haas W. Host-finding and host recognition of infective *Ancylostoma caninum* larvae. Int J Parasitol. 1991;21(4):429-40. PubMed PMID: 1917283.

19. Vetter JC, Vingerhoed J, Schoeman E, Wauters HW. Chemotactic attraction of infective hookworm larvae of *Ancylostoma caninum* by a dog serum factor. Z Parasitenkd. 1985;71(4):539-43. PubMed PMID: 4024709.

20. Koga M, Tada I. *Strongyloides ratti*: chemotactic responses of third-stage larvae to selected serum proteins and albumins. J Helminthol. 2000;74(3):247-52. PubMed PMID: 10953225.

21. Wang D, Jones LM, Urwin PE, Atkinson HJ. A synthetic peptide shows retro- and anterograde neuronal transport before disrupting the chemosensation of plant-pathogenic nematodes. PLoS One. 2011;6(3):e17475. doi: 10.1371/journal.pone.0017475. PubMed PMID: 21408216; PubMed Central PMCID: PMCPMC3049761.

22. Robinson AF, Perry RN. Behaviour and Sensory Perception. In: Perry RN, Moens M, editors. Plant Nematology. 2nd ed. Wallingford, Oxfordshire: CAB International; 2006. p. 210-33.

23. Kusaba T, Fujimaki Y, Vincent AL, Aoki Y. In vitro chemotaxis of *Brugia pahangi* infective larvae to the sera and hemolymph of mammals and lower animals. Parasitol Int. 2008;57(2):179-84. doi: 10.1016/j.parint.2007.12.006. PubMed PMID: 18243775.

24. Gunawardena NK, Fujimaki Y, Aoki Y. Chemotactic response of *Brugia pahangi* infective larvae to jird serum in vitro. Parasitol Res. 2003;90(4):337-42. doi: 10.1007/s00436-003-0838-1. PubMed PMID: 12695907.

25. Mitsui Y, Miura M, Bome DA, Aoki Y. In vitro chemotactic responses of *Brugia pahangi* infective larvae to sodium ions. J Helminthol. 2012;86(4):406-9. doi: 10.1017/S0022149X11000605. PubMed PMID: 22030560.

26. MacDonald WW. The selection of a strain of *Aedes aegypti* susceptible to infection with semi-periodic *Brugia malayi.* Annals of Tropical Medicine and Parasitology. 1962;56:368-72.

27. Hayes RO. Determination of a Physiological Saline Solution for *Aedes aegypti* (L.). Journal of Economic Entomology. 1953;46(4):624-7.

28. Margie OP, C.Chin-Sang, I. *C. elegans* chemotaxis assay. J Vis Exp. 2013;(74):e50069.

29. Bacaj T, Tevlin M, Lu Y, Shaham S. Glia are essential for sensory organ function in *C. elegans*. Science. 2008;322(5902):744-7. doi: 10.1126/science.1163074. PubMed PMID: 18974354; PubMed Central PMCID: PMCPMC2735448.

30. Perkins LA, Hedgecock EM, Thomson JN, Culotti JG. Mutant sensory cilia in the nematode *Caenorhabditis elegans*. Dev Biol. 1986;117(2):456-87. PubMed PMID: 2428682.

31. Wright KA. Nematode chemosensilla: form and function. J Nematol. 1983;15(2):151-8. PubMed PMID: 19295785; PubMed Central PMCID: PMCPMC2618269.

32. Mutafchiev Y, Dantas-Torres F, Giannelli A, Abramo F, Papadopoulos E, Cardoso L, et al. Redescription of *Onchocerca lupi* (Spirurida: Onchocercidae) with histopathological observations. Parasit Vectors. 2013;6(1):309. doi: 10.1186/1756-3305-6-309. PubMed PMID: 24499611; PubMed Central PMCID: PMCPMC3818983.

33. Uni S, Bain O, Agatsuma T, Harada M, Torii H, Fukuda M, et al. *Onchocerca eberhardi* n. sp. (Nematoda: Filarioidea) from sika deer in Japan; relationships between species parasitic in cervids and bovids in the Holarctic region. Parasite. 2007;14(3):199-211. PubMed PMID: 17933297.

34. Pradel E, Zhang Y, Pujol N, Matsuyama T, Bargmann CI, Ewbank JJ. Detection and avoidance of a natural product from the pathogenic bacterium *Serratia marcescens* by *Caenorhabditis elegans*. Proc Natl Acad Sci U S A. 2007;104(7):2295-300. doi: 10.1073/pnas.0610281104. PubMed PMID: 17267603; PubMed Central PMCID: PMCPMC1892944.

35. Jansen G, Weinkove D, Plasterk RH. The G-protein gamma subunit gpc-1 of the nematode *C.elegans* is involved in taste adaptation. EMBO J. 2002;21(5):986-94. doi: 10.1093/emboj/21.5.986. PubMed PMID: 11867526; PubMed Central PMCID: PMCPMC125897.

36. Matsuki M, Kunitomo H, Iino Y. Goalpha regulates olfactory adaptation by antagonizing Gqalpha-DAG signaling in *Caenorhabditis elegans*. Proc Natl Acad Sci U S A. 2006;103(4):1112-7. doi: 10.1073/pnas.0506954103. PubMed PMID: 16418272; PubMed Central PMCID: PMCPMC1347976.

37. Goater TM, Goater CP, Esch GW. Parasitism: the diversity and ecology of animal parasites: Cambridge University Press; 2013.

38. Tippawangkosol P, Choochote W, Na-Bangchang K, Jitpakdi A, Pitasawat B, Riyong D. The in vitro effect of albendazole, ivermectin, diethylcarbamazine, and their combinations against infective third-stage larvae of nocturnally subperiodic *Brugia malayi* (Narathiwat strain): scanning electron microscopy. J Vector Ecol. 2004;29(1):101-8. PubMed PMID: 15266747.

39. Hedgecock EM, Culotti JG, Thomson JN, Perkins LA. Axonal guidance mutants of *Caenorhabditis elegans* identified by filling sensory neurons with fluorescein dyes. Dev Biol. 1985;111(1):158-70. PubMed PMID: 3928418.

40. Srinivasan J, Durak O, Sternberg PW. Evolution of a polymodal sensory response network. BMC Biol. 2008;6:52. doi: 10.1186/1741-7007-6-52. PubMed PMID: 19077305; PubMed Central PMCID: PMCPMC2636771.

41. Zhu H, Li J, Nolan TJ, Schad GA, Lok JB. Sensory neuroanatomy of *Parastrongyloides trichosuri*, a nematode parasite of mammals: Amphidial neurons of

the first-stage larva. J Comp Neurol. 2011;519(12):2493-507. doi: 10.1002/cne.22637. PubMed PMID: 21456026; PubMed Central PMCID: PMCPMC3125480.

42. Han Z, Boas S, Schroeder NE. Unexpected Variation in Neuroanatomy among Diverse Nematode Species. Front Neuroanat. 2015;9:162. doi: 10.3389/fnana.2015.00162. PubMed PMID: 26778973; PubMed Central PMCID: PMCPMC4700257.

43. Smith HK, Luo L, O'Halloran D, Guo D, Huang XY, Samuel AD, et al. Defining specificity determinants of cGMP mediated gustatory sensory transduction in *Caenorhabditis elegans*. Genetics. 2013;194(4):885-901. doi: 10.1534/genetics.113.152660. PubMed PMID: 23695300; PubMed Central PMCID: PMCPMC3730918.

44. Ward S. Chemotaxis by the nematode *Caenorhabditis elegans*: identification of attractants and analysis of the response by use of mutants. Proc Natl Acad Sci U S A. 1973;70(3):817-21. PubMed PMID: 4351805; PubMed Central PMCID: PMCPMC433366.

45. Hallem EA, Nicole Fox A, Zwiebel LJ, Carlson JR. Olfaction: mosquito receptor for human-sweat odorant. Nature. 2004;427(6971):212-3. doi: 10.1038/427212a. PubMed PMID: 14724626.

46. Zwiebel LJ, Takken W. Olfactory regulation of mosquito-host interactions. Insect Biochem Mol Biol. 2004;34(7):645-52. doi: 10.1016/j.ibmb.2004.03.017. PubMed PMID: 15242705; PubMed Central PMCID: PMCPMC3100215.

47. Forbes WM, Ashton FT, Boston R, Zhu X, Schad GA. Chemoattraction and chemorepulsion of *Strongyloides stercoralis* infective larvae on a sodium chloride gradient is mediated by amphidial neuron pairs ASE and ASH, respectively. Vet Parasitol. 2004;120(3):189-98. doi: 10.1016/j.vetpar.2004.01.005. PubMed PMID: 15041094.

48. Garner CE, Smith S, de Lacy Costello B, White P, Spencer R, Probert CS, et al. Volatile organic compounds from feces and their potential for diagnosis of gastrointestinal disease. FASEB J. 2007;21(8):1675-88. doi: 10.1096/fj.06-6927com. PubMed PMID: 17314143.

49. Verhulst NO, Beijleveld H, Knols BG, Takken W, Schraa G, Bouwmeester HJ, et al. Cultured skin microbiota attracts malaria mosquitoes. Malar J. 2009;8:302. doi:

10.1186/1475-2875-8-302. PubMed PMID: 20017925; PubMed Central PMCID: PMCPMC2804688.

50. Goetz N, Kaba G, Good D. Detection and identification of volatile compounds evolved from human hair and scalp using headspace. J Soc Cosmet Chem. 1988;39:1-13.

51. Meijerink J, Braks M, Brack A, Adam W, Dekker T, Posthumus M, et al. Identification of olfactory stimulants for *Anopheles gambiae* from human sweat samples. Journal of Chemical Ecology. 2000;26(6):1367-82.

52. Qiu YT, van Loon JJ, Takken W, Meijerink J, Smid HM. Olfactory Coding in Antennal Neurons of the Malaria Mosquito, *Anopheles gambiae*. Chem Senses. 2006;31(9):845-63. doi: 10.1093/chemse/bjl027. PubMed PMID: 16963500.

53. Nguyen KB, Smart GC. Location of the Phasmids on Infective Juveniles of *Steinernema glaseri*. J Nematol. 1993;25(4):625-7. PubMed PMID: 19279819; PubMed Central PMCID: PMCPMC2619410.

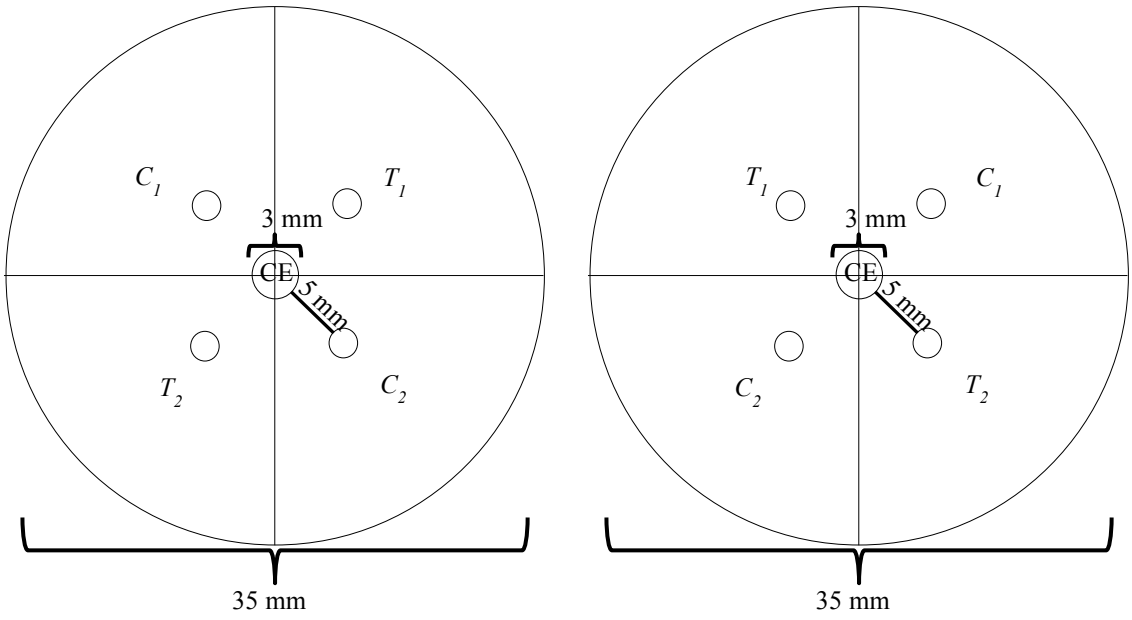

$$\text{CI} = \frac{[(\text{total \# of L3s at T1 and T2}) - (\text{total \# of L3s at C1 and C2})]}{[(\text{total \# of L3s at T1 and T2}) + (\text{total \# of L3s at C1 and C2})]}$$

Figure 1. *B. malayi* chemosensory behaviors are profiled using plate-based chemotaxis assays. Schematic of chemotaxis assay used. Infectious L3 *B. malayi* are placed in the center (CE) and allowed to distribute over the plate. After 30 minutes the number of parasites in T_1, T_2 (test compounds), C_1 and C_2 (control compounds) are counted and the chemotaxis index (C.I.) is calculated as indicated. Two plate arrangements were used to minimize any external or directional bias.

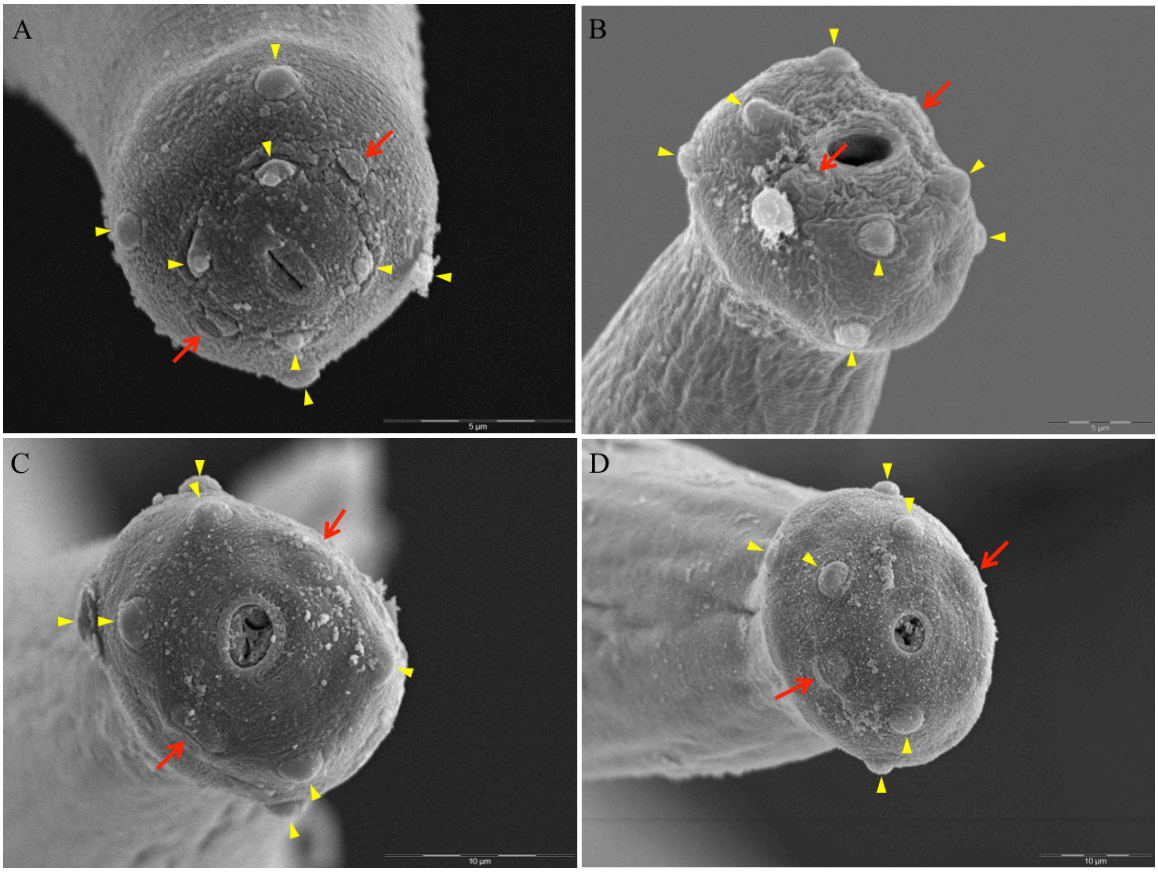

Figure 2. *B. malayi* parasites have conserved sensory ultrastructures across multiple life stages. Scanning electron images of the anterior portion of (A) L3, (B) L4, (C) adult male and (D) adult female *B. malayi* are shown. These data reveal that all life stages examined possess amphid pores (arrows) and cephalic papillae (arrow heads). Scale bars: 5 µm (A and B), 10 µm (C and D)

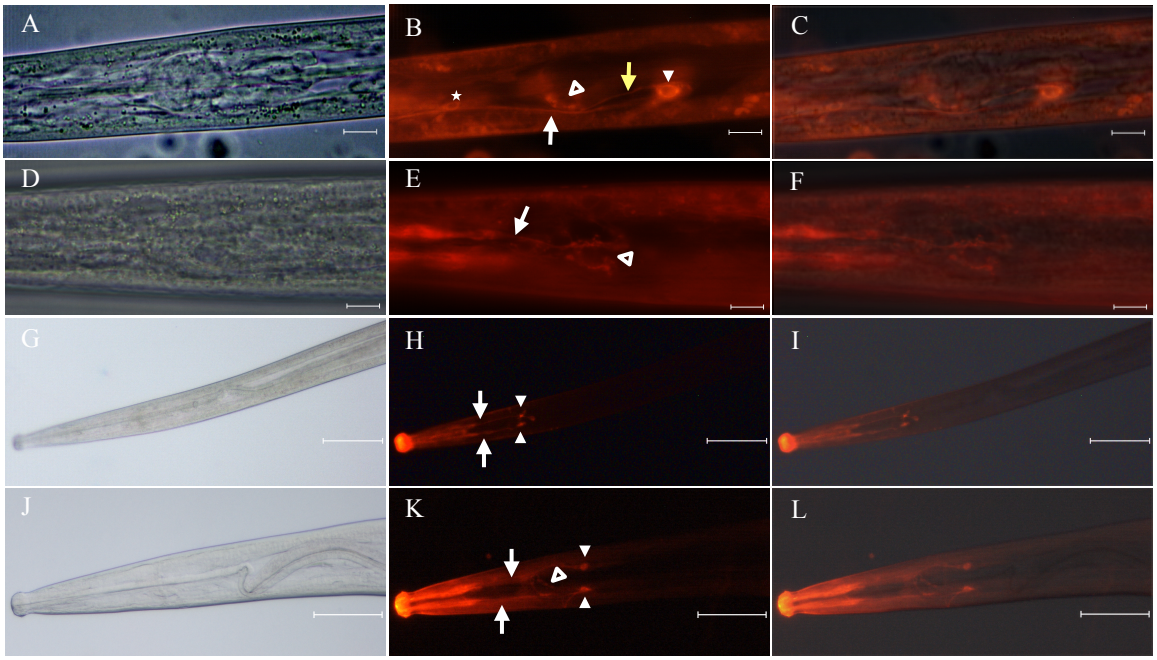

Figure 3. DiI staining reveals sensory neuroanatomy of *B. malayi*. Fluorescent images of anterior sensory structures in *B. malayi* using DiI stain show sheath cell bodies (*closed arrowheads*), nerve ring (*open arrowheads*), dendrites (*white arrows*), axons (*yellow arrow*) and socket cell bodies (*star*). Images are from L3 (A-C), L4 (D-F), adult male (G-I) and adult female (J-L) *B. malayi*. A-F show lateral views while G-L show dorsal-ventral views. Total magnification: 900x (A-F) and 150x (G-L). Scale bars: 10 µm (A-F) and 100 µm (G-L)

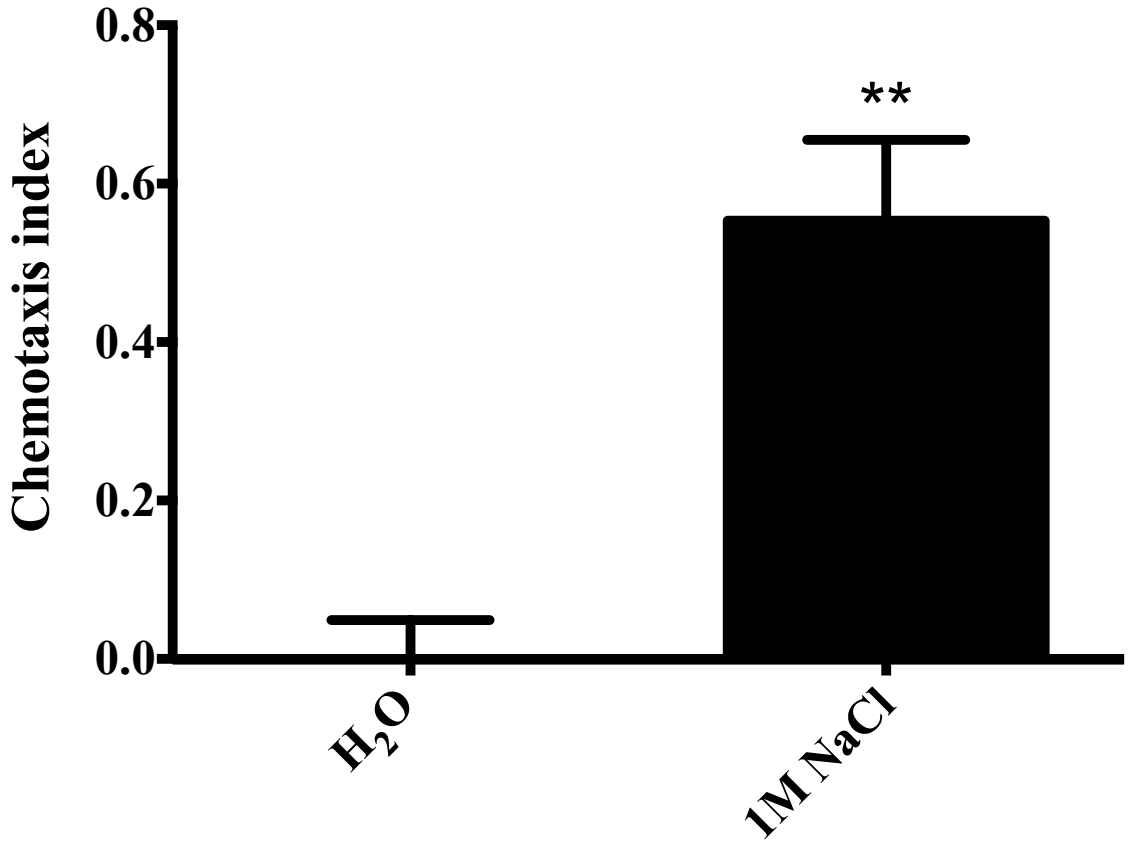

Figure 4. *B. malayi* is strongly attracted to sodium chloride. *B. malayi* L3 stage parasites are attracted to 1M sodium chloride (NaCl) when interrogated using chemotaxis assay plates. Statistical analysis: unpaired two-tailed t-test. **, p-value < 0.01 relative to control (H_2O). N = 3.

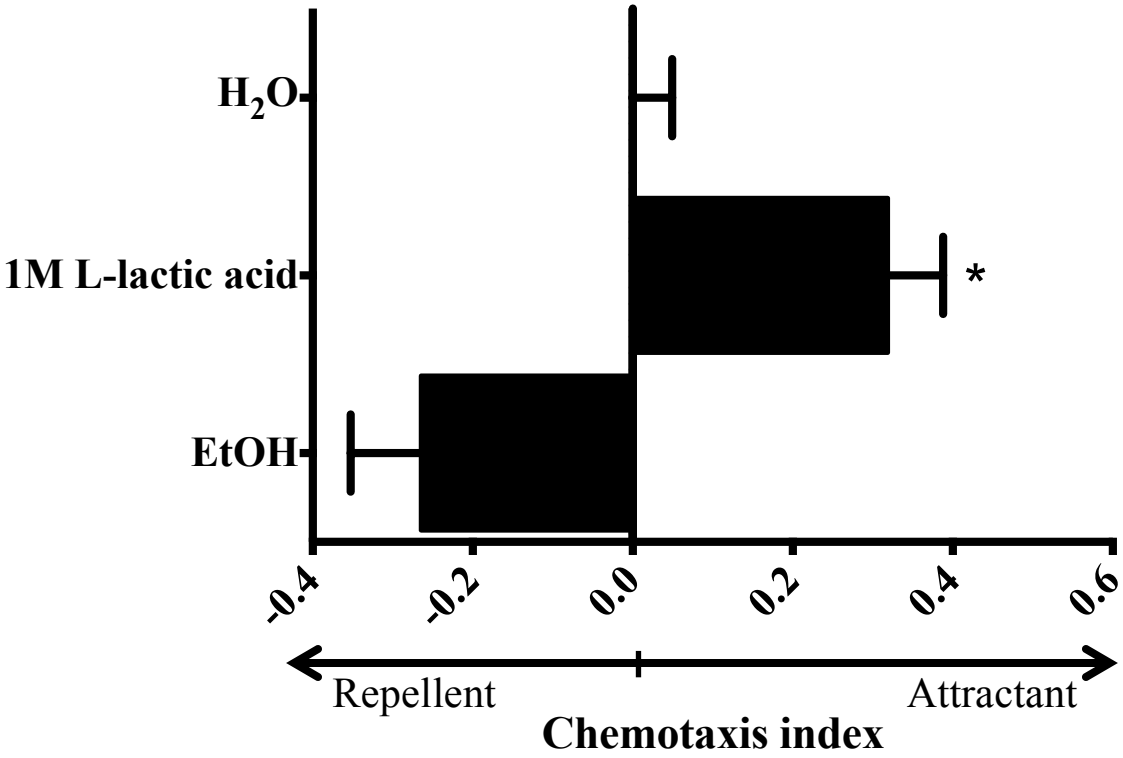

Figure 5. *B. malayi* is attracted to L-lactic acid. *B. malayi* L3s are attracted 1M L-lactic acid but are not significantly repelled by ethanol (EtOH). Arrows indicate responses that are either attractive or repellent. Statistical analysis: unpaired two-tailed t-test. *, p-value < 0.05 when compared to control (H_2O). N = 3.

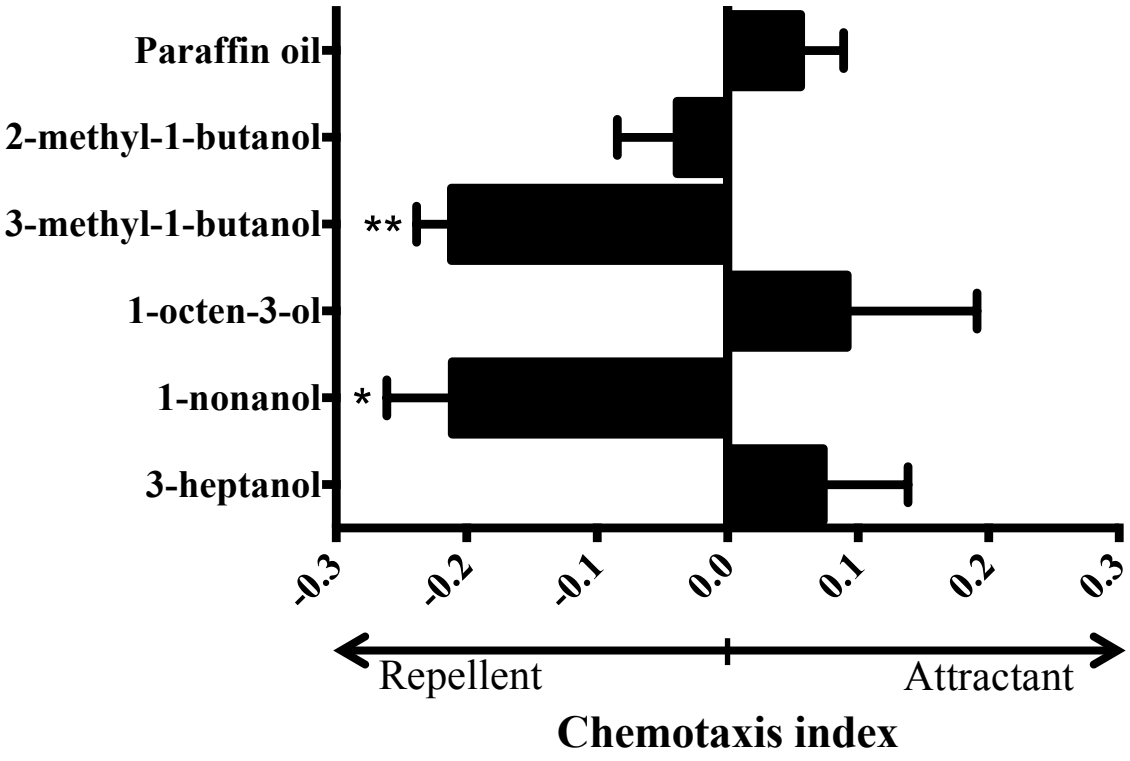

Figure 6. *B. malayi* is repelled by odorants present on human skin. L3 stage *B. malayi* are repelled or are neutral to a number of compounds found in human skin and sweat. Statistical analysis: unpaired two-tailed t-test. **, P-value < 0.01*, P-value < 0.05 relative to control (paraffin oil). N = 3.

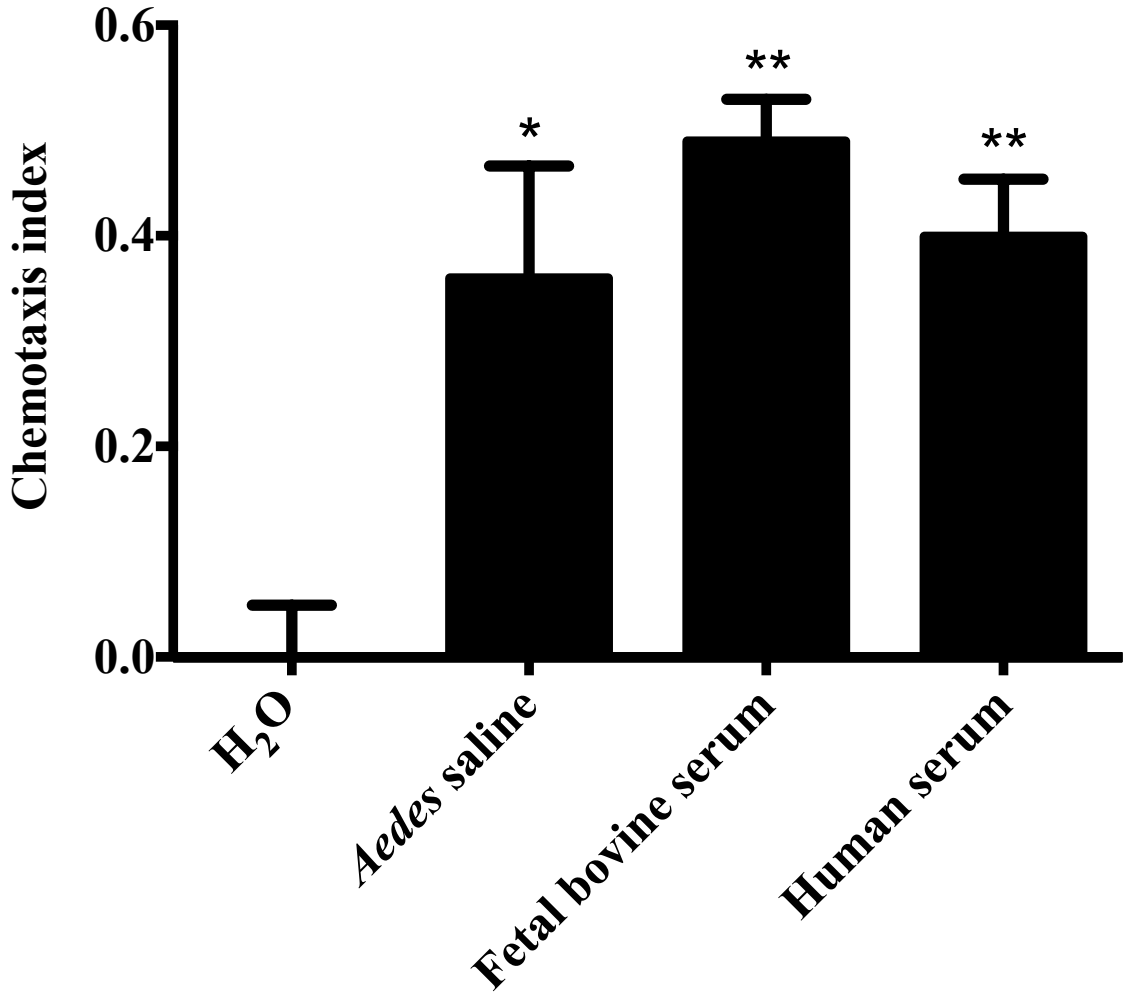

Figure 7. *B. malayi* is attracted to host-derived compounds. Complex compounds found within host such as serum are attractive to *B. malayi* L3s. However, no significant difference is found in *B. malayi* attraction to specific compounds indicating that these compounds do not dictate host specificity. *Aedes* saline composition: 154 mM NaCl, 1.36 mM $CaCl_2$, 2.68 mM KCl, 1.19 mM $NaHCO_3$ [3, 22, 29, 30, 44, 53]. Statistical analysis: unpaired two-tailed t-test. **, P-value < 0.01 *, P-value < 0.05 relative to the control (H_2O). N = 3

CHAPTER 3

MOLECULAR PHYLOGENETICS OF HETEROTRIMERIC G-PROTEINS REVEAL A NOVEL γ SUBUNIT IN PHYLUM NEMATODA

Lisa M. Fraser[1,2], Nicolas J. Wheeler[1], Lyric C. Bartholomay[2*] and Michael J. Kimber[1]

[1]Department of Biomedical Sciences, Iowa State University, Ames, Iowa, United States of America, [2]Department of Entomology, Iowa State University, Ames, Iowa, United States of America, [*]Current Address: Department of Pathobiological Sciences, University of Wisconsin-Madison, Madison, Wisconsin, United States of America

Abstract

Background

Heterotrimeric G-proteins, which are composed of α, β and γ subunits, play an integral role in G-protein signaling, which is involved in a number of essential behaviors in nematodes, including chemosensation. Previous research identified 22 heterotrimeric G-protein α subunits (GPAs), 2 heterotrimeric G-protein β subunits (GPBs) and 2 heterotrimeric G-protein γ subunits (GPCs) in the *C. elegans* genome. Of the GPAs identified, most have no clear homologs outside of phylum Nematoda and, therefore, are considered to be "nematode-specific". In contrast, GPBs in nematodes are highly conserved, even with organisms at great evolutionary distances, such as humans, while GPCs are very divergent, having no clear human homologs.

Results

Using the most comprehensive dataset available, we identified more than 1000 *C. elegans* GPA homologs and over 100 GPB and GPC homologs in various nematodes representing four clades (I, III, IV, and V) and two classes (Chromadorea and Enoplea). We show that nematode-specific heterotrimeric G-protein α subunits (GPAs) have expanded in class Chromadorea but not in class Enoplea. In addition, we determined that parasitic nematodes, such as *Brugia malayi*, possess far fewer nematode-specific GPAs than free-living nematodes. Further, heterotrimeric G-protein β subunits (GPBs) were found to be remarkably conserved within phylum Nematoda and fell within expected divisions (GPB-1 and GPB-2). Finally, we identified a novel heterotrimeric G-protein γ subunit (GPC-3) throughout the phylum, which was notably absent in *Caenorhabditis* spp.

Conclusion

G-protein signaling is involved in mediating numerous essential functions in nematodes, including chemosensation. Heterotrimeric G-proteins play a central role in these signal transduction pathways. Bioinformatic and phylogenetic analysis reveals nematodes have a diverse repertoire of heterotrimeric G-proteins. This work provides a basis for understanding basic nematode biology as well as highlights a potential set of targets that may be exploited for control of animal and plant parasitic nematodes.

Background

G-protein signaling pathways are a major mechanism used by eukaryotes to process extracellular signals and to translate those signals into cellular and subcellular

actions. Heterotrimeric G-proteins, which are composed of α, β and γ subunits, are the defining components of G-protein signaling. These proteins act as molecular switches that transduce signals from membrane bound G protein-coupled receptors (GPCRs) to a variety of intracellular effectors [1, 2]. In the inactive state, the G-protein α subunit (GPA) is bound to GDP (Gα-GDP) which promotes association between Gα-GDP, the Gβγ dimer and the cytoplasmic portions of GPCRs [3-5]. Once activated, GDP is released, which frees the α subunit to bind GTP (Gα-GTP); this event induces a conformational change in three flexible switch regions leading to the dissociation of Gα-GTP from the Gβγ dimer [4, 6]. Dissociated Gα-GTP and the Gβγ dimer can then each relay signals to activate a variety of downstream effectors [1, 4]. Termination of signaling occurs via hydrolysis of GTP by intrinsic GTPase activity of the GPA, which then can return to its inactive state, associated with Gβγ and the GPCR [1, 4, 7].

Heterotrimeric G-proteins are highly conserved even between evolutionarily distant organisms, from protists to mammals [8-11]. In humans, heterotrimeric G-protein α subunits (GPAs) are divided into four classes ($G\alpha_s$, $G\alpha_{i/o}$, $G\alpha_q$ and $G\alpha_{12}$) based on the intracellular signaling pathways they activate [9-12]. Interrogation of the genome sequence of the nematode *Caenorhabditis elegans* revealed the presence of 22 GPAs, while phylogenetic analysis identified at least one homologue for each of the four classes found in humans (GSA-1, $G\alpha_s$; GOA-1, $G\alpha_{i/o}$; EGL-30, $G\alpha_q$ and GPA-4, 12 & 16, $G\alpha_{12}$) suggesting general conservation of these four classes [8, 13, 14]. The remaining 16 GPAs (GPA 1-3, 5-11, 13-15, 17-18 and ODR-3) comprise a divergent class that is specific to nematodes [8, 13, 15]. Further investigation of these "nematode-specific" GPA genes revealed that 14 (*gpa* 1-3, 5-6, 8-11, 13-15 and *odr*-3) are expressed exclusively in

sensory neurons, suggesting that nematode-specific GPAs have a role in sensory behaviors such as chemosensation [8, 13, 16]. The *C. elegans* genome also encodes two G-protein β subunits (GPBs) [17, 18]. Both GPBs are expressed in most neurons but their functions appear to be very different. GPB-1 is essential for *C. elegans* development and taste adaptation, while GPB-2 functions in behaviors such as pharyngeal pumping and egg-laying [18-20]. Only two G-protein γ subunits (GPCs) have been identified in *C. elegans*, neither of which has a clear human homolog [20, 21]. *Gpc-1* expression is restricted to sensory neurons implying a function in chemosensation, while *gpc-2* is expressed in all neurons and muscles [20]. GPC-1 plays a role in plasticity to nematode responses to both salt and Cu^{2+} ions, illustrating its function in chemosensation [20, 22].

Much of what is known about heterotrimeric G-protein function in nematodes is restricted to research conducted in *C. elegans*. Studies in parasitic nematodes are incredibly limited and often restricted either to G-proteins that are broadly conserved such as homologs of the $G\alpha_s$, $G\alpha_{i/o}$, $G\alpha_q$ and $G\alpha_{12}$ subfamilies or to the identification of nematode-specific GPAs in specific species such as *Acanthocheilonema viteae* and *Strongyloides stercoralis* [8, 23, 24]. In order to better understand the heterotrimeric G-protein complement in nematodes, we conducted a pan-phylum search for these important signaling molecules in phylum Nematoda. Using a dataset that included over 70 nematode genomes representing four clades (I, III, IV and V) and both classes (Chromadorea and Enoplea), we show that several GPAs are broadly conserved throughout Nematoda. Further, we found that GPBs are remarkably conserved throughout phylum Nematoda. In addition, we determined that GPC-1 and GPC-2 were generally conserved throughout Nematoda. Finally, we identified a novel G-protein γ subunit

(GPC-3) that is present throughout Nematoda but notably absent in *Caenorhabditis* species. Increasing our understanding of these essential genes will not only provide insight into the biology of nematodes but may also identify novel targets that can be exploited for the development of new strategies of control for parasitic nematodes.

Materials and Methods

BLAST analysis

We downloaded the most recent versions of genomes and predicted proteins for more than 70 nematode species from Wormbase and Wormbase-Parasite [25] (Table 1). The representative nematode genomes were drawn from four clades (I, III, IV, and V) and two classes (Chromadorea and Enoplea). This overall dataset included free-living, plant and animal parasitic nematodes. Using *C. elegans* heterotrimeric G-protein amino acid sequences as our query sequences (Table 2) and predicted proteins from each nematode species as our subject sequence, we employed Basic Local Alignment Search Tool (blastp) to identify the top hits in each species. The resulting candidate heterotrimeric G-protein amino acid sequences were aligned using the MUSCLE multiple sequence alignment program [26] and manually curated to improve reliability of downstream analysis (Table 2). Manual curation included the removal of duplicate or severely truncated sequences and removal of any regions of poorly aligned sequence. The resulting alignment was used to generate probabilistic hidden Markov models (profile HMMs) using HMMER-3.1b2 [26, 27].

Post BLAST analysis

Using the multiple sequence alignments generated earlier, we employed HMMER-3.1b2 to build profile HMMs that were used as query sequences to identify homologous sequences in each of the genomes analyzed. Profile HMMs are probabilistic models that can be used to query sequence databases to identify homologous sequences [27]. This method is advantageous over BLAST analysis because of the underlying strength of its probabilistic inference methods, which facilitate the detection of remote homologs [27-29]. Profile HMMs were used as queries to identify homologous sequences in each nematode species using HMMsearch. Results were ranked according to e-value with our primary cutoff value set at the point where subsequent hits showed significant homology to other known proteins (Table 2). We identified this cutoff with a blastp search of all hits against the NCBI non-redundant (nr) database. The resulting datasets were used to generate multiple sequence alignments that would then be used for the generation of phylogenetic trees.

Phylogenetic analysis

GPA, GPB and GPC multiple sequence alignments were generated using the MUSCLE multiple sequence alignment program [26]. Resulting alignments were manually curated to remove any duplicates and false positives in order to improve reliability of the subsequent phylogenetic trees that were generated (Table 2). G-Blocks was then used to remove any poorly aligned or especially divergent regions of the multiple sequence alignments [30, 31]. Using the trimmed alignments, phylogenetic trees were constructed by maximum likelihood employing Randomized Axelerated Maximum

Likelihood (RAxML) using the general time-reversible (GTR) substitution matrix and visualized and edited with FigTree (http://tree.bio.ed.ac.uk/software/figtree/) [32, 33]. Phylogenetic trees shown here are the best-scoring maximum likelihood trees based on 100 bootstrap replicates.

Relative Semi-quantitative multiplex RT-PCR

Microfilariae (mf), L3, L4 adult male (AM) and adult female (AF) *B. malayi* were provided by the University of Georgia NIH/NIAID Filariasis Research Reagent Resource Center (FR3). Total RNA was extracted from mf, L3, L4, AM and AF *B. malayi* using RNAqueous Total RNA Isolation Kit (Thermo Fisher Scientific, Waltham, MA, USA) and quantified using a NanoDrop 2000 (Thermo Fisher Scientific, Waltham, MA, USA) prior to use. The resulting RNA served as a template for relative semi-quantitative multiplex RT-PCR using the SuperScript III one-step RT-PCR system with Platinum Taq DNA polymerase (Thermo Fisher Scientific, Waltham, MA, USA). The principle behind this reaction is to PCR amplify a target gene and compare its intensity to a multiplexed internal control during the linear phase of the reaction. The QuantumRNA Universal 18S internal standard (Thermo Fisher Scientific, Waltham, MA, USA) was used as the internal control. The oligonucleotide primers used for each gene are shown in Table 3. PCR reactions (50 µL) were carried out for each gene using the PCR conditions: cDNA synthesis at 50°C for 30 minutes, initial denaturation at 94°C for five minutes, 28 (*gpc-1* & *gpc-3*) or 29 (*gpc-2*) cycles of 94°C for 30 seconds, 55°C for 30 seconds, 72°C for 30 seconds followed by a final extension phase of 72°C for 5 minutes. Reactions were visualized on a 2% agarose gel containing ethidium bromide.

Results and Discussion

The advent of the 50 Helminth Genomes Initiative (Helminth Genomes Consortium, unpublished) and the Wormbase-Parasite project [25] has allowed access to an unprecedented number of nematode genomes for analysis. In this study, we used a blastp approach interfaced with hidden Markov models to identify putative homologs to *C. elegans* GPAs, GPBs and GPCs. Using this approach we identified over 1000 G-protein α subunit homologs, 144 G-protein β subunit homologs and 151 G-protein γ subunit homologs in more than 70 nematode species, representing four clades (I, III, IV and V) and both classes (Chromadorea and Enoplea). We believe these results represent the most comprehensive analysis of heterotrimeric G-proteins in nematodes to date.

G-protein α-subunits

Previously, 22 GPAs were identified in *C. elegans*, of which 16 (GPA 1-3, 5-11, 13-15, 17-18 and ODR-3) are considered nematode-specific [8, 13]. Since then, the vast majority of GPA sequence and functional analysis has been based in *Caenorhabditis* species, with only a very limited number of nematode-specific GPAs identified from 12 species of parasitic nematodes, none of which have been functionally characterized [8]. These studies which were primarily limited to *Caenorhabditis* began to reveal a lineage expansion of nematode-specific GPAs in phylum Nematoda [8]. Further analysis using ESTs from 12 nematode species spanning four clades revealed the presence of nematode-specific GPAs in all of these species suggesting that the evolution of nematode-specific GPAs occurred before the origin and divergence of Nematoda [8]. Using a greatly

expanded dataset than was previously available, we confirmed the lineage expansion of nematode-specific GPAs. Notably, nematode-specific GPA expansion appears to be predominantly restricted to class Chromadorea with the exception of a single nematode-specific GPA (GPA-7) evident in nematodes of class Enoplea, such as the swine parasite *Trichinella spiralis* (Table 4). This contrasting complexity between nematode classes is of particular interest because nematode-specific GPAs are thought to play an integral role in sensory behavior and the absence of these proteins in Enoplea leads to the question of what underlying mechanisms dictate sensory behavior in Enoplean nematodes. GPA-7, the one nematode-specific gene identified in Enopleans, is unique among the nematode-specific genes in that it is widely expressed in neuron and muscle cells instead of being restricted to sensory neurons in *C. elegans* [13]. Data presented here provide strong evidence that the majority of the nematode-specific GPA lineage expansion occurred following divergence of class Enoplea and Chromadorea, with the caveat that the database searched at this point was limited to seven Enoplean species (Table 4).

The data presented here also indicate that there are far fewer nematode-specific GPAs in parasitic nematodes when compared to free-living nematodes such as *C. elegans* (Table 4). This is especially evident in the clade III nematodes, which is composed exclusively of parasitic nematodes of animals (Table 4). Clade III nematodes spend their entire motile live within a host and thus only need to respond to a very specific set of host cues. In contrast, clade V nematodes such as *C. elegans* all have a free-living stage so must be able to distinguish between countless chemical cues present in the environment. The majority of nematode-specific GPAs are thought to function in sensory perception and have demonstrable functions in chemosensory behavior in *C. elegans* [13].

Chemosensation is the response to environmental compounds and is important in a variety of nematode behaviors such as finding food, mates and avoiding noxious conditions [34-36]. These behaviors are dictated by the nematode's life style so it would be reasonable to speculate that the underlying mechanisms that control these behaviors would also vary depending on the life strategy of the nematode.

To avoid any selection bias and identify highly divergent heterotrimeric G-proteins, we employed hidden Markov models (HMMER-3.1b2), an approach that builds probabilistic models called profile HMMs that can be used to identify homologous sequences throughout the phylum. Unlike BLAST, which provides one best-scoring alignment, the hidden Markov Model algorithm takes into account a sum of probabilities across the entire alignment which allows for the identification of more divergent homologs than would be found using BLAST. In addition to the more powerful HMM algorithm, we also built our profile HMMs using putative heterotrimeric G-protein homologs from the entire phylum in order minimize any bias that could arise as a result of using *C. elegans* heterotrimeric G-proteins as seed sequences.

G-protein β subunits

C. elegans have two G-protein β subunits, both of which show remarkable conservation with other GPBs even at great evolutionary distances (for example, percent shared identity with human homologs; GPB-1: 86% and GPB-2: 64%) [17, 18]. Nematode GPBs are incredibly conserved, with a high degree of similarity at the amino acid level, across the entire phylum (Table 5). Phylogenetic analysis further confirmed a high degree of GPB conservation within phylum Nematoda (Figure 1). GPB-1 is

important for olfactory adaption in *C. elegans* [21], however it remains to be seen if GPB-1 has a functional role in chemosensory behavior of parasitic nematodes. The high level of GPB-1 amino acid similarity (greater than 90% shared identity across Nematoda) found here may translate to like function and phenotype in all nematodes, but thorough pharmacological, genetic and/or reverse genetics studies would be necessary to fully elucidate the function of this β subunit in other members of the phylum.

GPB-2 is orthologous to a divergent vertebrate β subunit, GPB-5, which interacts with regulators of G-protein signaling (RGS) proteins in mammals [37]. RGS proteins negatively regulate G-protein signaling by accelerating the GTPase activity of α subunit thereby promoting inactivation of the GPA [37, 38]. In *C. elegans*, GPB-2 also appears to interact with RGS proteins, which is in contrast to GPB-1, which directly interacts with α subunits [37]. This demonstrates the remarkable functional conservation of these proteins. Like GPB-1, GPB-2 appears to be ubiquitous within phylum Nematoda (Table 5). Furthermore, GPB-2 amino acid similarity is very high (greater than 70% shared identity) within the phylum indicating that functional similarity may exist with this protein throughout Nematoda.

G-protein γ-subunits

Only two G-protein γ subunits (GPC-1 and GPC-2) have been identified in *C. elegans*, neither of which have any clear human homologs [13, 20]. The expression patterns of *gpc-1* and *gpc-2* are highly dissimilar [20]. *Gpc-1* is restricted to the sensory neurons in *C. elegans*, pointing to a specific role in sensory perception in this nematode

while *gpc-2* is ubiquitously expressed [20]. Additionally, GPC-1 is important for sensory adaptation to water-soluble compounds such as sodium chloride [20].

Bioinformatic analysis has shown that *gpc-1* and *gpc-2* can be found throughout phylum Nematoda (Table 6). Interestingly, we also identified a novel γ subunit (GPC-3) that was present throughout Nematoda but noticeably absent in *Caenorhabditis* species (Table 6). Like GPC-1 and GPC-2, GPC-3 is a short protein (~75 amino acids) with a gene structure that includes only 2 exons separated by a single intron demonstrating structural conservation of the genes that encode these proteins. Phylogenetic analysis confirmed that GPC-3 is unique but closely related to GPC-1 and GPC-2 (Figure 2). Using relative semi-quantitative RT PCR, we found that all three *gpc* genes are expressed throughout multiple life stages in *B. malayi* (Figure 3). Relative expression of *gpc-1* and *gpc-2* was comparable while relative expression of *gpc-3* was higher when compared to the 18S internal standard (Figure 3).

Of note, GPC-3 is absent in *Caenorhabditis species* (Table 6). That GPC-3 was found in all other nematodes analyzed indicates that this gene was lost prior to or during the divergence of *Caenorhabditis*. The absence of GPC-3 in *Caenorhabditis* highlights the limitation of regarding one genome as representative of an entire phylum and underscores the need to sequence additional nematode species in order to have a more accurate representation of this diverse phylum.

When we examined *Ascaris suum* transcriptomic datasets, we found *gpc*-3 transcript expression was highest in the pharyngeal region of the parasite, so it is possible that *gpc*-3, like *gpc*-1, is expressed at least in part in amphid sensory neurons [39]. Why

other nematodes would need to employ an additional γ subunit in the sensory neurons needs further study. However, it may be that GPC-3 represents a more ancestral chemosensory complement and its loss in *Caenorhabditis* came about as a result of an expansion in nematode-specific sensory GPAs in these nematodes. Other nematodes possess fewer GPAs, and thus GPC-3 may still have a functional role.

Conclusions

Heterotrimeric G-proteins are intimately involved in a number of essential functions in nematodes, including modulating the capacity to perceive and respond to sensory cues from the environment. Our bioinformatic and phylogenetic analysis that incorporated sequence data from more than 70 nematode species is the most comprehensive analysis of heterotrimeric G-proteins in nematodes to date. We have demonstrated that although GPAs, GPBs and GPCs are broadly conserved throughout Nematoda, there are some important differences. Notably, the nematode-specific GPA lineage expansion appears to primarily be a Chromadorean phenomenon. In addition, we found far fewer GPAs in parasitic nematodes and identified a novel GPC that is noticeably absent in *Caenorhabditis*. Characterization of these proteins not only provides insight into essential nematode behavior but may also provide novel targets that can be manipulated for use in control of parasitic nematodes of both plants and animals.

Author Contributions

Conceived and designed the experiments: LMF, NJW, LCB, MJK. Performed the experiments: LMF. Analyzed the data: LMF, NJW, LCB, MJK. Wrote the paper: LMF, NJW, LCB, MJK.

Acknowledgements

The authors would like to thank Dr. Mostafa Zamanian and Dr. John VanDyk for helpful discussions and technical guidance relating to bioinformatic analysis. The authors would also like to acknowledge parasite materials provided by Dr. Andrew Moorhead, Erica Burkman, Molly Riggs and the NIH-NIAID Filariasis Research Reagent Resource Center (FR3).

References

1. Oldham WM, Hamm HE: **Heterotrimeric G protein activation by G-protein-coupled receptors**. *Nat Rev Mol Cell Biol* 2008, **9**(1):60-71.

2. Gilman AG: **G proteins: transducers of receptor-generated signals**. *Annu Rev Biochem* 1987, **56**:615-649.

3. Johnston CA, Siderovski DP: **Receptor-mediated activation of heterotrimeric G-proteins: current structural insights**. *Mol Pharmacol* 2007, **72**(2):219-230.

4. Wall MA, Posner BA, Sprang SR: **Structural basis of activity and subunit recognition in G protein heterotrimers**. *Structure* 1998, **6**(9):1169-1183.

5. Bastiani C, Mendel J: **Heterotrimeric G proteins in *C. elegans***. *WormBook* 2006:1-25.

6. Hamm HE: **The many faces of G protein signaling**. *J Biol Chem* 1998, **273**(2):669-672.

7. McCudden CR, Hains MD, Kimple RJ, Siderovski DP, Willard FS: **G-protein signaling: back to the future**. *Cell Mol Life Sci* 2005, **62**(5):551-577.

8. O'Halloran DM, Fitzpatrick DA, McCormack GP, McInerney JO, Burnell AM: **The molecular phylogeny of a nematode-specific clade of heterotrimeric G-protein alpha-subunit genes**. *J Mol Evol* 2006, **63**(1):87-94.

9. Simon MI, Strathmann MP, Gautam N: **Diversity of G proteins in signal transduction**. *Science* 1991, **252**(5007):802-808.

10. Strathmann M, Simon MI: **G protein diversity: a distinct class of alpha subunits is present in vertebrates and invertebrates**. *Proc Natl Acad Sci U S A* 1990, **87**(23):9113-9117.

11. Strathmann MP, Simon MI: **G alpha 12 and G alpha 13 subunits define a fourth class of G protein alpha subunits**. *Proc Natl Acad Sci U S A* 1991, **88**(13):5582-5586.

12. Wettschureck N, Offermanns S: **Mammalian G proteins and their cell type specific functions**. *Physiol Rev* 2005, **85**(4):1159-1204.

13. Jansen G, Thijssen KL, Werner P, van der Horst M, Hazendonk E, Plasterk RH: **The complete family of genes encoding G proteins of *Caenorhabditis elegans***. *Nat Genet* 1999, **21**(4):414-419.

14. Consortium CeS: **Genome sequence of the nematode *C. elegans*: a platform for investigating biology**. *Science* 1998, **282**(5396):2012-2018.

15. Hart AC, Chao MY: **From odors to behaviors in *Caenorhabditis elegans***. In: *The neurobiology of olfaction.* Edited by Menini A. Boca Raton, FL: CRC Press; 2010: 1-33.

16. Cuppen E, van der Linden AM, Jansen G, Plasterk RH: **Proteins interacting with Caenorhabditis elegans Galpha subunits**. *Comp Funct Genomics* 2003, **4**(5):479-491.

17. van der Voorn L, Gebbink M, Plasterk RH, Ploegh HL: **Characterization of a G-protein beta-subunit gene from the nematode *Caenorhabditis elegans***. *J Mol Biol* 1990, **213**(1):17-26.

18. van der Linden AM, Simmer F, Cuppen E, Plasterk RH: **The G-protein beta-subunit GPB-2 in *Caenorhabditis elegans* regulates the G(o)alpha-G(q)alpha signaling network through interactions with the regulator of G-protein signaling proteins EGL-10 and EAT-16**. *Genetics* 2001, **158**(1):221-235.

19. Zwaal RR, Ahringer J, van Luenen HG, Rushforth A, Anderson P, Plasterk RH: **G proteins are required for spatial orientation of early cell cleavages in *C. elegans* embryos**. *Cell* 1996, **86**(4):619-629.

20. Jansen G, Weinkove D, Plasterk RH: **The G-protein gamma subunit gpc-1 of the nematode *C.elegans* is involved in taste adaptation**. *EMBO J* 2002, **21**(5):986-994.

21. Yamada K, Hirotsu T, Matsuki M, Kunitomo H, Iino Y: **GPC-1, a G protein gamma-subunit, regulates olfactory adaptation in *Caenorhabditis elegans***. *Genetics* 2009, **181**(4):1347-1357.

22. Hilliard MA, Apicella AJ, Kerr R, Suzuki H, Bazzicalupo P, Schafer WR: **In vivo imaging of *C. elegans* ASH neurons: cellular response and adaptation to chemical repellents**. *EMBO J* 2005, **24**(1):63-72.

23. Grant KR, Harnett MM, Milligan G, Harnett W: **Characterization of heterotrimeric G-proteins in adult *Acanthocheilonema viteae***. *Biochem J* 1996, **320 (Pt 2)**:459-466.

24. Massey HC, Ball CC, Lok JB: **PCR amplification of putative gpa-2 and gpa-3 orthologs from the (A+T)-rich genome of *Strongyloides stercoralis***. *Int J Parasitol* 2001, **31**(4):377-383.

25. Howe KL, Bolt BJ, Cain S, Chan J, Chen WJ, Davis P, Done J, Down T, Gao S, Grove C *et al*: **WormBase 2016: expanding to enable helminth genomic research**. *Nucleic Acids Res* 2016, **44**(D1):D774-780.

26. Edgar RC: **MUSCLE: multiple sequence alignment with high accuracy and high throughput**. *Nucleic Acids Res* 2004, **32**(5):1792-1797.

27. Eddy SR: **Profile hidden Markov models**. *Bioinformatics* 1998, **14**(9):755-763.

28. Eddy SR: **Accelerated Profile HMM Searches**. *PLoS Comput Biol* 2011, **7**(10):e1002195.

29. Eddy SR: **A new generation of homology search tools based on probabilistic inference**. *Genome Inform* 2009, **23**(1):205-211.

30. Talavera G, Castresana J: **Improvement of phylogenies after removing divergent and ambiguously aligned blocks from protein sequence alignments**. *Syst Biol* 2007, **56**(4):564-577.

31. Castresana J: **Selection of conserved blocks from multiple alignments for their use in phylogenetic analysis**. *Mol Biol Evol* 2000, **17**(4):540-552.

32. Stamatakis A: **RAxML version 8: a tool for phylogenetic analysis and post-analysis of large phylogenies**. *Bioinformatics* 2014, **30**(9):1312-1313.

33. Huelsenbeck JP, Joyce P, Lakner C, Ronquist F: **Bayesian analysis of amino acid substitution models**. *Philos Trans R Soc Lond B Biol Sci* 2008, **363**(1512):3941-3953.

34. Bargmann CI: **Chemosensation in *C. elegans***. *WormBook* 2006:1-29.

35. Castelletto ML, Gang SS, Okubo RP, Tselikova AA, Nolan TJ, Platzer EG, Lok JB, Hallem EA: **Diverse host-seeking behaviors of skin-penetrating nematodes**. *PLoS Pathog* 2014, **10**(8):e1004305.

36. Wang D, Jones LM, Urwin PE, Atkinson HJ: **A synthetic peptide shows retro- and anterograde neuronal transport before disrupting the chemosensation of plant-pathogenic nematodes**. *PLoS One* 2011, **6**(3):e17475.

37. Masuho I, Wakasugi-Masuho H, Posokhova EN, Patton JR, Martemyanov KA: **Type 5 G protein beta subunit (Gbeta5) controls the interaction of regulator of G protein signaling 9 (RGS9) with membrane anchors**. *J Biol Chem* 2011, **286**(24):21806-21813.

38. Watson N, Linder ME, Druey KM, Kehrl JH, Blumer KJ: **RGS family members: GTPase-activating proteins for heterotrimeric G-protein alpha-subunits**. *Nature* 1996, **383**(6596):172-175.

39. Rosa BA, Jasmer DP, Mitreva M: **Genome-wide tissue-specific gene expression, co-expression and regulation of co-expressed genes in adult nematode *Ascaris suum***. *PLoS Negl Trop Dis* 2014, **8**(2):e2678.

40. Schiffer PH, Kroiher M, Kraus C, Koutsovoulos GD, Kumar S, Camps JI, Nsah NA, Stappert D, Morris K, Heger P *et al*: **The genome of *Romanomermis***

***culicivorax*: revealing fundamental changes in the core developmental genetic toolkit in Nematoda**. *BMC Genomics* 2013, **14**:923.

41. Mitreva M, Jasmer DP, Zarlenga DS, Wang Z, Abubucker S, Martin J, Taylor CM, Yin Y, Fulton L, Minx P *et al*: **The draft genome of the parasitic nematode *Trichinella spiralis***. *Nat Genet* 2011, **43**(3):228-235.

42. Foth BJ, Tsai IJ, Reid AJ, Bancroft AJ, Nichol S, Tracey A, Holroyd N, Cotton JA, Stanley EJ, Zarowiecki M *et al*: **Whipworm genome and dual-species transcriptome analyses provide molecular insights into an intimate host-parasite interaction**. *Nat Genet* 2014, **46**(7):693-700.

43. Jex AR, Nejsum P, Schwarz EM, Hu L, Young ND, Hall RS, Korhonen PK, Liao S, Thamsborg S, Xia J *et al*: **Genome and transcriptome of the porcine whipworm *Trichuris suis***. *Nat Genet* 2014, **46**(7):701-706.

44. Wang J, Mitreva M, Berriman M, Thorne A, Magrini V, Koutsovoulos G, Kumar S, Blaxter ML, Davis RE: **Silencing of germline-expressed genes by DNA elimination in somatic cells**. *Dev Cell* 2012, **23**(5):1072-1080.

45. Jex AR, Liu S, Li B, Young ND, Hall RS, Li Y, Yang L, Zeng N, Xu X, Xiong Z *et al*: ***Ascaris suum* draft genome**. *Nature* 2011, **479**(7374):529-533.

46. Ghedin E, Wang S, Spiro D, Caler E, Zhao Q, Crabtree J, Allen JE, Delcher AL, Guiliano DB, Miranda-Saavedra D *et al*: **Draft genome of the filarial nematode parasite *Brugia malayi***. *Science* 2007, **317**(5845):1756-1760.

47. Godel C, Kumar S, Koutsovoulos G, Ludin P, Nilsson D, Comandatore F, Wrobel N, Thompson M, Schmid CD, Goto S *et al*: **The genome of the heartworm, *Dirofilaria immitis*, reveals drug and vaccine targets**. *FASEB J* 2012, **26**(11):4650-4661.

48. Tallon LJ, Liu X, Bennuru S, Chibucos MC, Godinez A, Ott S, Zhao X, Sadzewicz L, Fraser CM, Nutman TB *et al*: **Single molecule sequencing and genome assembly of a clinical specimen of *Loa loa*, the causative agent of loiasis**. *BMC Genomics* 2014, **15**:788.

49. Desjardins CA, Cerqueira GC, Goldberg JM, Dunning Hotopp JC, Haas BJ, Zucker J, Ribeiro JM, Saif S, Levin JZ, Fan L *et al*: **Genomics of *Loa loa*, a Wolbachia-free filarial parasite of humans**. *Nat Genet* 2013, **45**(5):495-500.

50. Kikuchi T, Cotton JA, Dalzell JJ, Hasegawa K, Kanzaki N, McVeigh P, Takanashi T, Tsai IJ, Assefa SA, Cock PJ *et al*: **Genomic insights into the origin of parasitism in the emerging plant pathogen *Bursaphelenchus xylophilus***. *PLoS Pathog* 2011, **7**(9):e1002219.

51. Srinivasan J, Dillman AR, Macchietto MG, Heikkinen L, Lakso M, Fracchia KM, Antoshechkin I, Mortazavi A, Wong G, Sternberg PW: **The draft genome and transcriptome of *Panagrellus redivivus* are shaped by the harsh demands of a free-living lifestyle**. *Genetics* 2013, **193**(4):1279-1295.

52. Hunt VL, Tsai IJ, Coghlan A, Reid AJ, Holroyd N, Foth BJ, Tracey A, Cotton JA, Stanley EJ, Beasley H *et al*: **The genomic basis of parasitism in the *Strongyloides* clade of nematodes**. *Nat Genet* 2016, **48**(3):299-307.

53. Dillman AR, Macchietto M, Porter CF, Rogers A, Williams B, Antoshechkin I, Lee MM, Goodwin Z, Lu X, Lewis EE *et al*: **Comparative genomics of *Steinernema* reveals deeply conserved gene regulatory networks**. *Genome Biol* 2015, **16**:200.

54. Cotton JA, Lilley CJ, Jones LM, Kikuchi T, Reid AJ, Thorpe P, Tsai IJ, Beasley H, Blok V, Cock PJ *et al*: **The genome and life-stage specific transcriptomes of *Globodera pallida* elucidate key aspects of plant parasitism by a cyst nematode**. *Genome Biol* 2014, **15**(3):R43.

55. Lunt DH, Kumar S, Koutsovoulos G, Blaxter ML: **The complex hybrid origins of the root knot nematodes revealed through comparative genomics**. *PeerJ* 2014, **2**:e356.

56. Opperman CH, Bird DM, Williamson VM, Rokhsar DS, Burke M, Cohn J, Cromer J, Diener S, Gajan J, Graham S *et al*: **Sequence and genetic map of *Meloidogyne hapla*: A compact nematode genome for plant parasitism**. *Proc Natl Acad Sci U S A* 2008, **105**(39):14802-14807.

57. Abad P, Gouzy J, Aury JM, Castagnone-Sereno P, Danchin EG, Deleury E, Perfus-Barbeoch L, Anthouard V, Artiguenave F, Blok VC *et al*: **Genome sequence of the metazoan plant-parasitic nematode *Meloidogyne incognita***. *Nat Biotechnol* 2008, **26**(8):909-915.

58. Schwarz EM, Hu Y, Antoshechkin I, Miller MM, Sternberg PW, Aroian RV: **The genome and transcriptome of the zoonotic hookworm *Ancylostoma***

ceylanicum **identify infection-specific gene families**. *Nat Genet* 2015, **47**(4):416-422.

59. Mortazavi A, Schwarz EM, Williams B, Schaeffer L, Antoshechkin I, Wold BJ, Sternberg PW: **Scaffolding a *Caenorhabditis* nematode genome with RNA-seq**. *Genome Res* 2010, **20**(12):1740-1747.

60. Stein LD, Bao Z, Blasiar D, Blumenthal T, Brent MR, Chen N, Chinwalla A, Clarke L, Clee C, Coghlan A *et al*: **The genome sequence of *Caenorhabditis briggsae*: a platform for comparative genomics**. *PLoS Biol* 2003, **1**(2):E45.

61. Huang RE, Ren X, Qiu Y, Zhao Z: **Description of *Caenorhabditis sinica* sp. n. (Nematoda: Rhabditidae), a nematode species used in comparative biology for *C. elegans***. *PLoS One* 2014, **9**(11):e110957.

62. Koutsovoulos G, Makepeace B, Tanya VN, Blaxter M: **Palaeosymbiosis revealed by genomic fossils of Wolbachia in a strongyloidean nematode**. *PLoS Genet* 2014, **10**(6):e1004397.

63. McNulty SN, Strübe C, Rosa BA, Martin JC, Tyagi R, Choi YJ, Wang Q, Hallsworth Pepin K, Zhang X, Ozersky P *et al*: ***Dictyocaulus viviparus*** **genome, variome and transcriptome elucidate lungworm biology and support future intervention**. *Sci Rep* 2016, **6**:20316.

64. Laing R, Kikuchi T, Martinelli A, Tsai IJ, Beech RN, Redman E, Holroyd N, Bartley DJ, Beasley H, Britton C *et al*: **The genome and transcriptome of *Haemonchus contortus*, a key model parasite for drug and vaccine discovery**. *Genome Biol* 2013, **14**(8):R88.

65. Schwarz EM, Korhonen PK, Campbell BE, Young ND, Jex AR, Jabbar A, Hall RS, Mondal A, Howe AC, Pell J *et al*: **The genome and developmental transcriptome of the strongylid nematode *Haemonchus contortus***. *Genome Biol* 2013, **14**(8):R89.

66. Bai X, Adams BJ, Ciche TA, Clifton S, Gaugler R, Kim KS, Spieth J, Sternberg PW, Wilson RK, Grewal PS: **A lover and a fighter: the genome sequence of an entomopathogenic nematode *Heterorhabditis bacteriophora***. *PLoS One* 2013, **8**(7):e69618.

67. Tang YT, Gao X, Rosa BA, Abubucker S, Hallsworth-Pepin K, Martin J, Tyagi R, Heizer E, Zhang X, Bhonagiri-Palsikar V *et al*: **Genome of the human hookworm *Necator americanus***. *Nat Genet* 2014, **46**(3):261-269.

68. Rödelsperger C, Neher RA, Weller AM, Eberhardt G, Witte H, Mayer WE, Dieterich C, Sommer RJ: **Characterization of genetic diversity in the nematode *Pristionchus pacificus* from population-scale resequencing data**. *Genetics* 2014, **196**(4):1153-1165.

Table 1. Nematode genomes used in this study

Species	Genome provider	BioProject ID	Assembly version	Reference
Romanomermis culicivorax	University of Cologne	PRJEB1358	nRc.2.0	[40]
Soboliphyme baturini[1]	Wellcome Trust Sanger Institute	PRJEB516	S_baturini_Dall_Island_v1_0_4	
Trichinella nativa[1]	Genome Institute of Washington University	PRJNA179527	T_nativa_rf_gd	
Trichinella spiralis	Genome Institute of Washington University	PRJNA12603	Trichinella_spiralis-3.7.1	[41]
Trichuris muris	Wellcome Trust Sanger Institute	PRJEB126	TMUE2.2	[42]
Trichuris suis[1]	Genome Institute of Washington University	PRJNA179528	T_suis_1.0.allpaths	
Trichuris suis	University of Melbourne	PRJNA208415	Tsuis_adult_male_1.0	[43]
Trichuris suis	University of Melbourne	PRJNA208416	Tsuis_adult_female_1.0	[43]
Trichuris trichiura	Wellcome Trust Sanger Institute	PRJEB535	TTRE2.1	[42]
Acanthocheilonema viteae	University of Edinburgh	PRJEB4306	nAv1.0	
Anisakis simplex[1]	Wellcome Trust Sanger Institute	PRJEB496	A_simplex_v1_5_4	
Ascaris lumbricoides[1]	Wellcome Trust Sanger Institute	PRJEB4950	A_lumbricoides_Ecuador_v1_5_4	
Ascaris suum	University of Colorado	PRJNA62057	ASU_2.0	[44]
Ascaris suum	University of Melbourne	PRJNA808881	AscSuum_1.0_submitted	[45]
Brugia malayi	University of Pittsburgh	PRJNA10729	B_malayi-3.1	[46]
Brugia pahangi[1]	Wellcome Trust Sanger Institute	PRJEB497	B_pahangi_Glasgow_v1_5_4	
Brugia timori[1]	Wellcome Trust Sanger Institute	PRJEB4663	B_timori_Indonesia_v1_0_4	
Dirofilaria immitis	University of Edinburgh	PRJEB1797	nDi.2.2	[47]
Dracunculus medinensis[1]	Wellcome Trust Sanger Institute	PRJEB500	D_medinensis_Ghana_v2_0_4	
Elaeophora elaphi[1]	Wellcome Trust Sanger Institute	PRJEB502	E_elaphi_v1_0_4	
Enterobius vermicularis[1]	Wellcome Trust Sanger Institute	PRJEB503	E_vermicularis_Canary_Islands_v1_0_4	
Gongylonema pulchrum[1]	Wellcome Trust Sanger Institute	PRJEB505	G_pulchrum_Hokkaido_v1_0_4	
Litomosoides sigmodontis	University of Edinburgh	PRJEB3075	nLs.2.1	
Loa loa	University of Maryland	PRJNA246086	Lloa-hgap-1	[48]
Loa loa	Broad Institute	PRJNA60051	Loa_loa_V3	[49]

Table 1. Nematode genomes used in this study (continued)

Species	Genome provider	BioProject ID	Assembly version	Reference
Onchocerca flexuosa[1]	Wellcome Trust Sanger Institute	PRJEB512	O_flexuosa_Cordoba_v1_0_4	
Onchocerca ochengi[1]	Wellcome Trust Sanger Institute	PRJEB1204	O_ochengi_Ngaoundere_v1_0_4	
Onchocerca ochengi	University of Edinburgh	PRJEB1809	nOo.2.0	
Onchocerca volvulus[1]	Wellcome Trust Sanger Institute	PRJEB513	O_volvulus_Cameroon_v3	
Parascaris equorum[1]	Wellcome Trust Sanger Institute	PRJEB514	P_equorum_v1_0_4	
Syphacia muris[1]	Wellcome Trust Sanger Institute	PRJEB524	S_muris_Valencia_v1_0_4	
Thelazia callipaeda[1]	Wellcome Trust Sanger Institute	PRJEB1205	T_callipaeda_Ticino_v1_0_4	
Toxocara canis[1]	Wellcome Trust Sanger Institute	PRJEB533	T_canis_Equador_v1_5_4	
Wuchereria bancrofti[1]	Wellcome Trust Sanger Institute	PRJEB536	W_bancrofti_Jakarta_v2_0_4	
Bursaphelenchus xylophilus	Wellcome Trust Sanger Institute	PRJEA64437	ASM23113v1_submitted	[50]
Panagrellus redivivus	California Institute of Technology	PRJNA186477	Pred3	[51]
Parastrongyloides trichosuri	Wellcome Trust Sanger Institute	PRJEB515	P_trichosuri_KNP_v2_0_4	[52]
Rhabditophanes sp KR3021	Wellcome Trust Sanger Institute	PRJEB1297	Rhabditophanes_sp_KR3021_v2_0_4	[52]
Steinernema carpocapsae	California Institute of Technology	PRJNA202318	S_carpo_v1_submitted	[53]
Steinernema feltiae	California Institute of Technology	PRJNA204661	S_felt_v1_submitted	[53]
Steinernema glaseri	California Institute of Technology	PRJNA204943	S_glas_v1_submitted	[53]
Steinernema monticolum	California Institute of Technology	PRJNA205067	S_monti_v1_submitted	[53]
Steinernema scapterisci	California Institute of Technology	PRJNA204942	S_scapt_v1_submitted	[53]
Strongyloides papillosus	Wellcome Trust Sanger Institute	PRJEB525	S_papillosus_LIN_v2_1_4	[52]
Strongyloides ratti	Wellcome Trust Sanger Institute	PRJEB125	S_ratti_ED321_v5_0_4	[52]
Strongyloides stercoralis	Wellcome Trust Sanger Institute	PRJEB528	S_stercoralis_PV0001_v2_0_4	[52]
Strongyloides venezuelensis	Wellcome Trust Sanger Institute	PRJEB530	S_venezuelensis_HH1_v2_0_4	[52]
Globodera pallida	Wellcome Trust Sanger Institute	PRJEB123	GPAL001	[54]
Meloidogyne floridensis	University of Edinburgh	PRJEB6016	nMf.1.0	[55]
Meloidogyne hapla	North Carolina State University	PRJNA29083	Freeze_1	[56]

Table 1. Nematode genomes used in this study (continued)

Species	Genome provider	BioProject ID	Assembly version	Reference
Meloidogyne incognita	INRA	PRJEA28837	ASM18041v1a	[57]
Ancylostoma caninum[1]	Genome Institute of Washington University	PRJNA72585	A_caninum_9.3.2.ec.cg.pg	
Ancylostoma ceylanicum	Cornell University	PRJNA231479	Acey_2013.11.30.genDNA	[58]
Ancylostoma ceylanicum[1]	Genome Institute of Washington University	PRJNA72583	A_ceylanicum1.3.ec.cg.pg	
Ancylostoma duodenale[1]	Genome Institute of Washington University	PRJNA72581	A_duodenale_2.2.ec.cg.pg	
Angiostrongylus cantonensis[1]	Wellcome Trust Sanger Institute	PRJEB493	A_cantonensis_Taipei_v1_5_4	
Angiostrongylus costaricensis[1]	Wellcome Trust Sanger Institute	PRJEB494	A_costaricensis_Costa_Rica_v1_5_4	
Caenorhabditis angaria	California Institute of Technology	PRJNA51225	13mar2012	[59]
Caenorhabditis brenneri	Genome Institute of Washington University	PRJNA20035	C_brenneri-6.0.1b	
Caenorhabditis briggsae	Genome Institute of Washington University	PRJNA10731	CB4	[60]
Caenorhabditis elegans	Wellcome Trust Sanger Institute	PRJNA13758	WBcel235	[14]
Caenorhabditis japonica	Genome Institute of Washington University	PRJNA12591	C_japonica-7.0.1	
Caenorhabditis remani	Genome Institute of Washington University	PRJNA53967	C_remani-15.0.1	
Caenorhabditis sinica	University of Edinburgh	PRJNA194557	1.0	[61]
Caenorhabditis tropicalis	Genome Institute of Washington University	PRJNA53597	Caenorhabditis_sp11_JU1373-3.0.1	
Cylicostephanus goldi[1]	Wellcome Trust Sanger Institute	PRJEB498	C_goldi_Cheshire_v1_0_4	
Dictyocaulus viviparus	University of Edinburgh	PRJEB5116	nDv.1.0	[62]
Dictyocaulus viviparus	Genome Institute of Washington University	PRJNA72587	D_viviparus_9.2.1.ec.pg	[63]
Haemonchus contortus	Wellcome Trust Sanger Institute	PRJEB506	Haemonchus_contortus_MHco3-2.0	[64]
Haemonchus contortus	University of Melbourne	PRJNA205202	Hco_v4_coding_submitted	[65]
Haemonchus placei[1]	Wellcome Trust Sanger Institute	PRJEB509	H_placei_MHpl1_v1_5_4	
Heligmosomoides bakeri[1]	Wellcome Trust Sanger Institute	PRJEB1203	H_bakeri_Edinburgh_v1_5_4	
Heterorhabditis bacteriophora	The Ohio State University	PRJNA13977	Heterorhabditis_bacteriophora-7.0	[66]
Necator americanus	Genome Institute of Washington University	PRJNA72135	N_americanus_v1	[67]
Nippostrongylus brasiliensis[1]	Wellcome Trust Sanger Institute	PRJEB511	N_brasiliensis_RM07_v1_5_4	

Table 1. Nematode genomes used in this study (continued)

Species	Genome provider	BioProject ID	Assembly version	Reference
Oesophagostomum dentatum[1]	Genome Institute of Washington University	PRJNA72579	O_dentatum_10.0.ec.cg.pg	
Pristionchus exspectatus	Max-Planck Institute for Developmental Biology	PRJEB6009	P_exspectatus_v1	[68]
Pristionchus pacificus	Max-Planck Institute for Developmental Biology	PRJNA12644	P_pacificus-v2	[68]
Strongylus vulgaris[1]	Wellcome Trust Sanger Institute	PRJEB531	S_vulgaris_Kentucky_v1_0_4	
Teladorsagia circumcincta[1]	Genome Institute of Washington University	PRJNA72569	T_circumcincta.14.0.ec.cg.pg	

[1] Genome sequenced as part of the Helminth Genomes Consortium (unpublished)

Table 2. Putative heterotrimeric G-proteins identified in Nematoda

	Seed	BLAST	HMMs
GPA	22	473	1038
GPB	2	163	144
GPC	2	149	151

To focus our search on heterotrimeric G-proteins we downloaded all known heterotrimeric G-proteins in *C. elegans* (Seed). Local blastp searches were performed using the predicted proteins from each nematode species as subjects and *C. elegans* heterotrimeric G-protein sequences as queries. The top hits for each these searches were aligned using the MUSCLE multiple sequence alignment program and manually curated. The putative heterotrimeric G-proteins identified (BLAST) were used to build profile HMMs that were then used as query sequences to identify putative homologs using HMMsearch. This data set was aligned and manually curated to identify putative heterotrimeric G-proteins in Nematoda (HMMs). GPA = G-protein α subunit, GPB = G-protein β subunit, GPC = G-protein γ subunit.

Table 3. Oligonucleotides used to amplify GPC genes from *B. malayi*

Target	Oligonucleotide sequence (5' to 3')	Amplicon size (Bp)
GPC1	Forward: GATCAGGTTCGAGRACAGACC Reverse: CAGCACAAGATTTCTTTTCCTG	178
GPC2	Forward: GACAAGTGCGACATGCAGCGG Reverse: GGATTGCATCGTTTATCAACGGGAT	158
GPC3	Forward: GCAAGAGATACTCATTCCATTCAA Reverse: GCAAACACTGGAAGGAACTT	208

Table 4. Heterotrimeric G-protein α subunits in Nematoda

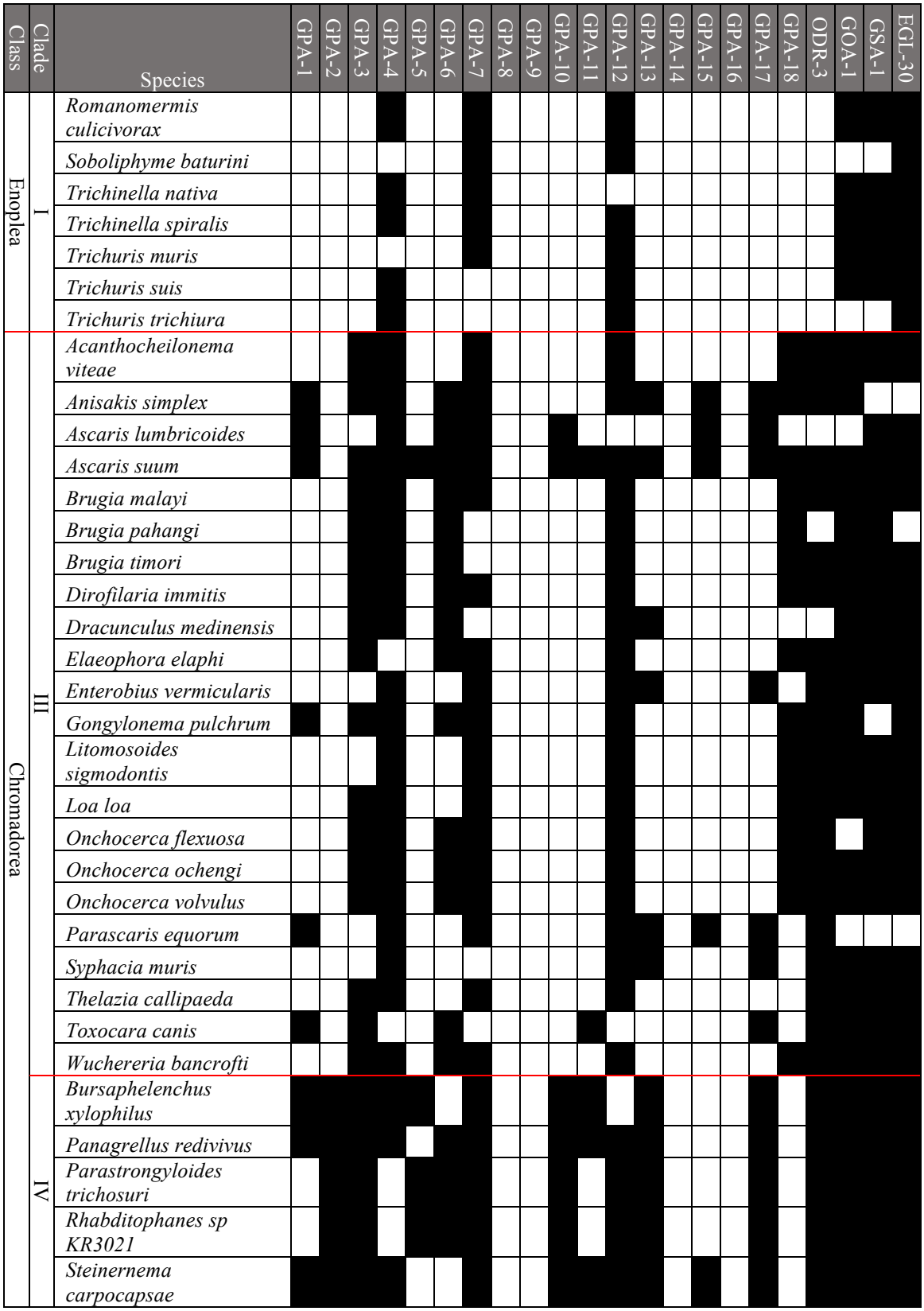

Table 4. Heterotrimeric G-protein α subunits in Nematoda (continued)

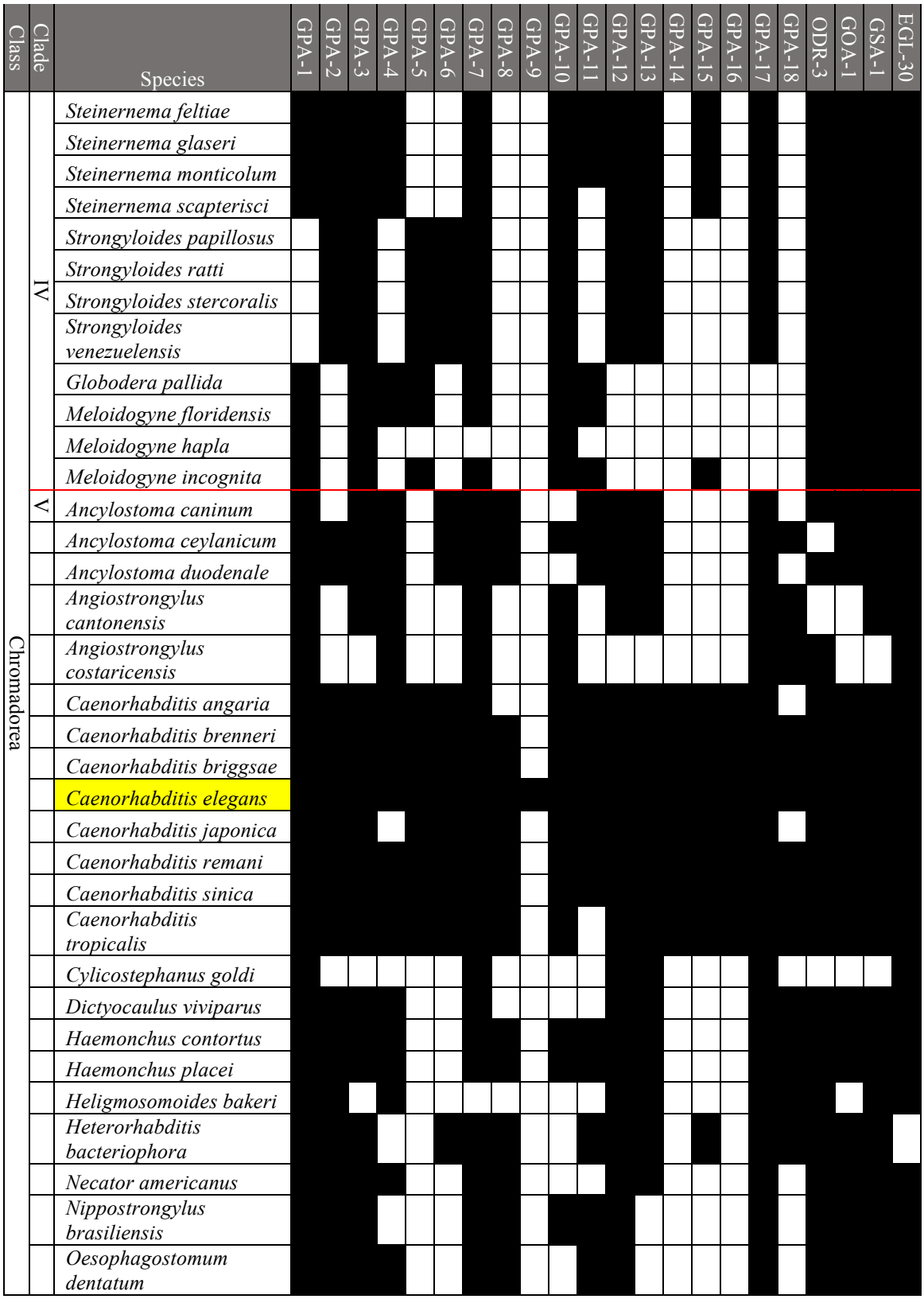

Table 4. Heterotrimeric G-protein α subunits in Nematoda (continued)

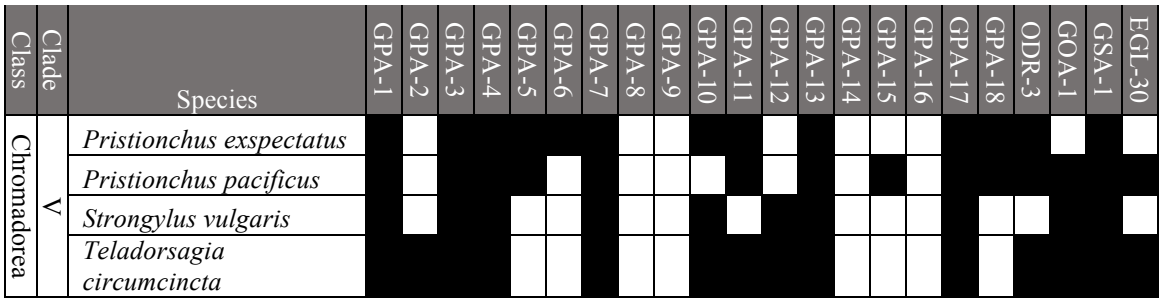

Putative heterotrimeric G-protein α subunits in phylum Nematoda. Black boxes indicate the presence of a GPA homolog, as identified via blastp and HMMER, in genomes analyzed in this study. GPAs from *C. elegans* (highlighted in yellow) were used to seed homology searches.

Table 5. Heterotrimeric G-protein β subunits in Nematoda

Class	Clade	Species	GPB-1	GPB-2
Enoplea	I	*Romanomermis culicivorax*	■	■
		Soboliphyme baturini	■	□
		Trichinella nativa	■	■
		Trichinella spiralis	■	□
		Trichuris muris	■	■
		Trichuris suis	■	■
		Trichuris trichiura	■	■
Chromadorea	III	*Acanthocheilonema viteae*	■	■
		Anisakis simplex	■	■
		Ascaris lumbricoides	■	□
		Ascaris suum	■	■
		Brugia malayi	■	■
		Brugia pahangi	■	■
		Brugia timori	■	■
		Dirofilaria immitis	■	■
		Dracunculus medinensis	■	□
		Elaeophora elaphi	■	□
		Enterobius vermicularis	■	■
		Gongylonema pulchrum	□	□
		Litomosoides sigmodontis	■	■
		Loa loa	■	■
		Onchocerca flexuosa	■	■
		Onchocerca ochengi	■	■
		Onchocerca volvulus	■	■
		Parascaris equorum	■	■
		Syphacia muris	■	□
		Thelazia callipaeda	■	□
		Wuchereria bancrofti	■	■
	IV	*Bursaphelenchus xylophilus*	■	■
		Panagrellus redivivus	■	■
		Parastrongyloides trichosuri	■	■
		Rhabditophanes sp KR3021	■	■
		Steinernema carpocapsae	■	■
		Steinernema feltiae	■	■
		Steinernema glaseri	■	■
		Steinernema monticolum	■	■
		Steinernema scapterisci	■	■
		Strongyloides papillosus	■	■

Table 5. Heterotrimeric G-protein β subunits in Nematoda (continued)

Class	Clade	Species	GPB-1	GPB-2
Chromadorea	IV	*Strongyloides ratti*	■	■
		Strongyloides stercoralis	■	■
		Strongyloides venezuelensis	■	■
		Globodera pallida	■	■
		Meloidogyne floridensis	■	■
		Meloidogyne hapla	■	■
		Meloidogyne incognita	■	■
	V	*Ancylostoma caninum*	■	■
		Ancylostoma ceylanicum	■	■
		Ancylostoma duodenale	■	■
		Angiostrongylus cantonensis	■	
		Angiostrongylus costaricensis		
		Caenorhabditis angaria	■	■
		Caenorhabditis brenneri	■	■
		Caenorhabditis briggsae	■	■
		Caenorhabditis elegans	■	■
		Caenorhabditis japonica	■	■
		Caenorhabditis remani	■	■
		Caenorhabditis sinica	■	■
		Caenorhabditis tropicalis	■	■
		Cylicostephanus goldi		
		Dictyocaulus viviparus	■	■
		Haemonchus contortus	■	■
		Haemonchus placei	■	■
		Heligmosomoides bakeri	■	
		Heterorhabditis bacteriophora	■	■
		Necator americanus	■	■
		Nippostrongylus brasiliensis	■	■
		Oesophagostomum dentatum	■	■
		Pristionchus exspectatus	■	■
		Pristionchus pacificus	■	■
		Strongylus vulgaris	■	■
		Teladorsagia circumcincta	■	■

Putative heterotrimeric G-protein β subunits in phylum Nematoda. Black boxes indicate the presence of a GPB homolog, as identified via blastp and HMMER, in genomes analyzed in this study. GPBs from *C. elegans* (highlighted in yellow) were used to seed homology searches.

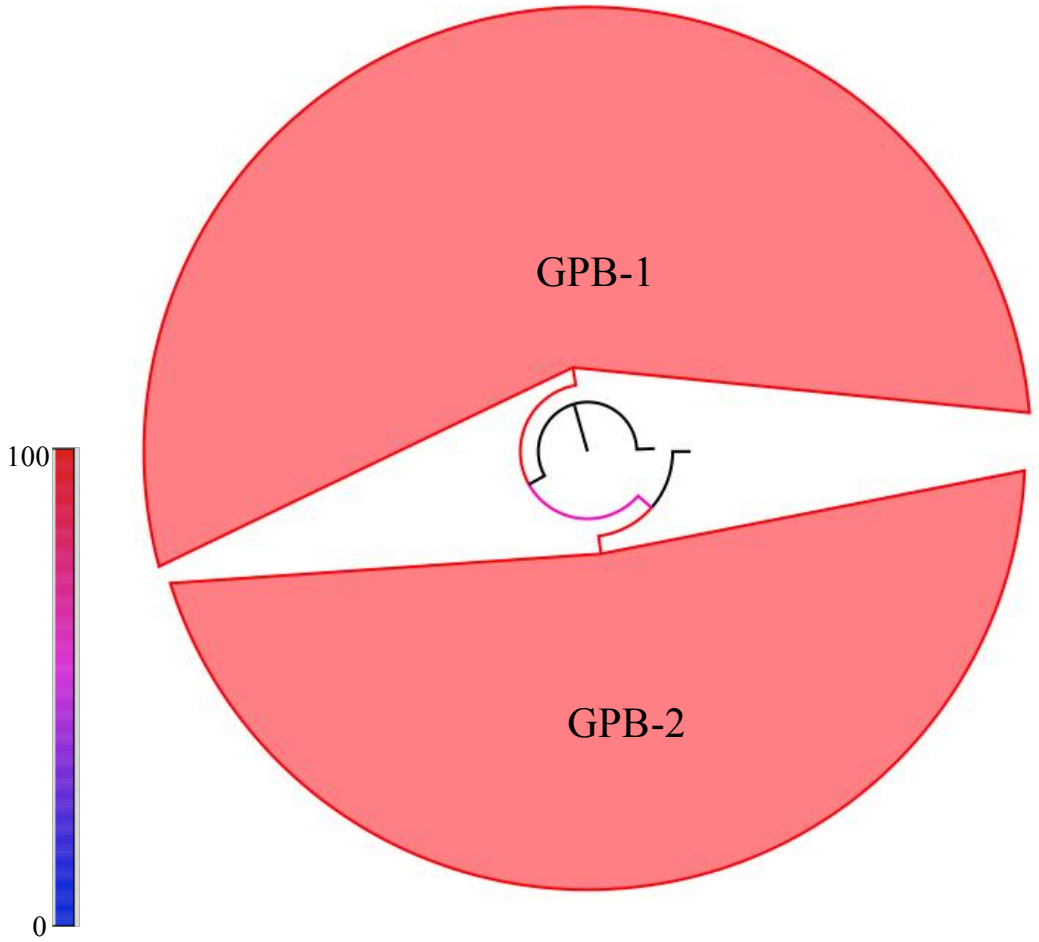

Figure 1. Phylogeny reveals that heterotrimeric G-protein β subunits (GPB) are highly conserved in phylum Nematoda. Maximum likelihood phylogeny of heterotrimeric GPBs in phylum Nematoda. Phylogenetic tree was constructed using RAxML and visualized with FigTree [32, 34]. Phylogenetic tree shown is the best-scoring maximum likelihood tree based on 100 bootstrap replicates.

Table 6. Heterotrimeric G-protein γ subunits in Nematoda

Class	Clade	Species	GPC-1	GPC-2	GPC-3
Enoplea	I	*Romanomermis culicivorax*	■	■	■
		Soboliphyme baturini			■
		Trichinella nativa	■	■	■
		Trichinella spiralis	■	■	■
		Trichuris muris	■	■	■
		Trichuris suis	■	■	■
		Trichuris trichiura	■	■	■
Chromadorea	III	*Acanthocheilonema viteae*		■	■
		Anisakis simplex			■
		Ascaris lumbricoides	■	■	■
		Ascaris suum	■	■	■
		Brugia malayi	■	■	■
		Brugia pahangi	■	■	■
		Brugia timori	■	■	■
		Dirofilaria immitis	■	■	■
		Dracunculus medinensis	■	■	■
		Elaeophora elaphi	■	■	■
		Enterobius vermicularis		■	■
		Gongylonema pulchrum		■	■
		Litomosoides sigmodontis		■	■
		Loa loa	■	■	■
		Onchocerca flexuosa		■	■
		Onchocerca ochengi	■	■	■
		Onchocerca volvulus	■	■	■
		Parascaris equorum	■		■
		Syphacia muris		■	■
		Thelazia callipaeda	■	■	■
		Toxocara canis	■	■	■
		Wuchereria bancrofti	■	■	■
	IV	*Bursaphelenchus xylophilus*		■	■
		Panagrellus redivivus	■		■
		Parastrongyloides trichosuri	■	■	■
		Rhabditophanes sp KR3021	■	■	■
		Steinernema carpocapsae			■
		Steinernema feltiae			■
		Steinernema glaseri			■
		Steinernema monticolum			■

Table 6. Heterotrimeric G-protein γ subunits in Nematoda (continued)

Class	Clade	Species	GPC-1	GPC-2	GPC-3
Chromadorea	IV	*Steinernema scapterisci*		■	■
		Strongyloides papillosus	■	■	■
		Strongyloides ratti	■	■	■
		Strongyloides stercoralis	■	■	■
		Strongyloides venezuelensis	■	■	■
		Globodera pallida			■
		Meloidogyne floridensis	■	■	■
		Meloidogyne hapla		■	■
		Meloidogyne incognita	■	■	■
	V	*Ancylostoma caninum*	■		■
		Ancylostoma ceylanicum	■	■	■
		Ancylostoma duodenale		■	■
		Angiostrongylus cantonensis		■	■
		Angiostrongylus costaricensis	■	■	■
		Caenorhabditis angaria	■		
		Caenorhabditis briggsae	■	■	
		Caenorhabditis elegans	■	■	
		Caenorhabditis japonica	■		
		Caenorhabditis remani	■	■	
		Cylicostephanus goldi		■	■
		Dictyocaulus viviparus	■	■	■
		Haemonchus contortus		■	■
		Haemonchus placei	■	■	■
		Heligmosomoides bakeri		■	■
		Heterorhabditis bacteriophora		■	■
		Necator americanus		■	■
		Nippostrongylus brasiliensis		■	■
		Oesophagostomum dentatum			■
		Pristionchus exspectatus		■	■
		Pristionchus pacificus	■	■	■
		Strongylus vulgaris		■	■
		Teladorsagia circumcincta	■		■

Putative heterotrimeric G-protein γ subunits in phylum Nematoda. Black boxes indicate the presence of a GPC homolog, as identified via blastp and HMMER, in genomes analyzed in this study. GPCs from *C. elegans* (highlighted in yellow) were used to seed homology searches.

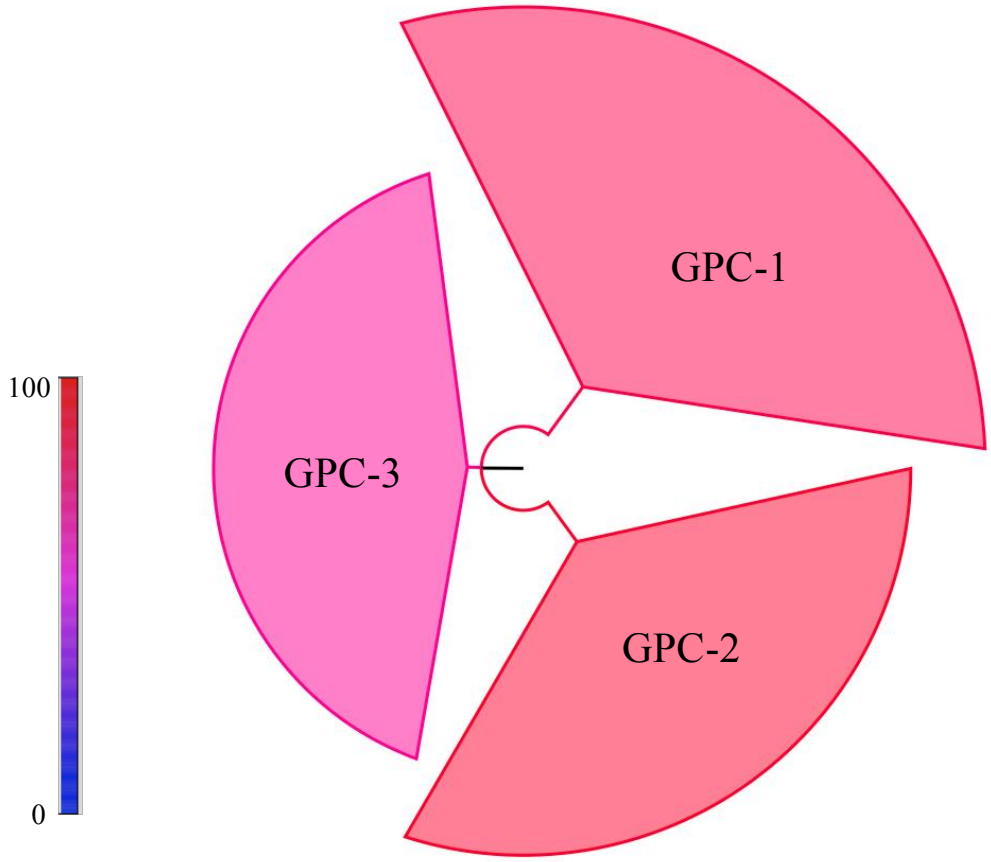

Figure 2. Phylogenetic analysis of G-protein γ subunits (GPCs) reveals novel γ subunit (GPC-3) in phylum Nematoda. Maximum-likelihood phylogeny of GPCs in phylum Nematoda. Phylogenetic tree was constructed using RAxML and visualized with FigTree [32, 34]. Phylogenetic tree shown is the best-scoring maximum likelihood tree based on 100 bootstrap replicates.

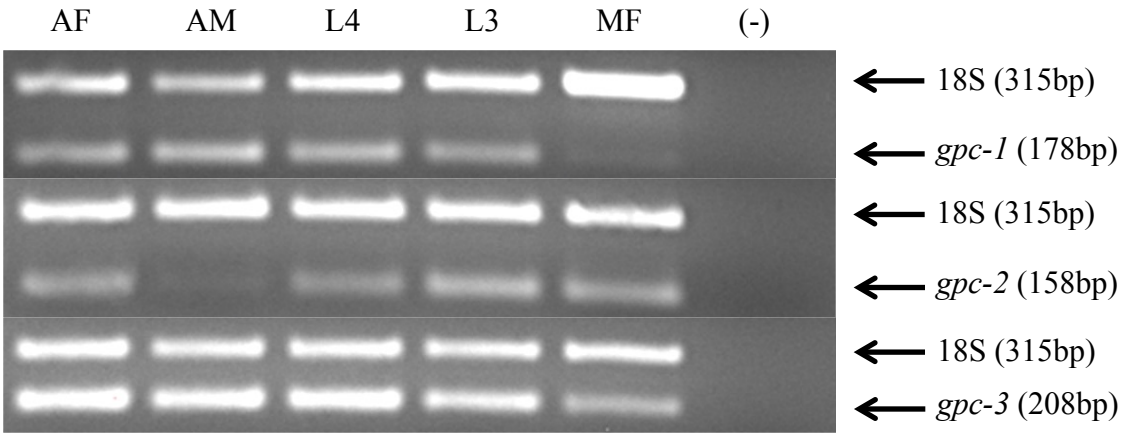

Figure 3. GPC genes are transcribed throughout the life of *B. malayi*. Micrograph shows ethidium bromide stained 2% agarose gel of relative semi-quantitative RT-PCR of adult female (AF), adult male (AM), L4, L3 and microfilariae (MF) stage *B. malayi*. Top: *gpc-1*, middle: *gpc-2*, bottom: *gpc-3*. QuantumRNA Universal 18S internal standards were used as an internal control.

CHAPTER 4

RELEASE OF SMALL RNA-CONTAINING EXOSOME-LIKE VESICLES FROM THE HUMAN FILARIAL PARASITE *BRUGIA MALAYI*

Modified from a paper published in *PLOS Neglected Tropical Diseases*

Mostafa Zamanian[1,2•], Lisa M. Fraser[1•], Prince N. Agbedanu[1], Hiruni Harischandra[1], Andrew R. Moorhead[3], Tim A. Day[1], Lyric C. Bartholomay[4], Michael J. Kimber[1]*

[1]Department of Biomedical Sciences, Iowa State University, Ames, Iowa, United States of America, [2]Department of Molecular Biosciences, Northwestern University, Evanston, Illinois, United States of America, [3]Department of Infectious Disease, University of Georgia, Athens, Georgia, United States of America, [4]Department of Pathobiological Sciences, University of Wisconsin-Madison, Madison, Wisconsin, United States of America

•These authors contributed equally to this work

*michaelk@iastate.edu

Abstract

Lymphatic Filariasis (LF) is a socio-economically devastating mosquito-borne Neglected Tropical Disease caused by parasitic filarial nematodes. The interaction between the parasite and host, both mosquito and human, during infection, development and persistence is dynamic and delicately balanced. Manipulation of this interface to the

detriment of the parasite is a promising potential avenue to develop disease therapies but is prevented by our very limited understanding of the host-parasite relationship. Exosomes are bioactive small vesicles (30–120 nm) secreted by a wide range of cell types and involved in a wide range of physiological processes. Here, we report the identification and partial characterization of exosome-like vesicles (ELVs) released from the infective L3 stage of the human filarial parasite *Brugia malayi*. Exosome-like vesicles were isolated from parasites in culture media and electron microscopy and nanoparticle tracking analysis were used to confirm that vesicles produced by juvenile *B. malayi* are exosome-like based on size and morphology. We show that loss of parasite viability correlates with a time-dependent decay in vesicle size specificity and rate of release. The protein cargo of these vesicles is shown to include common exosomal protein markers and putative effector proteins. These *Brugia*-derived vesicles contain small RNA species that include microRNAs with host homology, suggesting a potential role in host manipulation. Confocal microscopy shows J774A.1, a murine macrophage cell line, internalize purified ELVs, and we demonstrate that these ELVs effectively stimulate a classically activated macrophage phenotype in J774A.1. To our knowledge, this is the first report of exosome-like vesicle release by a human parasitic nematode and our data suggest a novel mechanism by which human parasitic nematodes may actively direct the host responses to infection. Further interrogation of the makeup and function of these bioactive vesicles could seed new therapeutic strategies and unearth stage-specific diagnostic biomarkers.

Introduction

The parasitic filarial nematodes *Wuchereria bancrofti*, *Brugia malayi* and *B. timori* are etiological agents of Lymphatic Filariasis (LF), a chronic and debilitating disease infecting over 120 million people in 73 endemic countries [1]. Adult parasites reside in the lymphatic vasculature of infected individuals and release larvae called microfilariae, which are taken up by vector mosquitoes during the blood meal. Parasites rapidly develop within the mosquito, molting twice to the infective L3 stage [2, 3] before transmission to the definitive host during a subsequent blood meal. Following penetration of the vertebrate host via the puncture wound left by the mosquito, L3 stage parasites migrate to the lymphatics and undergo further growth and development, molting to the L4 stage and again to adulthood. The longevity of patent infection is remarkable; adults live for at least 8–10 years by general consensus. The ability of larval stages to successfully invade the host, and for adult worms to maintain infection for such an extended period of time, suggest filarial worms have developed strategies to both facilitate the establishment of infection and evade or manipulate the host immune response. Although the immunomodulatory capabilities of infecting larval and adult stage filarial worms have been well documented and reviewed [4-8], the parasite effector molecules responsible for manipulating host biology and their mechanisms of release have been difficult to define. Actively secreted proteins have historically been considered the principal candidates and several secreted proteins have been identified with demonstrable bioactivity at the host-parasite interface [9-12]. Adding to these, the characterization of parasitic nematode secretomes has revealed a complex array of potential proteinaceous effectors [13-16]. Other types of effector, including molecules

expressed on the parasite surface may have a role [17] and the emergence of small noncoding RNAs as cell-to-cell agents of genetic regulation [18-22] hint at exciting alternative mechanisms.

Exosomes are a subtype of extracellular vesicle categorized by size (30–120 nm diameter) and defined by a particular biogenic pathway [23]; exosomes are formed by inward budding of vesicles in the late endosomal pathway to create multivesicular endosomes that fuse with the plasma membrane to effect release [24, 25]. Originally thought to be a means of cellular waste disposal, exosomes are now considered highly bioactive extracellular vesicles that facilitate cell-to-cell communication and are the focus of renewed investigation. The cargo of exosomes is complex and variable, containing bioactive proteins, functional mRNA, miRNA and other small non-coding RNA species [18, 26], likely reflecting both source and target environments. Fusion of the exosome to a target cell delivers this heterogeneous bioactive cargo and selectively alters the biology of the target tissue [19, 21, 26, 27]; the isolation of exosomes from circulatory systems and an array of biofluids suggests effector sites can be far from the point of release. Parasites are known to release exosome-like vesicles [27-30] and it is compelling to hypothesize that bioactive molecules secreted by parasitic nematodes, packaged in exosomes, function as cell-to-cell effectors in the host-parasite interaction. Indeed recently, extracellular vesicles secreted by the gastrointestinal nematode *Heligmosomoides polygyrus*, containing proteins and small RNA species, have been shown to alter gene expression in host cells and suppress innate immune responses in mice [26].

Here we show that larval and adult stage *B. malayi* secrete prodigious quantities of extracellular vesicles in vitro whose size and morphology are consistent with exosomes. These exosome-like extracellular vesicles (ELVs) contain small RNA species, including specific miRNA and are enriched in miRNA that are identical to host miRNAs with known immunomodulatory roles [31-34]. The protein cargo of the vesicles is relatively scant but includes bioactive proteins, proteins with putative RNA binding properties and proteins commonly associated with exosomes [35]. The parasite ELVs are internalized by host macrophages and elicit a classically activated phenotype in these cells. The demonstration that filarial nematodes secrete exosomal RNA and proteins that potentially function at the host-parasite interface is significant. Defining this parasite effector toolkit exposes an array of new molecules that may be exploited in novel LF control strategies.

Results and Discussion

Infective-stage *B. malayi* release exosome-like vesicles

In order to ascertain whether exosomes are released by *B. malayi*, extracellular vesicles were isolated from parasites incubated in culture media using a filtration and ultracentrifugation protocol. We focused our initial discovery efforts on larval and adult stage parasites. L3, adult male, and adult female *B. malayi* were incubated in vitro for 24 hour periods under standard culture conditions, and purified vesicle preparations were evaluated with electron microscopy (EM). Infectious stage L3 parasites in culture release abundant 50–120 nm microvesicles consistent with the classical "deflated ball" morphology of mammalian and non-mammalian exosomes reported in the literature [36]

(Fig 1A & 1B). We refer to these as exosome-like vesicles (ELVs) throughout this manuscript, in recognition that they cannot be unequivocally designated as exosomes, rather than another class of extracellular vesicles, because their biogenesis has not been determined. Preparations from adult stage *B. malayi* were more heterogenous and dilute, not allowing for the definitive categorization of putative exosome-like vesicles (Fig 1C). This, despite the fact a much higher mass of total parasite tissue was used for adult preparations as compared to larval preparations. These data suggest ELV release to be a predominantly larval phenomenon in *B. malayi*, a working hypothesis supported by analysis of RNA associated with the vesicles. We therefore chose to focus our subsequent experiments on L3 stage parasites. A compelling overall hypothesis for the function of *B. malayi* ELVs is that they mediate the secretion and trafficking to host cells of effector molecules that facilitate parasitism and the observation that ELV secretion occurs primarily in those parasite stages that infect the host and establish parasitemia is consistent with this narrative.

Time course profile of exosome-like vesicle release from infectious stage *B. malayi*

To more accurately resolve the dynamics of ELV release in L3 *B. malayi*, we used a nanoparticle tracking analysis (NTA) system to measure vesicle output in a 72 hr *in vitro* time course. Media was collected from 300 worms after three successive 24 hr incubation periods, vesicles were purified by ultracentrifugation as before and individual vesicle preparations were analyzed via NanoSight LM10 as shown in Fig 2. Day 1 (0–24 hr in culture) preparations reveal a prolific ELV release rate (> 9,000 ELVs/parasite/min) with a very narrow size distribution centered at ~90 nm. Day 2 (24–48 hr in culture) preparations show an essentially equivalent rate of release, but a stark broadening of the

size distribution. Day 3 (48–72 hr in culture) preparations are associated with significantly lower levels of release (<4,000 ELVs/parasite/min) and an even wider multimodal size distribution. These data suggest an overall time-dependent decay in vesicle rate of release and size specificity, which correlates to decreased L3 viability *in vitro*. The release of considerable quantities of precisely sized ELVs in viable worms (Days 1–2) is followed by the release of smaller quantities of a broader size range of particles that potentially include larger membrane vesicles and apoptotic blebs (Days 2–3). This suggests an active and regulated mechanism of ELV release in healthy and viable L3 stage parasites, as opposed to a passive mode of noisy cellular deterioration.

The protein cargo of *Brugia* exosome-like vesicles

The protein content of *B. malayi* ELVs was determined using nanoscale liquid chromatography coupled to tandem mass spectrometry (nano LC/MS/MS). A total of 32 proteins each containing at least two unique peptides were identified using MASCOT (Table 1). Specific proteins identified within the pellet included characteristic markers of exosomes including Hsp70, elongation factor-1α, elongation factor-2, actin, and Rab-1. In addition, over 80% of the proteins identified are orthologous to proteins identified in mammalian exosome proteomes, strongly suggesting that these vesicles are exosome-like in nature and supporting our ELV designation here. Interestingly, this set of vesicle-specific proteins is entirely distinct from the proteins previously identified in pre- and post-molt L3 secretions [15].

UniProt-GOA and quickGO were used to sort proteins into functional groups based on assigned gene ontology (GO) terms [37, 38], as shown in Fig 3. Based on GO

annotations, 20% of the proteins identified are involved in binding of bioactive molecules including nucleic acids and other proteins, 16% function in the transport of various ions and proteins and 14% are ribosomal proteins. In addition, a large fraction of proteins identified (21%) appear to be involved in various metabolic processes including hydrolase and transferase activities while the remaining 29% comprises proteins with translational, cytoskeletal and other functions.

Included in the list of *Brugia* ELV proteins are potential effector molecules. Bm-CPL-1 is a cathepsin L-like cysteine protease robustly expressed across the *B. malayi* life cycle [39]. Upregulation of *Bm-cpl-1* expression coincides with transition between life cycle stages and an important role in the modulation of parasite molting has been confirmed [40-42]. This is the first demonstration that *B. malayi* secretes CPL-1 although other cathepsin-like cysteine proteases have been identified in the *B. malayi* secretome [14, 15] and a cathepsin L-like molecule is secreted by intra-mammalian stage *Haemonchus contortus* [43]. The exogenous function of exosomal Bm-CPL-1 is not clear but evidence points to some manipulation of the host-parasite interface. In a previous study, we suppressed *Bm-cpl-1* expression using *in vivo* RNAi during the mosquito life stages [41]. Loss-of-function reduced prevalence of infection in mosquitoes by nearly 40%, suggesting Bm-CPL-1 is important for establishing or maintaining parasitemia. In flatworms, an immunomodulatory role for secreted cathepsin L-like proteases is better established [44]; in *Fasciola* infection cathepsin L contributes to the permissive polarized Th2 > Th1 host response.

The proteomic profiles of parasitic helminth exosomes are broad in range; for example, over 350 proteins were identified in the putative exosomes secreted by

Heligmosomoides polygyrus [26] whilst 45 and 79 proteins were identified in exosome-like vesicles from *Echinostoma caproni* and *Fasciola hepatica*, respectively [28]. The *B. malayi* L3 stage profile identified here is relatively scant but consistent with this broad distribution. It may be that this is a stage-specific observation and ELV secreted by other *B. malayi* life stages display a more complex and abundant protein cargo tailored to distinct functional demands. Reflecting the small RNA component of these ELVs (see later sections), it may also be that larval stage *Brugia* ELVs are primarily vehicles for protected RNA secretion. Replication of the experiments conducted here might add depth to the MS data set and identify further ELV-associated proteins.

B. malayi ELVs contain small RNA including miRNAs with potential host targets

We probed larval and adult microvesicle preparations for the presence of small RNA species. Exosomes have been found to contain both non-coding RNAs (ncRNAs) and messenger RNAs (mRNAs) in a diverse range of species and cell types. Of particular interest to us was the potential presence of small non-coding RNAs, including microRNAs (miRNAs) that could potentially mediate parasite-parasite communication or modulate host gene expression. Small RNA species were preferentially isolated from putative ELV-containing pellets and examined with an Agilent Bioanalyzer. The microvesicle fractions of L3 *B. malayi* (24 hr incubations of 300 worms) revealed an abundance of small RNA species in the 25–200 nt range (Fig 4). Much less RNA was detected from incubations of adult male and female *B. malayi* (24 hr incubations of 30 adult worms), despite the much higher mass of tissue in adult stage culture media. This lack of correlation between total parasite tissue material and RNA yield, coupled to the differential quality of larval and adult microvesicle preparations as evaluated by EM,

further indicates that ELV release is primarily a characteristic of larval-stage parasites and perhaps more biologically relevant to early parasite infection.

To more fully investigate the nucleic acid contents of these newly discovered vesicles, we carried out RNA-Seq with both L3 ELV and tissue-derived small RNAs. Reads generated by Illumina sequencing were processed and used to seed an miRNA discovery and abundance estimation pipeline using miRDeep2 [45]. To compare ELV and cellular RNA abundance, miRNA expression was normalized to the total miRNA read count within each sample. miRNA discovery and profiling was augmented with data from previously discovered miRNAs in closely related nematode species to help overcome gaps in the *B. malayi* draft genome assembly (see Methods). Fig 5A compares normalized miRNA expression between ELV and tissue for the 20 most abundant miRNAs in each sample. Although there is considerable conservation in relative miRNAs abundances, there are some notable observations and exceptions.

Bma-let-7 is significantly enriched in L3 ELVs as compared to L3 tissue, where it does not appear among the 20 most abundant miRNAs. Bma-let-7, along with four other *B. malayi* mature miRNAs found in ELVs (bma-miR-1, bma-miR-9, bma-miR-92, and bma-miR-100b), share perfect sequence identity with host (*Homo sapiens*) mature miRNAs, as shown in Fig 5B. Additionally, bma-miR-34 shares near perfect sequence identity with its *H. sapiens* homolog. 11 *B. malayi* miRNAs also share common seed sites with *H. sapiens* miRNAs (Fig 5C). *Brugia* ELV miRNA sequences were more broadly clustered by putative seed site and aligned to miRNAs from the soil-transmitted parasitic nematode *Ascaris suum*, the free living model nematode *Caenorhabditis elegans*, and mammalian host species *H. sapiens* and *Mus musculus* (Fig 6). In all cases, *Brugia* ELV

miRNAs that share common seed sites with host miRNAs have one-to-one *A. suum* orthologs. In some cases, parasite miRNAs are better conserved in mammalian hosts than in *C. elegans* (e.g., bma-miR-9, bma-miR-993, and bma-miR-100b/c).

We examined the complement of the most abundant *Brugia* ELV-associated miRNAs with respect to very recent investigations of miRNAs released by other parasitic nematode species and found circulating in host biofluids [26, 46-48]. Common markers include let-7, lin-4, miR-34, miR-71, miR-92, and miR-100c (Fig 7A and 7B). While all members of this subset share seed site sequence identity with mammalian host miRNAs, lin-4, miR-34, miR-71, and miR-100c are sufficiently diverged from host miRNAs over their full length mature miRNA sequence and can potentially serve as biomarkers of filarial infection. Additionally, we compared the complements of the 20 most abundant *Brugia* ELV and *H. polygyrus* exosomal [26] miRNAs, identifying six miRNAs shared between these vesicles and a large number of miRNAs unique to each species (Fig 7C).

Enrichment of bma-let-7 and the high fractional presence of other parasite miRNAs sharing perfect or high homology to host miRNAs, leads us to speculate about a potential ELV mediated mechanism by which parasite RNAs can be used to efficiently direct aspects of gene expression in host cells. Targets of endogenous let-7 family miRNAs in vertebrates include oncogenes, as well as genes involved in proliferation, apoptosis, and innate immunity [49-51]. Let-7 is intricately involved in macrophage polarization and responses to pathogen challenge [31, 33, 52], and the altering of host let-7 expression therefore represents a potentially advantageous point of intervention for an invading parasite. Live pathogens down-regulate the expression of let-7 family miRNAs, and let-7 miRNAs act on toll-like receptors (e.g. TLR4) that directly mediate macrophage

responses [52-54]. Clearly, there is an important association between macrophage response to pathogens and let-7 expression. Our observation that *B. malayi* secrete let-7 and other potential modulators of host gene expression identifies a mechanism by which this host immune response might be manipulated. Supporting this hypothesis, let-7 and other miRNAs with host conservation have been identified in immunomodulatory *H. polygyrus* adult stage exosomes [26]. To fully dissect this hypothesis, a broad investigation of the interaction of ELV miRNAs and host immune cells *in vivo* is needed.

Brugia ELVs are internalized by host macrophages

Macrophages are critical mediators of the early immune response to invasive *Brugia* parasites [8]. To test the hypothesis that secreted *Brugia* ELVs interact with host macrophages, we used fluorescent lipophilic dyes to visualize the interaction between J774A.1 murine macrophages and ELVs. This cell line was chosen because it is commercially available, can be cultured readily and because it recapitulates the biology of primary macrophages and dendritic cells [55]. ELVs were labeled with PKH67, a green fluorescent dye, and incubated with J774A.1 labeled with PKH26, a red fluorescent dye. Confocal microscopy revealed efficient internalization of the ELVs by this macrophage cell line (Fig 8). Internalization was observed diffusely throughout the cell cytoplasm with focus around membrane-rich puncta associated with the surface of the macrophages (Fig 8B). This pattern of internalization is consistent with other studies describing a phagocytic route of vesicle internalization [56, 57]. Macrophages were counterstained with DAPI to determine the efficiency of cell labeling and ELV uptake. PKH26-labeling of J774A.1 was very efficient and all cells were visualized although intensity of labeling was variable (Fig 8D). Approximately 40–50% of macrophages

internalized labeled ELVs to some degree (Fig 8E) with approximately 10% of macrophages internalizing ELVs at markedly higher levels (Fig 8E). There was no correlation between strong PKH 26-labelling of macrophages and vesicle uptake indicating internalization is not a factor of receptiveness to labeling.

Brugia ELVs elicit a classically activated phenotype in host macrophages

Macrophage activation is dichotomous; classically activated macrophages (CAMΦ) are elicited by LPS or IFN-γ and have a generally pro-inflammatory phenotype whereas alternatively activated macrophages (AAMΦ), driven by IL-4 and IL-13, appear immunosuppressive or anti-inflammatory. Helminth infection is typically associated with the AAMΦ pathway although both CAMΦ and AAMΦ are involved in the immune response to, and immunopathology caused by, *Brugia* infection. Experiments demonstrate different *Brugia* preparations can generate both CAMΦ and AAMΦ activation phenotypes; dead and moribund worms and worm lysates produce CAMΦ [58] but live worms and complete excretory/secretory (ES) preparations drive AAMΦ [59-61]. To test the hypothesis that ELVs activate host macrophages, J774A.1 were treated with purified ELV preparations and their cytokine/chemokine responses monitored. J774A.1 were treated for 48 hrs with approximately 4 × 108 L3 stage vesicles, purified from *in vitro* culture medium by ultracentrifugation. The macrophage response was assayed using the Milliplex MAP Mouse Cytokine/Chemokine kit (EDM Millipore) interfaced with a Bio-Plex System (Bio-Rad) utilizing Luminex xMAP technology, a platform capable of simultaneously identifying and quantifying 32 cytokines/chemokines. Vesicle treatment effectively activated J774A.1 macrophages with significant increases in G-CSF, MCP-1, IL-6 and MIP-2 levels compared to control macrophages treated with

naïve RPMI 1640 culture media, ($p \leq 0.001$) (Fig 9A). Smaller increases in LIX, RANTES and TNF-α were also noted. Healthy, viable L3 stage parasites produced an almost identical response (Fig 9A), the only difference being a modest but significant enhancement of G-CSF stimulation by the viable parasites ($p < 0.001$), suggesting that the dominant parasite immunogen(s) are found in the vesicle pellet. Finally, parasite culture media from which the ELVs had been removed by centrifugation did not produce this response, nor did live schistosomes (*S. mansoni* cercaria) or their secreted vesicles suggesting the *Brugia*-associated activation is specific to this parasite and not a general response to helminths or their secreted vesicles.

The activation profile observed would be considered more indicative of a CAMΦ response than AAMΦ; to confirm the response was CAMΦ-like, we compared it to the response elicited by LPS (200 ng/mL). The only significant differences were that ELV treatment stimulated G-CSF and IL-6 less effectively ($p < 0.001$) and stimulated MCP-1 more effectively ($p < 0.001$) than LPS (Fig 9B). The overall conservation of response, however, indicates these ELVs generate a CAMΦ phenotype. Since *Wolbachia*, the endosymbiont present in filarial nematodes, lack LPS biosynthetic capacity it seemed unlikely our CAMΦ-like response was driven by LPS like contamination but to rule this out, endotoxin levels in our vesicle preparation were determined commercially (Lonza, Walkersville, MD). LPS-like activity was present (0.003 ng/mL) but at a concentration several orders of magnitude lower than the minimum dose required to stimulate J774A.1 macrophages [62]. As expected, treatment of macrophages with this low LPS dose was insufficient for activation (Fig 9C) indicating that the CAMΦ response we observe is not due to an LPS-like component in our preparation.

Since the stimulation of an AAMΦ phenotype by live *Brugia* and ES preparations thereof *in vivo* and *in vitro* has been well established [59-61] it might be expected that *Brugia* ELV preparations also stimulate a AAMΦ phenotype, especially since complete *Brugia* ES preparations are likely to include ELVs similar to those examined here, albeit at reduced concentrations. We observed a response consistent with a CAMΦ phenotype, however, although without the acute elevation in IL-β and TNF-α production others have seen in response to LPS [58]. One interpretation is that the CAMΦ > AAMΦ phenotype may be a somewhat artificial function of the homogenous J774A.1 monoculture used here as other studies describing a AAMΦ phenotype often use PBMC or other heterogeneous primary cell types. It would be instructive to monitor the responses of such mixed cell populations to the ELV preparation. Additionally, although the murine model is regarded as valuable for illuminating both how parasites establish themselves and the early host immune response, J774A.1 may not be optimal for studying this particular *Brugia*-host interaction and optimization with other murine or human cells may be required. Another interpretation, however, is that the purified ELVs examined here should be considered a distinct and specific fraction of the highly complex immunogenic facade presented by filarial parasites and may elicit a genuine CAMΦ phenotype when examined in isolation. Supporting this interpretation, exosomes isolated from other biological systems effectively generate a CAMΦ phenotype [57, 63, 64]. A key mediator of this pro-inflammatory response is Hsp70 [63], which was identified in our ELV proteomic profile. In summary, irrespective of the polarity of macrophage activation phenotype, our results unequivocally identify secreted ELVs as distinct parasite-derived structures capable of activating the host immune system.

A picture is emerging that parasitic helminths secrete functional exosome-like vesicles. The protein and small RNA cargo of these vesicles have putative effector functions at the host-parasite interface and potentially serve to create conditions favorable to the establishment or maintenance of infection. The identification of these cell-to-cell effector structures is exciting and prompts further investigation of their functional relevance. In particular, it will be important to describe the roles of individual miRNAs and proteins contained within the ELVs, to identify the host molecular targets being manipulated in vivo, and reveal any conserved or stage-specific effectors secreted across the parasite life cycle. Another intriguing question is whether or not there is any specificity or selectivity in host cells or tissues targeted and if so, what molecular mechanisms underscore this specificity. Addressing such questions will illuminate the fundamental interactions that occur between parasite and host, and may open previously unexploited opportunities for parasite control and diagnostics.

Materials and Methods

Mosquito maintenance

Aedes aegypti (Black eyed Liverpool strain, LVP), previously selected for susceptibility to infection with *Brugia malayi* [65], were maintained in controlled conditions (27°C ± 1°C and 75% ± 5% relative humidity) with a 16:8 photoperiod. Adult mosquitoes were fed a diet of 10% sucrose. Approximately 4,000 and 2,600 mosquitos were used for proteomics and RNA sequencing, respectively.

Establishing *Brugia malayi* infection

For proteomics and transcriptomics, *B. malayi* microfilaria (mf) infected cat blood was obtained from the University of Georgia NIH/NIAID Filariasis Research Reagent Resource Center (FR3). Blood containing the parasites was diluted with defibrinated sheep's blood (Hemostat Laboratories, CA, USA) to achieve a concentration of 80–100 mf per 20μL. To establish infection, 3- to 5-day-old *Ae. Aegypti* (LVP) were allowed to feed for one hour on a glass membrane feeder. Mosquitoes were sucrose-starved for 24 hrs prior to blood feeding and those that did not take a blood meal were removed. Infected mosquitoes were maintained in the above described conditions for 13–15 days post infection (dpi) to allow development of parasites.

***Brugia malayi* maintenance and collection of vesicle-containing media**

In exploratory studies, larval (300 L3) and adult (30 male or 30 female) *B. malayi* were procured from the FR3. On arrival, parasites were cultured in 50 mL RPMI 1640 (Sigma-Aldrich, St. Louis, MO) at 37°C (5% CO2). Cell culture media was collected and replaced at 24 hr intervals for up to 72 hrs to collect secreted ELVs. For downstream sequencing and proteomics, *B. malayi* (13–15 dpi) were locally collected using methods described by FR3. Briefly, infected mosquitoes were immobilized by cooling to 4°C for 15 minutes. Immobilized mosquitoes were crushed in a mortar containing 5 ml of chilled Hanks' balanced salt solution (HBSS, pH 7.0) containing pen-strep (0.4 units penicillin/ml, 0.4 mcg streptomycin/ml). Mosquitoes were then rinsed onto a 150 mesh sieve contained in a deep well plastic petri dish and washed 3–4 times using fresh chilled HBSS + pen-strep. Sieves were then placed into petri dishes containing warm (40°C)

HBSS + pen-strep to allow infective larvae to migrate out. Sieves were transferred to new deep well petri dishes containing fresh warm HBSS every 30 minutes. Collected parasites were washed twice with warm HBSS + pen-strep, placed into 25 mL RPMI 1640 containing pen-strep (0.4 units penicillin/ml, 0.4 mcg streptomycin/ml) and held at 37°C, 5% CO2 for 24 hrs to collect secreted ELVs.

Exosome-like vesicle purification

Differential centrifugation was used to isolate ELVs from 25 or 50 mL aliquots of *Brugia* culture media. Aliquots were collected from 24 hr incubations of larval or adult worms in culture media. Lower speed centrifugation and filtration steps were used to remove contaminating cells (300 × g, 10 minutes) and cellular debris (10,000 × g, 15 minutes). The resulting supernatants underwent filtration through 0.22 μm filters and ultracentrifugation at 105,000 × g for 90 minutes to pellet ELVs. Pellets were then washed with cold phosphate-buffered saline (PBS) and a final spin was carried out at 105,000 × g for 90 minutes. Supernatants were discarded and pellets were resuspended in small volumes (30–250 uL) of PBS for imaging, sequencing, and proteomics, and RPMI for immunological assays. Samples were kept on ice and centrifugation steps were carried out at 4°C. Resuspended ELVs were stored at –80°C.

Electron microscopy and nanoparticle tracking analysis

Small aliquots of ELV suspension (3 μl) were applied to carbon coated 200 mesh copper grids and negatively stained with 2% uranyl acetate. Images were taken using a JEOL 2100 scanning and transmission electron microscope (Japan Electron Optics Laboratories, Akishima, Japan) at the Microscopy and NanoImaging Facility (Iowa State

University). Nanoparticle tracking analysis was carried out with the NanoSight LM10 (NanoSight Ltd., Amesbury, UK) to ascertain the size and frequency distribution of individual vesicle preparations, assayed in triplicate. The Brownian motion of particles in solution is related back to particle sizes and numbers, allowing better statistical resolution of vesicle size and concentration [66].

LC-MS/MS and proteomic analysis

Protein was isolated from purified exosome-like vesicles for proteomic analysis (System Biosciences). Briefly, samples were modified with 10% SDS to a final concentration of 2% SDS, heated at 100°C for 15 minutes and clarified by centrifugation. Protein concentration was determined using a Qubit fluorometry assay (Invitrogen). 15 µg of material was processed by SDS-PAGE using a 10% Bis-Tris homogeneous gel and the MES buffer system. In-gel digestion with trypsin was done at 37°C for 4 hrs using a ProGest robot (DigiLab, Marlborough, MA). The digested sample was analyzed by nano LC-MS/MS analysis using a Waters NanoAcquity HPLC system interfaced to a ThermoFisher Q Exactive. Data were searched against a copy of the *B. malayi* UniProt database (taxon ID: 6278) using a locally running copy of MASCOT (Matrix Science Ltd., London, UK). The search was restricted using the following parameters; maximum missed cleavages = 2, fixed modifications = carbamidomethyl (C), variable modifications = Oxidation (M), Acetyl (N-term), Pyro-Glu (N-term Q) and Deamidation (N, Q), a peptide mass tolerance of 10 ppm, and a fragment mass tolerance of 0.02 Da. Mascot DAT files were parsed into the Scaffold software for validation, filtering and to create a nonredundant list per sample. Data were filtered using a minimum protein value of 90%,

a minimum peptide value of 50% (Prophet scores) and requiring at least two unique peptides per protein.

RNA isolation and sequencing

For detection of RNA species in ELV preparations, small RNAs were preferentially isolated from vesicle-containing pellets using the miRCURY RNA Isolation Kit (Exiqon, Vedbaek, Denmark) and RNA samples were examined with an Agilent 2100 Bioanalyzer using the RNA 6000 Nano Kit. For small RNA sequencing (RNA-Seq), total RNA was isolated from ELVs released by ~5,000 L3s over a 24 hr incubation period using the Total RNA and Protein Isolation Kit (Invitrogen, Carlsbad, CA). In parallel, total RNA was isolated from whole worm tissue using a TRIzol (Invitrogen) protocol, where a 6 hr precipitation step was carried out at -80°C to improve small RNA recovery. RNA NGS libraries were constructed using modified Illumina adapter methods using SBI's XRNA Sample Preparation Kit (System Biosciences, Mountain View, CA) and indexed with separate bar codes for multiplex sequencing on an Illumina MiSeq v3 instrument using a 2 × 75 bp paired end run setting.

miRNA discovery and abundance estimation

Raw reads were trimmed to remove adapter sequences, filtered by quality score, and de-multiplexed using the FASTX-Toolkit [67] (sequencing data are deposited with the NCBI SRA under project number PRJNA285132). The miRDeep2 pipeline was used to map short RNA reads (>15 nt) to the *B. malayi* genome for miRNA discovery, and to estimate and normalize miRNA abundances with respect to total miRNA read count. Nematode precursor and mature miRNA sequences deposited into miRBase [68] were

used in the pipeline, including known *B. pahangi*, *Caenorhabditis elegans*, *Ascaris suum*, *Haemonchus contortus*, and *Strongyloides ratti* miRNAs. Non-mapped reads were ranked by abundance, filtered for homology against known miRNAs in the phylum Nematoda using BLASTn [69], and incorporated for final quantification of abundance with the miRDeep quantifier script, allowing for capture of miRNAs that did not map to the *B. malayi* assembly due to sequencing gaps. The ggplot2 package [70] of the statistical programming language *R* was used to organize and visualize comparisons between vesicular and tissue RNA samples.

Cell culture

J774A.1 murine macrophages (ATCC, Manassas, VA) were maintained in complete tissue culture medium (Dulbecco's modified Eagle's medium, 25 mM HEPES, pH 7.4 supplemented with 2 mM L-glutamine, 100 U/mL penicillin, 100 μg/mL streptomycin, 0.05 μM 2-mercaptoethanol, and 10% heat-inactivated fetal bovine serum) at 37°C and 5% CO2. 24 hrs prior to assays, 400 μL cells were plated in standard 24-well plates at a density of 5 × 105 cells/well.

Vesicle labeling and uptake

Exosome-like vesicles were purified from a 24 hr culture of 300 *Brugia malayi* L3 parasites as described above and labeled with the green fluorescent dye, PKH67 (Sigma-Aldrich, St Louis, MO, USA), according to the manufacturer's instructions. ELVs were incubated with PKH67 for 5 minutes at room temperature and the reaction terminated by addition of 1% BSA in PBS. RPMI 1640 media was added, mixed and centrifuged at 105,000 × g for 1 hr to separate ELV-bound PKH67 from excess PKH67.

Labeled ELV were washed again then resuspended in an appropriate volume of complete tissue culture medium (Dulbecco's modified Eagles medium, 25 mM HEPES, pH 7.4 supplemented with 2 mM L-glutamine, 100 U/mL penicillin, 100 µg/mL streptomycin, 0.05 µM 2-mercaptoethanol and 10% heat-inactivated fetal bovine serum).

J774A.1 were labeled with red fluorescent lipophilic dye, PKH26 (Sigma-Aldrich, St Louis, MO), according to the manufacturer's instructions. Macrophages were incubated with PKH26 for 5 minutes at room temperature and the reaction terminated by addition of 1% BSA. To remove excess unbound dye, samples were centrifuged at 400 × g for 10 minutes at room temperature and the supernatant discarded. Centrifugation was repeated three more times using 10 ml of complete media to ensure full removal of unbound dye and the cells were re-suspended in 1 mL of complete medium. Approximately 3×10^5 labeled cells were plated onto sterile coverslips and incubated overnight at 37°C/5% CO2. Labeled ELV suspension (approximately 3×10^7 per coverslip) was added to labeled J774A.1 and incubated for 6 hrs. Cells were washed 5 times with ice-cold PBS to remove excess labeled ELVs, the cells fixed in 4% paraformaldehyde (Sigma-Aldrich), washed and counterstained with DAPI before mounting and storage at 4°C. Preparations were visualized using a Leica TCS SP5 X Confocal/multiphoton microscope system (Leica Microsystems Inc., Buffalo Grove, IL).

Detection of macrophage modulation by Luminex assay

Triplicate wells of adhered J774A.1 were treated with approximately 4×10^8 purified L3 stage ELVs. The ELVs were purified by ultracentrifugation as previously described, resuspended in RPMI 1640 medium (Gibco/Life Technologies, Carlsbad, CA)

and quantified by nanoparticle tracking analysis. Other treatments were similar volumes of vesicle depleted L3 culture medium (supernatant created following pelleting of ELV fraction from spent parasite culture medium), live *B. malayi* L3 parasites (10 worms/well), lipopolysaccharide (LPS; final concentration 200 ng/mL)(Sigma-Aldrich, St. Louis, MO), naïve RPMI 1640 culture medium and various combinations of these conditions. Supernatants from these cell cultures (400 µL/well) were collected 24 or 48 hrs post-treatment and centrifuged briefly (2,000 × g for 10 minutes) to remove non-adhered cells and cell debris before being analyzed for the presence of cytokines/ chemokines. The Milliplex MAP Mouse Cytokine/Chemokine kit (EDM Millipore, Billerica, MA) interfaced with a Bio-Plex System (Bio-Rad, Hercules, CA) utilizing Luminex xMAP technology (Luminex, Austin, TX) allowed the simultaneous identification and quantification of the following analytes in the cell culture supernatant: Eotaxin, G-CSF, GM-CSF, IFNγ, IL-1α, M-CSF, IL-1β, IL-2, IL-3, IL-4, IL-5, IL-6, IL-7, IL-10, IL-12 (p40), IL-13, IL-15, IL-17, IP-10, MIP-2, KC, LIF, LIX, MCP-1, MIP-1α, MIP-1β, MIG, RANTES, TNFα, IL-12(p70), VEGF, IL-9. Briefly, experimental samples, background, standards and controls were added to a 96-well plate and combined with equal volumes of pre-mixed, antibody coated magnetic beads; the plate was sealed and incubated overnight at 4°C. Following washing, 25 µL of detection antibody was added and the plate incubated for one hour at room temperature with shaking. Streptavidin-Phycoerythrin (25 µL) was added to each well and the plate incubated for a further hour at room temperature before washing. Finally, 150 µL assay buffer was added to all wells and fluorescence immediately recorded. Median fluorescent intensity data

were analyzed as recommended using a five-parameter logistic curve-fitting method for calculating cytokine/ chemokine concentration.

G-CSF ELISA

Triplicate wells of adhered J774A.1 cells, prepared as described above, were treated with LPS (final concentration 200 ng/mL or 0.003 ng/mL), approximately 4×10^8 purified L3 stage ELVs as described above, or RPMI 1640 as negative control. Cell culture supernatants were collected 24 hrs after treatment, cleared via centrifugation as described previously and assayed for G-CSF using a Mouse G-CSF Quantikine ELISA kit (R&D Systems, Minneapolis, MN). Standard curves were generated using Prism 6 software (GraphPad Software, San Diego, CA) and sample G-CSF concentrations determined by regression analysis.

Statistical analysis

For analysis of Luminex data, Tukey's test was used to compare overall treatments while multiple t-tests, incorporating the Holm-Sidak method to correct for multiple comparisons, were used to compare individual chemokines/cytokines following treatments. T-tests were used to compare treatment groups following ELISA analysis. All statistical analyses were performed using Prism 6 for Mac (GraphPad).

Author Contributions

Conceived and designed the experiments: MZ LMF LCB MJK ARM. Performed the experiments: MZ LMF HH PNA. Analyzed the data: MZ LMF TAD LCB MJK.

Contributed reagents/materials/analysis tools: ARM. Wrote the paper: MZ LMF LCB MJK.

Acknowledgments

The authors would like to thank Marie Bockenstedt, Mary J. Long, and Dr. Douglas E. Jones for helpful discussions and technical guidance relating to the Luminex experiments. The authors would also like to acknowledge parasite materials provided by Erica Burkman and the NIH-NIAID Filariasis Research Reagent Resource Center (FR3). The authors thank Michael Nazarchyk and Brendan Dunphy for technical assistance with mosquito infections and mosquito maintenance, and Morgan Pearson for assistance with vesicle isolation.

References

1. Global programme to eliminate lymphatic filariasis: progress report, 2011. Wkly Epidemiol Rec. 2012;87(37):346-56. PubMed PMID: 22977953.

2. Bartholomay LC, Christensen BM. Vector-parasite interactions in mosquito-borne filariasis. In: Klei TR, Rajan TV, editors. The Filaria. World Class Parasites. Norwell, MA: Kluwer Academic Press; 2002. p. 9-20.

3. Erickson SM, Xi Z, Mayhew GF, Ramirez JL, Aliota MT, Christensen BM, et al. Mosquito infection responses to developing filarial worms. PLoS Negl Trop Dis. 2009;3(10):e529. doi: 10.1371/journal.pntd.0000529. PubMed PMID: 19823571; PubMed Central PMCID: PMCPMC2752998.

4. Allen JE, Maizels RM. Diversity and dialogue in immunity to helminths. Nat Rev Immunol. 2011;11(6):375-88. doi: 10.1038/nri2992. PubMed PMID: 21610741.

5. Maizels RM, Pearce EJ, Artis D, Yazdanbakhsh M, Wynn TA. Regulation of pathogenesis and immunity in helminth infections. J Exp Med. 2009;206(10):2059-66.

doi: 10.1084/jem.20091903. PubMed PMID: 19770272; PubMed Central PMCID: PMCPMC2757871.

6. van Riet E, Hartgers FC, Yazdanbakhsh M. Chronic helminth infections induce immunomodulation: consequences and mechanisms. Immunobiology. 2007;212(6):475-90. doi: 10.1016/j.imbio.2007.03.009. PubMed PMID: 17544832.

7. Hoerauf A, Satoguina J, Saeftel M, Specht S. Immunomodulation by filarial nematodes. Parasite Immunol. 2005;27(10-11):417-29. doi: 10.1111/j.1365-3024.2005.00792.x. PubMed PMID: 16179035.

8. Devaney E, Osborne J. The third-stage larva (L3) of *Brugia*: its role in immune modulation and protective immunity. Microbes Infect. 2000;2(11):1363-71. PubMed PMID: 11018453.

9. Zang X, Yazdanbakhsh M, Jiang H, Kanost MR, Maizels RM. A novel serpin expressed by blood-borne microfilariae of the parasitic nematode *Brugia malayi* inhibits human neutrophil serine proteinases. Blood. 1999;94(4):1418-28. PubMed PMID: 10438730.

10. Zang X, Atmadja AK, Gray P, Allen JE, Gray CA, Lawrence RA, et al. The serpin secreted by *Brugia malayi* microfilariae, Bm-SPN-2, elicits strong, but short-lived, immune responses in mice and humans. J Immunol. 2000;165(9):5161-9. PubMed PMID: 11046048.

11. Falcone FH, Loke P, Zang X, MacDonald AS, Maizels RM, Allen JE. A *Brugia malayi* homolog of macrophage migration inhibitory factor reveals an important link between macrophages and eosinophil recruitment during nematode infection. J Immunol. 2001;167(9):5348-54. PubMed PMID: 11673551.

12. Zang X, Taylor P, Wang JM, Meyer DJ, Scott AL, Walkinshaw MD, et al. Homologues of human macrophage migration inhibitory factor from a parasitic nematode. Gene cloning, protein activity, and crystal structure. J Biol Chem. 2002;277(46):44261-7. doi: 10.1074/jbc.M204655200. PubMed PMID: 12221083.

13. Hewitson JP, Harcus YM, Curwen RS, Dowle AA, Atmadja AK, Ashton PD, et al. The secretome of the filarial parasite, *Brugia malayi*: proteomic profile of adult excretory-secretory products. Mol Biochem Parasitol. 2008;160(1):8-21. doi: 10.1016/j.molbiopara.2008.02.007. PubMed PMID: 18439691.

14. Moreno Y, Geary TG. Stage- and gender-specific proteomic analysis of *Brugia malayi* excretory-secretory products. PLoS Negl Trop Dis. 2008;2(10):e326. doi: 10.1371/journal.pntd.0000326. PubMed PMID: 18958170; PubMed Central PMCID: PMCPMC2569413.

15. Bennuru S, Semnani R, Meng Z, Ribeiro JM, Veenstra TD, Nutman TB. *Brugia malayi* excreted/secreted proteins at the host/parasite interface: stage- and gender-specific proteomic profiling. PLoS Negl Trop Dis. 2009;3(4):e410. doi: 10.1371/journal.pntd.0000410. PubMed PMID: 19352421; PubMed Central PMCID: PMCPMC2659452.

16. Geary J, Satti M, Moreno Y, Madrill N, Whitten D, Headley SA, et al. First analysis of the secretome of the canine heartworm, *Dirofilaria immitis*. Parasit Vectors. 2012;5:140. doi: 10.1186/1756-3305-5-140. PubMed PMID: 22781075; PubMed Central PMCID: PMCPMC3439246.

17. Tawill S, Le Goff L, Ali F, Blaxter M, Allen JE. Both free-living and parasitic nematodes induce a characteristic Th2 response that is dependent on the presence of intact glycans. Infect Immun. 2004;72(1):398-407. PubMed PMID: 14688121; PubMed Central PMCID: PMCPMC343992.

18. Valadi H, Ekström K, Bossios A, Sjöstrand M, Lee JJ, Lötvall JO. Exosome-mediated transfer of mRNAs and microRNAs is a novel mechanism of genetic exchange between cells. Nat Cell Biol. 2007;9(6):654-9. doi: 10.1038/ncb1596. PubMed PMID: 17486113.

19. Mittelbrunn M, Gutiérrez-Vázquez C, Villarroya-Beltri C, González S, Sánchez-Cabo F, González M, et al. Unidirectional transfer of microRNA-loaded exosomes from T cells to antigen-presenting cells. Nat Commun. 2011;2:282. doi: 10.1038/ncomms1285. PubMed PMID: 21505438; PubMed Central PMCID: PMCPMC3104548.

20. Vickers KC, Palmisano BT, Shoucri BM, Shamburek RD, Remaley AT. MicroRNAs are transported in plasma and delivered to recipient cells by high-density lipoproteins. Nat Cell Biol. 2011;13(4):423-33. doi: 10.1038/ncb2210. PubMed PMID: 21423178; PubMed Central PMCID: PMCPMC3074610.

21. Montecalvo A, Larregina AT, Shufesky WJ, Stolz DB, Sullivan ML, Karlsson JM, et al. Mechanism of transfer of functional microRNAs between mouse dendritic cells via exosomes. Blood. 2012;119(3):756-66. doi: 10.1182/blood-2011-02-338004. PubMed PMID: 22031862; PubMed Central PMCID: PMCPMC3265200.

22. Chen X, Liang H, Zhang J, Zen K, Zhang CY. Secreted microRNAs: a new form of intercellular communication. Trends Cell Biol. 2012;22(3):125-32. doi: 10.1016/j.tcb.2011.12.001. PubMed PMID: 22260888.

23. Kalra H, Simpson RJ, Ji H, Aikawa E, Altevogt P, Askenase P, et al. Vesiclepedia: a compendium for extracellular vesicles with continuous community annotation. PLoS Biol. 2012;10(12):e1001450. doi: 10.1371/journal.pbio.1001450. PubMed PMID: 23271954; PubMed Central PMCID: PMCPMC3525526.

24. van Niel G, Porto-Carreiro I, Simoes S, Raposo G. Exosomes: a common pathway for a specialized function. J Biochem. 2006;140(1):13-21. doi: 10.1093/jb/mvj128. PubMed PMID: 16877764.

25. Lakkaraju A, Rodriguez-Boulan E. Itinerant exosomes: emerging roles in cell and tissue polarity. Trends Cell Biol. 2008;18(5):199-209. doi: 10.1016/j.tcb.2008.03.002. PubMed PMID: 18396047; PubMed Central PMCID: PMCPMC3754907.

26. Buck AH, Coakley G, Simbari F, McSorley HJ, Quintana JF, Le Bihan T, et al. Exosomes secreted by nematode parasites transfer small RNAs to mammalian cells and modulate innate immunity. Nat Commun. 2014;5:5488. doi: 10.1038/ncomms6488. PubMed PMID: 25421927.

27. Twu O, de Miguel N, Lustig G, Stevens GC, Vashisht AA, Wohlschlegel JA, et al. Trichomonas vaginalis exosomes deliver cargo to host cells and mediate host：parasite interactions. PLoS Pathog. 2013;9(7):e1003482. doi: 10.1371/journal.ppat.1003482. PubMed PMID: 23853596; PubMed Central PMCID: PMCPMC3708881.

28. Marcilla A, Trelis M, Cortés A, Sotillo J, Cantalapiedra F, Minguez MT, et al. Extracellular vesicles from parasitic helminths contain specific excretory/secretory proteins and are internalized in intestinal host cells. PLoS One. 2012;7(9):e45974. doi: 10.1371/journal.pone.0045974. PubMed PMID: 23029346; PubMed Central PMCID: PMCPMC3454434.

29. Bernal D, Trelis M, Montaner S, Cantalapiedra F, Galiano A, Hackenberg M, et al. Surface analysis of *Dicrocoelium dendriticum*. The molecular characterization of exosomes reveals the presence of miRNAs. J Proteomics. 2014;105:232-41. doi: 10.1016/j.jprot.2014.02.012. PubMed PMID: 24561797.

30. Silverman JM, Clos J, de'Oliveira CC, Shirvani O, Fang Y, Wang C, et al. An exosome-based secretion pathway is responsible for protein export from Leishmania and communication with macrophages. J Cell Sci. 2010;123(Pt 6):842-52. doi: 10.1242/jcs.056465. PubMed PMID: 20159964.

31. Chen XM, Splinter PL, O'Hara SP, LaRusso NF. A cellular micro-RNA, let-7i, regulates Toll-like receptor 4 expression and contributes to cholangiocyte immune responses against *Cryptosporidium parvum* infection. J Biol Chem. 2007;282(39):28929-38. doi: 10.1074/jbc.M702633200. PubMed PMID: 17660297; PubMed Central PMCID: PMCPMC2194650.

32. Kumar M, Ahmad T, Sharma A, Mabalirajan U, Kulshreshtha A, Agrawal A, et al. Let-7 microRNA-mediated regulation of IL-13 and allergic airway inflammation. J Allergy Clin Immunol. 2011;128(5):1077-85.e1-10. doi: 10.1016/j.jaci.2011.04.034. PubMed PMID: 21616524.

33. Banerjee S, Xie N, Cui H, Tan Z, Yang S, Icyuz M, et al. MicroRNA let-7c regulates macrophage polarization. J Immunol. 2013;190(12):6542-9. doi: 10.4049/jimmunol.1202496. PubMed PMID: 23667114; PubMed Central PMCID: PMCPMC3679284.

34. Lodish HF, Zhou B, Liu G, Chen CZ. Micromanagement of the immune system by microRNAs. Nat Rev Immunol. 2008;8(2):120-30. doi: 10.1038/nri2252. PubMed PMID: 18204468.

35. Simpson RJ, Kalra H, Mathivanan S. ExoCarta as a resource for exosomal research. J Extracell Vesicles. 2012;1. doi: 10.3402/jev.v1i0.18374. PubMed PMID: 24009883; PubMed Central PMCID: PMCPMC3760644.

36. Chen CY, Hogan MC, Ward CJ. Purification of exosome-like vesicles from urine. Methods Enzymol. 2013;524:225-41. doi: 10.1016/B978-0-12-397945-2.00013-5. PubMed PMID: 23498743; PubMed Central PMCID: PMCPMC4028690.

37. Binns D, Dimmer E, Huntley R, Barrell D, O'Donovan C, Apweiler R. QuickGO: a web-based tool for Gene Ontology searching. Bioinformatics. 2009;25(22):3045-6. doi: 10.1093/bioinformatics/btp536. PubMed PMID: 19744993; PubMed Central PMCID: PMCPMC2773257.

38. Huntley RP, Sawford T, Mutowo-Meullenet P, Shypitsyna A, Bonilla C, Martin MJ, et al. The GOA database: gene Ontology annotation updates for 2015. Nucleic Acids

Res. 2015;43(Database issue):D1057-63. doi: 10.1093/nar/gku1113. PubMed PMID: 25378336; PubMed Central PMCID: PMCPMC4383930.

39. Guiliano DB, Hong X, McKerrow JH, Blaxter ML, Oksov Y, Liu J, et al. A gene family of cathepsin L-like proteases of filarial nematodes are associated with larval molting and cuticle and eggshell remodeling. Mol Biochem Parasitol. 2004;136(2):227-42. PubMed PMID: 15478801.

40. Ford L, Zhang J, Liu J, Hashmi S, Fuhrman JA, Oksov Y, et al. Functional analysis of the cathepsin-like cysteine protease genes in adult *Brugia malayi* using RNA interference. PLoS Negl Trop Dis. 2009;3(2):e377. doi: 10.1371/journal.pntd.0000377. PubMed PMID: 19190745; PubMed Central PMCID: PMCPMC2634747.

41. Song C, Gallup JM, Day TA, Bartholomay LC, Kimber MJ. Development of an *in vivo* RNAi protocol to investigate gene function in the filarial nematode, *Brugia malayi*. PLoS Pathog. 2010;6(12):e1001239. doi: 10.1371/journal.ppat.1001239. PubMed PMID: 21203489; PubMed Central PMCID: PMCPMC3009605.

42. Lustigman S, Zhang J, Liu J, Oksov Y, Hashmi S. RNA interference targeting cathepsin L and Z-like cysteine proteases of *Onchocerca volvulus* confirmed their essential function during L3 molting. Mol Biochem Parasitol. 2004;138(2):165-70. doi: 10.1016/j.molbiopara.2004.08.003. PubMed PMID: 15555728.

43. Rhoads ML, Fetterer RH. Developmentally regulated secretion of cathepsin L-like cysteine proteases by *Haemonchus contortus*. J Parasitol. 1995;81(4):505-12. PubMed PMID: 7623189.

44. Dalton JP, Neill SO, Stack C, Collins P, Walshe A, Sekiya M, et al. *Fasciola hepatica* cathepsin L-like proteases: biology, function, and potential in the development of first generation liver fluke vaccines. Int J Parasitol. 2003;33(11):1173-81. PubMed PMID: 13678633.

45. Friedländer MR, Mackowiak SD, Li N, Chen W, Rajewsky N. miRDeep2 accurately identifies known and hundreds of novel microRNA genes in seven animal clades. Nucleic Acids Res. 2012;40(1):37-52. doi: 10.1093/nar/gkr688. PubMed PMID: 21911355; PubMed Central PMCID: PMCPMC3245920.

46. Tritten L, Burkman E, Moorhead A, Satti M, Geary J, Mackenzie C, et al. Detection of circulating parasite-derived microRNAs in filarial infections. PLoS Negl Trop Dis. 2014;8(7):e2971. doi: 10.1371/journal.pntd.0002971. PubMed PMID: 25033073; PubMed Central PMCID: PMCPMC4102413.

47. Tritten L, O'Neill M, Nutting C, Wanji S, Njouendoui A, Fombad F, et al. *Loa loa* and *Onchocerca ochengi* miRNAs detected in host circulation. Mol Biochem Parasitol. 2014;198(1):14-7. doi: 10.1016/j.molbiopara.2014.11.001. PubMed PMID: 25461483.

48. Quintana JF, Makepeace BL, Babayan SA, Ivens A, Pfarr KM, Blaxter M, et al. Extracellular *Onchocerca*-derived small RNAs in host nodules and blood. Parasit Vectors. 2015;8:58. doi: 10.1186/s13071-015-0656-1. PubMed PMID: 25623184; PubMed Central PMCID: PMCPMC4316651.

49. Johnson SM, Grosshans H, Shingara J, Byrom M, Jarvis R, Cheng A, et al. RAS is regulated by the let-7 microRNA family. Cell. 2005;120(5):635-47. doi: 10.1016/j.cell.2005.01.014. PubMed PMID: 15766527.

50. Johnson CD, Esquela-Kerscher A, Stefani G, Byrom M, Kelnar K, Ovcharenko D, et al. The let-7 microRNA represses cell proliferation pathways in human cells. Cancer Res. 2007;67(16):7713-22. doi: 10.1158/0008-5472.CAN-07-1083. PubMed PMID: 17699775.

51. Roush S, Slack FJ. The let-7 family of microRNAs. Trends Cell Biol. 2008;18(10):505-16. doi: 10.1016/j.tcb.2008.07.007. PubMed PMID: 18774294.

52. Schulte LN, Eulalio A, Mollenkopf HJ, Reinhardt R, Vogel J. Analysis of the host microRNA response to *Salmonella* uncovers the control of major cytokines by the let-7 family. EMBO J. 2011;30(10):1977-89. doi: 10.1038/emboj.2011.94. PubMed PMID: 21468030; PubMed Central PMCID: PMCPMC3098495.

53. Androulidaki A, Iliopoulos D, Arranz A, Doxaki C, Schworer S, Zacharioudaki V, et al. The kinase Akt1 controls macrophage response to lipopolysaccharide by regulating microRNAs. Immunity. 2009;31(2):220-31. doi: 10.1016/j.immuni.2009.06.024. PubMed PMID: 19699171; PubMed Central PMCID: PMCPMC2865583.

54. Liu G, Abraham E. MicroRNAs in immune response and macrophage polarization. Arterioscler Thromb Vasc Biol. 2013;33(2):170-7. doi: 10.1161/ATVBAHA.112.300068. PubMed PMID: 23325473; PubMed Central PMCID: PMCPMC3549532.

55. van Helden SF, van Leeuwen FN, Figdor CG. Human and murine model cell lines for dendritic cell biology evaluated. Immunol Lett. 2008;117(2):191-7. doi: 10.1016/j.imlet.2008.02.003. PubMed PMID: 18384885.

56. Feng D, Zhao WL, Ye YY, Bai XC, Liu RQ, Chang LF, et al. Cellular internalization of exosomes occurs through phagocytosis. Traffic. 2010;11(5):675-87. doi: 10.1111/j.1600-0854.2010.01041.x. PubMed PMID: 20136776.

57. Atay S, Gercel-Taylor C, Taylor DD. Human trophoblast-derived exosomal fibronectin induces pro-inflammatory IL-1β production by macrophages. Am J Reprod Immunol. 2011;66(4):259-69. doi: 10.1111/j.1600-0897.2011.00995.x. PubMed PMID: 21410811.

58. Taylor MJ, Cross HF, Bilo K. Inflammatory responses induced by the filarial nematode *Brugia* malayi are mediated by lipopolysaccharide-like activity from endosymbiotic Wolbachia bacteria. J Exp Med. 2000;191(8):1429-36. PubMed PMID: 10770808; PubMed Central PMCID: PMCPMC2193140.

59. Osborne J, Hunter SJ, Devaney E. Anti-interleukin-4 modulation of the Th2 polarized response to the parasitic nematode *Brugia pahangi*. Infect Immun. 1996;64(9):3461-6. PubMed PMID: 8751885; PubMed Central PMCID: PMCPMC174249.

60. Allen JE, MacDonald AS. Profound suppression of cellular proliferation mediated by the secretions of nematodes. Parasite Immunol. 1998;20(5):241-7. PubMed PMID: 9651925.

61. Weinkopff T, Mackenzie C, Eversole R, Lammie PJ. Filarial excretory-secretory products induce human monocytes to produce lymphangiogenic mediators. PLoS Negl Trop Dis. 2014;8(7):e2893. doi: 10.1371/journal.pntd.0002893. PubMed PMID: 25010672; PubMed Central PMCID: PMCPMC4091784.

62. Amano F, Akamatsu Y. A lipopolysaccharide (LPS)-resistant mutant isolated from a macrophagelike cell line, J774.1, exhibits an altered activated-macrophage phenotype in response to LPS. Infect Immun. 1991;59(6):2166-74. PubMed PMID: 1645329; PubMed Central PMCID: PMCPMC257982.

63. Anand PK, Anand E, Bleck CK, Anes E, Griffiths G. Exosomal Hsp70 induces a pro-inflammatory response to foreign particles including mycobacteria. PLoS One. 2010;5(4):e10136. doi: 10.1371/journal.pone.0010136. PubMed PMID: 20405033; PubMed Central PMCID: PMCPMC2853569.

64. Atay S, Gercel-Taylor C, Suttles J, Mor G, Taylor DD. Trophoblast-derived exosomes mediate monocyte recruitment and differentiation. Am J Reprod Immunol. 2011;65(1):65-77. doi: 10.1111/j.1600-0897.2010.00880.x. PubMed PMID: 20560914.

65. MacDonald WW. The selection of a strain of *Aedes aegypti* susceptible to infection with semi-periodic *Brugia malayi.* Annals of Tropical Medicine and Parasitology. 1962;56:368-72.

66. Filipe V, Hawe A, Jiskoot W. Critical evaluation of Nanoparticle Tracking Analysis (NTA) by NanoSight for the measurement of nanoparticles and protein aggregates. Pharm Res. 2010;27(5):796-810. doi: 10.1007/s11095-010-0073-2. PubMed PMID: 20204471; PubMed Central PMCID: PMCPMC2852530.

67. A G, G H. FASTQ/A short-reads pre-processing tools 2010. Available from: hannonlab.cshl.edu/fastx_toolkit.

68. Griffiths-Jones S, Saini HK, van Dongen S, Enright AJ. miRBase: tools for microRNA genomics. Nucleic Acids Res. 2008;36(Database issue):D154-8. doi: 10.1093/nar/gkm952. PubMed PMID: 17991681; PubMed Central PMCID: PMCPMC2238936.

69. Altschul SF, Gish W, Miller W, Myers EW, Lipman DJ. Basic local alignment search tool. J Mol Biol. 1990;215(3):403-10. doi: 10.1016/S0022-2836(05)80360-2. PubMed PMID: 2231712.

70. H W. ggplot2 2009.

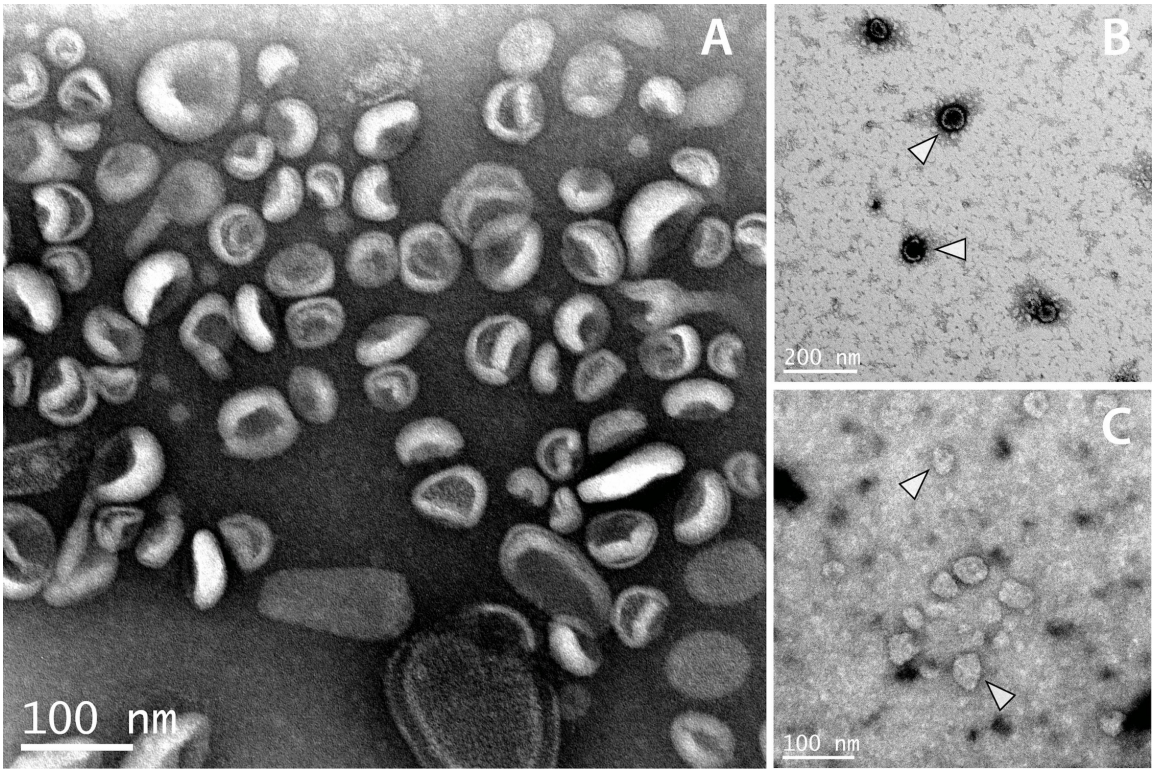

Fig 1. Electron microscopy confirms secretion of exosome-like vesicles in intra-host stages of *B. malayi*. TEM images of L3 (A and B) and adult female (C) ELV preparations are shown. L3 vesicles take on a distinct morphology often reported in the literature. Adult isolations are more heterogenous and may require further optimization to achieve uniform vesicle preparation. White arrows show canonical L3 ELVs (B) and putative adult ELVs (C). This provides evidence for the release of exosome-like vesicles in the human-infective L3 stage of the parasite and much of the rest of the work we report is focused on vesicles derived from this larval stage.

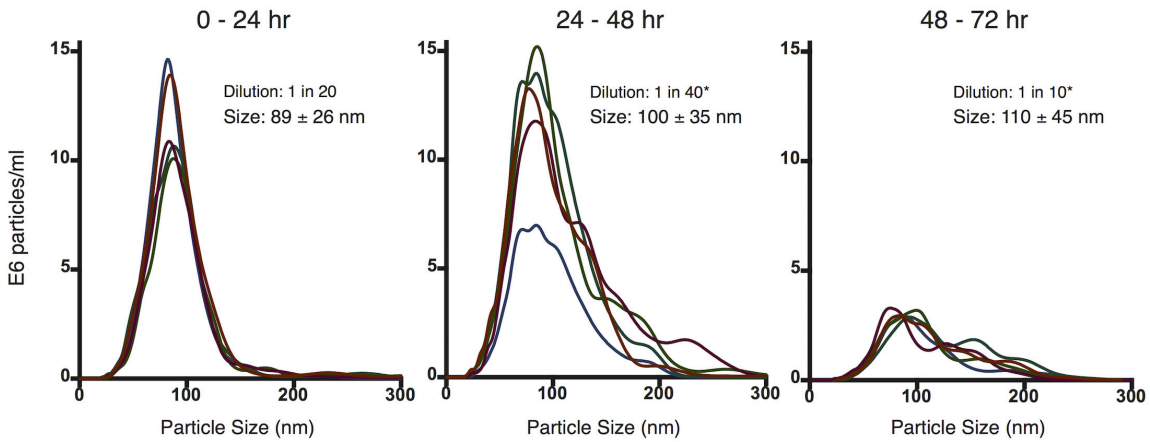

	ELVs	/parasite/min
0 - 24 hr	4.0×10^9	9,300
24 - 48 hr	4.5×10^9	10,400
48 - 72 hr	1.7×10^9	3,900

Fig 2. Particle tracking analysis reveals prolific larval *Brugia* exosome-like vesicle release rate. Profile of ELVs isolated from culture media incubated with 300 L3 parasites for successive 24 hr incubations. The size distribution of L3-derived ELVs from Day 1 (left), Day 2 (center) and Day 3 (right) incubations are shown (mean ± SD). Calculated vesicle release rates are provided in tabular format. ELV rate of release and size specificity decay in a time-dependent manner *in vitro*. * re-scaled based on dilution for comparison to 0–24 hour (1:20) dilution.

Table 1. Annotation of *Brugia* ELV proteome.

Brugia Protein ID	UniProt ID	Annotation
BM-ACT-5	A8P5A0_BRUMA	Actin
Bm-HSP-1	A8P6Q6_BRUMA	HSP70
Bm5195	A8PJ17_BRUMA	Elongation factor 1-alpha
BM-EEF-2	A8PJV1_BRUMA	Elongation factor 2
Bm4733	A8PHP7_BRUMA	Beta-tubulin
BM-MEC-12	A8PN52_BRUMA	Alpha-tubulin like
BM-DPY-23	A8PZJ6_BRUMA	Adaptin
Bm13837	A8QAR6_BRUMA	ATP synthase subunit alpha
Bm-ATP-2	A8Q895_BRUMA	ATP synthase subunit beta
Bm5931	A8P4C6_BRUMA	Alpha-1,4 glucan phosphorylase
BM-CPL-1	A8NCV6_BRUMA	Cathepsin L-like cysteine protease
BM-EAT-6	A8Q4C9_BRUMA	Na^+K^+ATPase
Bm-SCA-1	A8QET1_BRUMA	Calcium-transporting ATPase
BM-RAB-1	A8Q8U0_BRUMA	Ras-related protein
Bm4628	A8NSV0_BRUMA	Ubiquitin
Bm5528	A8NHQ1_BRUMA	1,4-alpha-glucan branching enzyme
BM-DLST-1	A8PU77_BRUMA	2-oxoglutarate dehydrogenase
Bm3206	A8NHD8_BRUMA	Histone H2B
Bm3425	A8NHD2_BRUMA	Histone H3
Bm4113	A8Q1K1_BRUMA	Histone H4
Ribosomal Proteins		
BM-RPS-16	A8P1D4_BRUMA	40S ribosomal protein S16
Bm2853	A8Q0J1_BRUMA	40S ribosomal protein S2
Bm2320	A8NXR7_BRUMA	40S ribosomal protein S3
BM-SECS-1	A8PJH5_BRUMA	40S ribosomal protein S5
BM-RPS-9	A8P2X1_BRUMA	40S ribosomal protein S9
Bm13774	A8PTY7_BRUMA	60S ribosomal protein L10
Bm13718	A8NKQ0_BRUMA	60S ribosomal protein L11
BM-RPL-3	A8P136_BRUMA	60S ribosomal protein L3
BM-RPL-9	A8QHP9_BRUMA	60S ribosomal protein L9
Bm3930	A8ND23_BRUMA	Ribosomal protein
BM-RPL-1	A8NG31_BRUMA	Ribosomal protein

Homology-based annotation of *B. malayi* ELV proteins reveals hallmarks of mammalian exosomes, including HSP70 and translation elongation factors. Ribosomal proteins, histones, ras-related proteins, cathepsins, ATP synthase subunits, and other homologs of identified *Brugia* ELV proteins have also been reported in exosomes derived from various cell types.

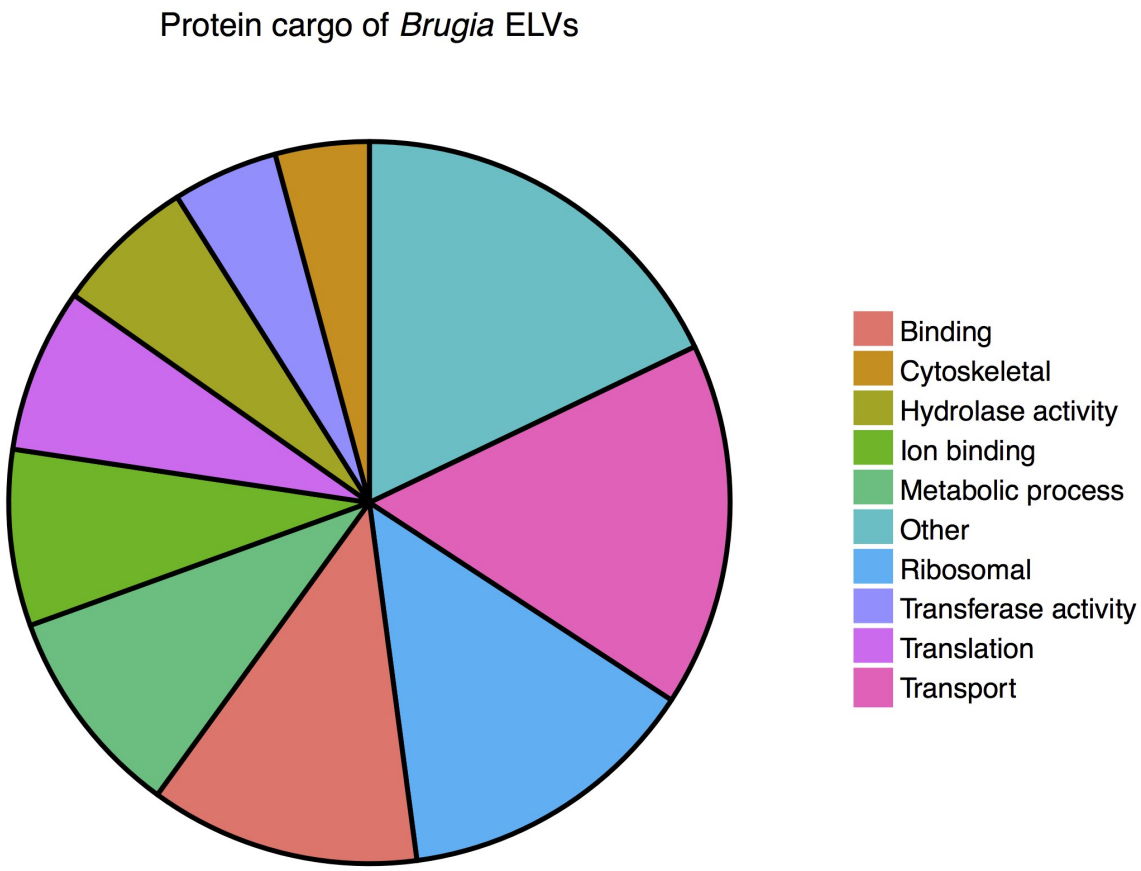

Fig 3. Protein content of *B. malayi* exosome-like vesicles. GO functional annotation of 32 proteins identified in ELVs isolated from *B. malayi* L3 stage parasites.

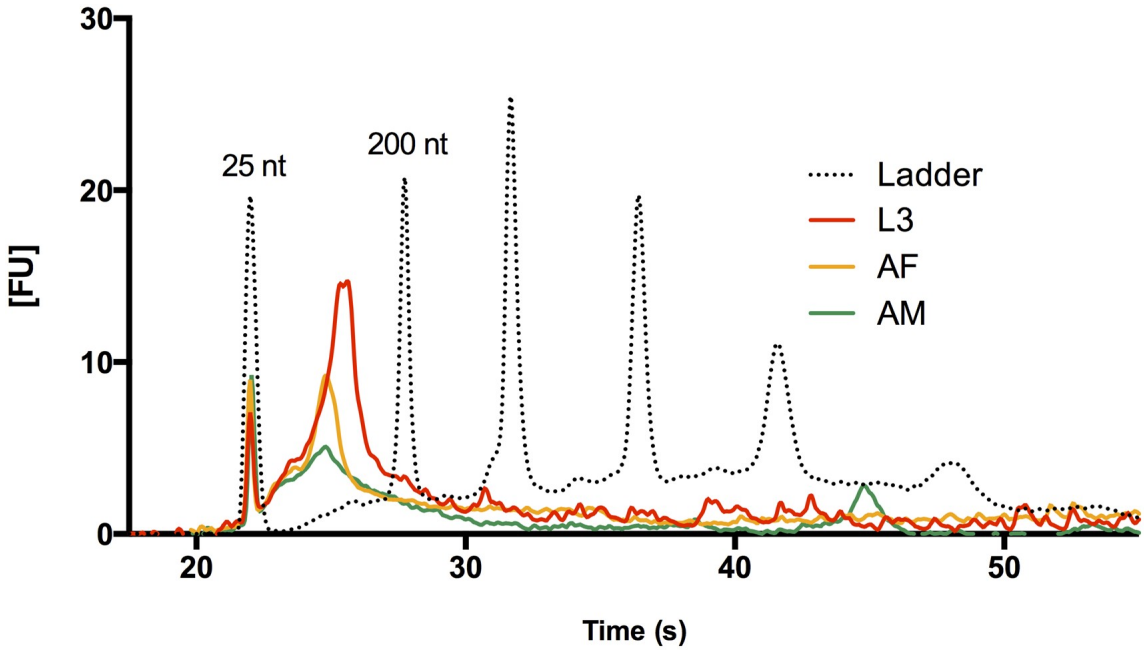

Fig 4. Isolation of Small RNAs from larval and adult *B. malayi* ELV fractions. Bioanalyzer data are shown for RNAs isolated from L3, adult male, and adult female *Brugia* preparations. L3 ELVs contain significant amounts of small RNAs in the 25–200 nt range (25 and 200 nt reference peaks labeled), while adult male and female vesicle preparations yield fewer RNAs. Vesicle fractions were prepared from 300 L3 and 30 adults in 24 hr culture incubations. Despite the much higher total tissue amounts used in adult culture, we detect much higher levels of small RNAs in L3-derived ELVs.

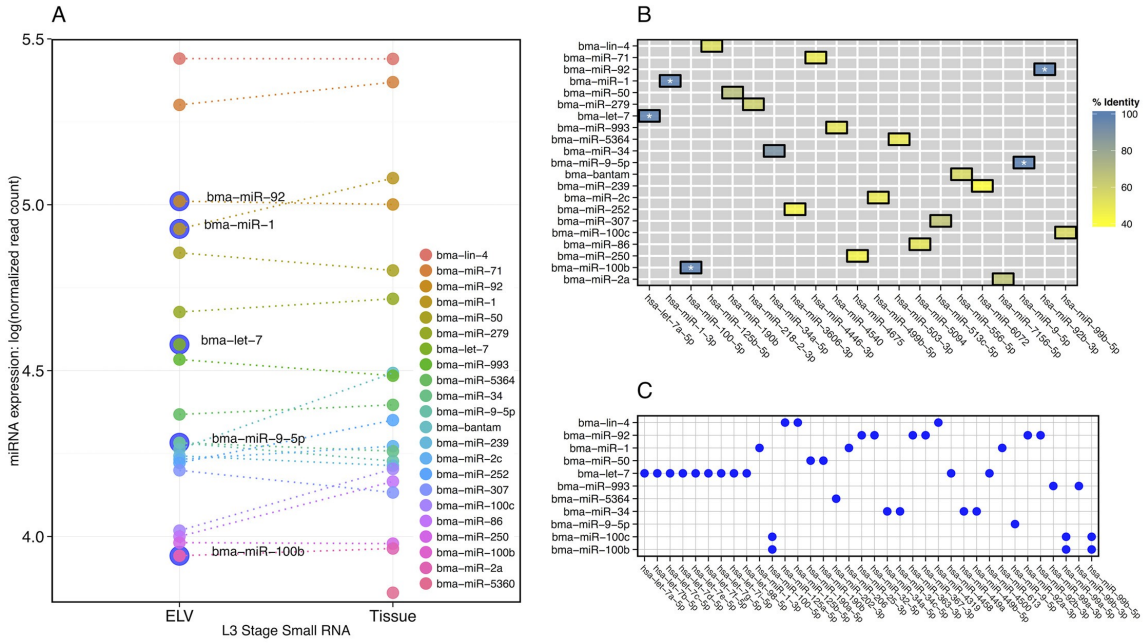

Fig 5. Discovery and profiling of miRNAs in *B. malayi* exosome-like vesicles. (A) Comparative abundance of miRNAs in L3 ELV and tissue-derived samples. miRNA discovery and abundance estimation was carried out using the mirDeep2 pipeline. The 20 miRNAs with highest expression in each sample were retained for comparison and abundance was normalized with respect to total miRNA-mapping reads within each sample. Normalized read count is plotted on a log scale for ELV and tissue miRNAs to provide a relative ordering of fractional abundance. Bma-let-7 only appears in the highly expressed subset, and a number of miRNAs with perfect mature sequence identity to host homologs are highlighted (outer blue circle). (B) Sequence conservation between *B. malayi* ELV-origin miRNAs and the host (H. *sapiens)* miRNA complement. Reduced heat map showing one-to-one homology between a given *B. malayi* miRNA and its nearest matching human counterpart in terms of percent identity. Bma-let-7, bma-miR-1, bma-miR-9, bma-miR-92, and bma- miR-100b (white asterisks) share 100% identity with a host miRNA, while bma-miR-34 shows high identity with a host miRNA (21/23 nucleotides). This *B. malayi* miRNA subset (shown in blue) contains potential modulators of host gene expression. (C) Sequence conservation between *B. malayi* ELV-origin miRNA seed sites and host (H. *sapiens)* miRNA seed sites. miRNAs sharing perfectly conserved seed sites, defined here as nucleotides 2–8 of the mature miRNA, are marked (blue circles).

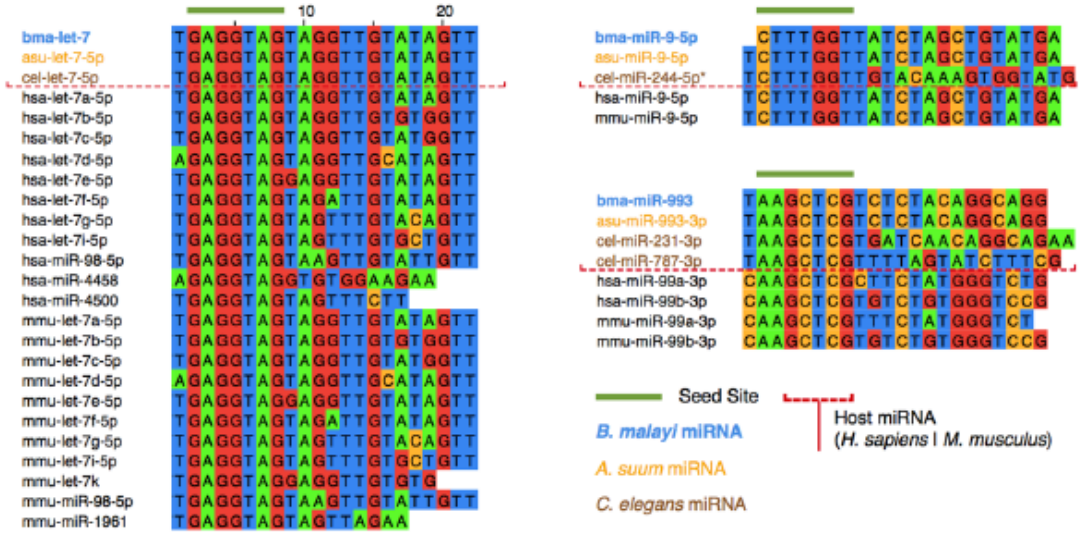

Fig 6. *Brugia malayi* ELV miRNA sequence homology to nematode and mammalian host miRNAs. miRNAs from *B. malayi*, *A. suum*, *C. elegans*, *H. sapiens*, and *M. musculus* were grouped by seed site sequence identity (nucleotides 2–8) for multiple sequence alignments. Alignments are shown for bma-let-7, bma-miR-9 and bma-miR-993. bma-let-7 is shown as an example of a *Brugia* ELV miRNA that exhibits both seed site and full length sequence conservation extending to other parasitic and free-living nematodes, as well as to mammalian host species. bma-miR-9 and bma-miR-993 are presented as examples where conserved parasite miRNAs have clear host homologs, yet lack one-to-one *C. elegans* orthologs.

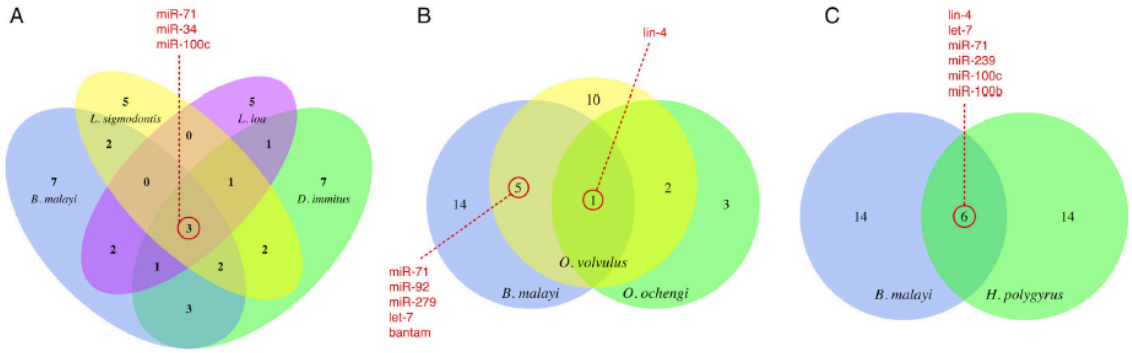

Fig 7. Comparison of the B. malayi ELV miRNA complement to miRNAs secreted by other parasitic nematodes species. (A & B) Comparison of the 20 most abundant B. malayi ELV miRNAs with the complements of miRNAs found circulating in the serum and plasma of definitive and model mammal hosts burdened with filarial infection (*Litomosoides sigmodontis* [26], *Dirofilaria immitis* [46], *Loa loa* [47], *Onchocerca volvulus* [46, 48], and *Onchocerca ochengi* [47]). The *D. immitis* miRNAs in (A) are restricted to the 20 most abundant miRNAs, and the *O. volvulus* miRNAs in (B) represent the combination of two non- overlapping sets arising from separate reports. (C) Comparison of the 20 most abundant miRNAs identified in *B. malayi* ELVs and *H. polygyrus* exosomes. These analyses reveal sets of common markers and a number of miRNAs unique to each species.

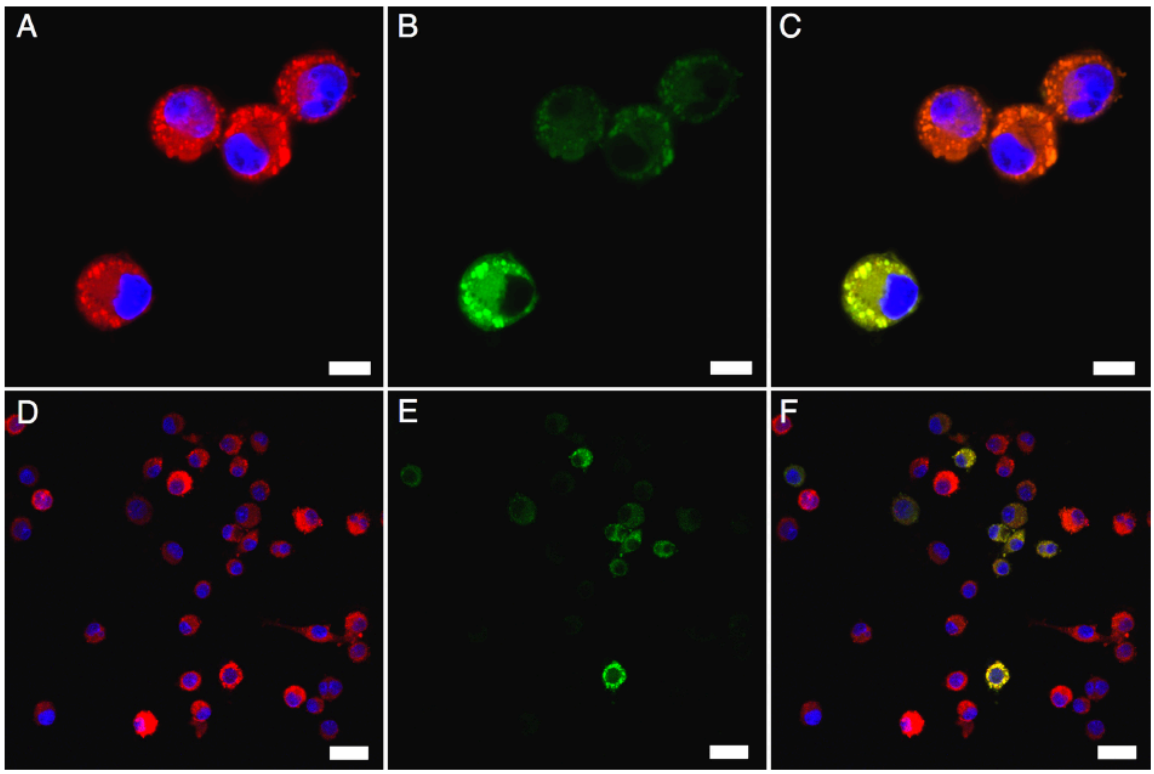

Fig 8. *Brugia* exosome-like vesicles (ELVs) are internalized by J774A.1 macrophages. (A and D) J774A.1 macrophages were labeled with PKH26 (red) and counterstained with DAPI (blue) to visualize nuclei. (B and E) *B. malayi* L3 stage ELVs were purified from a 24 hr parasite culture and labeled with PKH67 (green). 3 × 105 J774A.1 were co-incubated with approximately 3 × 107 labeled ELVs for 6 hrs at 37°C and washed repeatedly to remove unbound ELVs. Vesicles internalized by macrophages appear diffusely throughout cytoplasm and focused in discrete puncta associated with the cell membrane. (C and F) Merged images showing internalization of parasite ELVs. All images were acquired using a using a Leica TCS SP5 X Confocal/multiphoton microscope system with 20X (A-C) or 60X (D-F) objectives. Scale bars: 10 μm (A-C) and 25 μm (D-F).

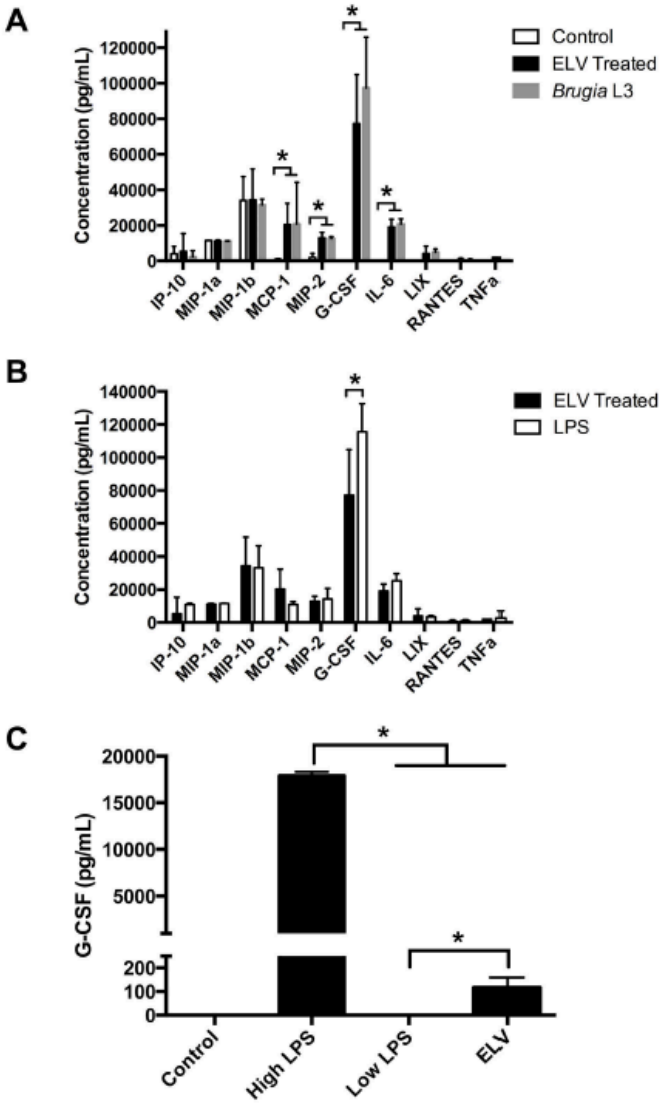

Fig 9. *Brugia* exosome-like vesicles (ELVs) elicit a classically activated phenotype in J774A.1 macrophages. (A) J774A.1 (5 × 105) were treated with approximately 4 × 108 purified L3 stage ELVs, live L3 stage parasites (10 worms) or naïve culture media (control) and supernatents collected after 48 hr. The presence of 32 cytokines/chemokines was simultaneously assayed using the Milliplex MAP Mouse Cytokine/ Chemokine kit (EDM Millipore) interfaced with a Bio-Plex System (Bio-Rad) utilizing Luminex xMAP technology (Luminex). The quantification of identified cytokines is presented. The cytokine profile generated by ELV treatment is consistent with a classically activated phenotype. (B) Cytokine response to ELV treatment is compared to LPS (200 ng/mL). The close correlation of responses indicates ELV treatment generates a classically activated phenotype. (C) J774A.1 (5 × 105) were treated with high dose LPS (200 ng/mL), low dose LPS (0.003 ng/mL), ELV or naïve culture media (control) for 24 hr, supernatant collected and assayed for G-CSF using a Mouse G-CSF Quantikine ELISA kit (R&D Systems). The absence of response to low dose LPS suggests the classically activated response is not due to LPS-like contamination.

CHAPTER 5

SUMMARY AND CONCLUSIONS

Nematodes are an incredibly diverse group of organisms that inhabit terrestrial, freshwater and marine environments and exhibit both free-living and parasitic lifestyles [1]. To date, over 23,000 species of nematodes have been described; however, the actual number of species may exceed one million [1]. Their simple body plan belies the molecular intricacy that has allowed these organisms not only to adapt but also to flourish in a wide assortment of ecological niches.

Here we explore chemosensation, which is an essential behavior used to detect environmental cues [2]. Chemosensory perception is critical for nematodes to find food, mates, avoid noxious condition and even in behaviors that allow parasites to identify and invade their hosts [3]. Our study of chemosensation focused on the response of *B. malayi* to environmental cues and how this response may facilitate transmission of this parasite. To further our understanding of chemosensation in nematodes, we conducted a pan-phylum analysis to survey heterotrimeric G-proteins, which are vital for sensory perception in nematodes [4-6].

Chapter 2 of this dissertation represents the first description of chemosensory behavior in *B. malayi*. This study, which focused on the infectious L3 stage of the parasite, demonstrated that these parasites possess the major structures required for sensory perception and exhibit specific tactic behaviors when exposed to different chemical compounds.

More specifically, we identified amphids in multiple life stages (L3, L4, adult male and adult female) of *B. malayi* using scanning electron microscopy. Amphids are the major sensory organs of nematodes, located in the head [7-9]. The pore shape of the amphids is highly variable among nematodes, ranging from simple slits to large complex structures found in many marine nematodes. This extreme anatomical variation may arise as a result of specific environmental adaptations. Our studies showed that amphid pores in *B. malayi* are simple, crescent shaped openings that are similar to amphid pores of a closely related species, *Onchocerca eberhardi* and less prominent than those of *C. elegans* [10]. The simplicity of amphid pore shape in *B. malayi* could be an adaptation to the niche this nematode occupies. *B. malayi* is a parasitic nematode that infects humans and is transmitted by mosquitoes. Mammalian and insect vector hosts are required for development and successful completion of this parasite's life cycle, so no free-living stage occurs. As a result, *B. malayi* is exposed to relatively few chemical compounds compared to free-living counterparts and thus is unlikely to require specific anatomical adaptations that would enhance the acuity of the chemosensory system in order to thrive in its ecological niche.

We used the fluorescent lipophilic dye DiI (1,1'-dioctadecyl-3,3,3',3'-tetramethylindocarbocyanine perchlorate) to visualize internal sensory neuroanatomy across multiple life stages. Our results showed stage-specific variations in dye-filling patterns. For example, while amphid channels were found to dye-fill in all life stages, dye-filling of amphid associated socket cell bodies was only observed in L3 stage worms. Sheath cell bodies were observed in all but L4 stage parasites, while we were able to visualize the nerve ring in all but adult male *B. malayi*. Of note, no amphidial neurons

were found to dye-fill in any stage of the parasite. This is a significant departure from what has been observed in *C. elegans*, where six amphid neurons (ASH, ASI, ASK, ADL and AWB) were visualized using DiI [11]. Traditionally it was thought that the neuroanatomy of nematodes in the class Chromadorea (which includes *C. elegans* and *B. malayi*) is highly conserved, so the variation in dye-filling patterns observed herein was perhaps unexpected although not unprecedented [11-18]. Previous studies using DiI have shown that parasitic nematodes exhibit variation in dye-filling patterns [19, 20]. For example, only a single pair of amphid neurons dye-filled in the L1 stage of the APN *Parastrongyloides trichosuri* [19]. More recently, Han *et al.* (2015) compared dye-filling patterns in a number of nematode species[20]. Their research incorporated a more diverse group of nematodes than previous studies and demonstrated significant variation in dye-filling between species and even between life stages within the same species [20]. Their results showed that like APNs, far fewer amphid neurons stain in PPNs when compared to free-living nematodes like *C. elegans* [20]. In the same study, examination of DiI staining in entomopathogenic parasitic nematodes (EPNs) showed stage specific variations [20]. No dye-filling of any sensory neuron was observed in the non-feeding infectious juvenile (IJ) stage (analogous to dauer stage of *C. elegans*) of either *Heterorhabditis bacteriophora* or in *Steinernema carpocapsae* [20]. In the non-IJ stages, amphid neuron staining was only periodically observed in either species, but the authors observed robust staining in other sensory neurons such as inner labial and phasmid neurons in *S. carpocapsae* [20]. Our results are consistent with these findings and suggest that, although the architecture of sensory anatomy is generally considered conserved

across the phylum, modifications to sensory neurons exist between species and that these alterations may be a result of stage- and niche-specific adaptations.

Identification of the sensory neuroanatomy in *B. malayi* led us to question whether or not these parasites would exhibit distinct behavioral responses when exposed to different stimuli. Previous investigations of chemosensation in *C. elegans* showed that this nematode has a robust chemosensory response with the ability to respond to hundreds of compounds in a concentration-dependent manner [21]. In contrast, our understanding of chemosensory behavior in parasitic nematodes is very limited. Those studies performed show that parasites have the capacity to respond to environmental cues and that this behavior plays roles in the parasite's ability to identify and invade suitable hosts [3]. Based on the data, parasitic nematodes appear to exhibit differential responses to chemical compounds and that these responses are reflective of the host-specificity of the parasite [22-26]. However, chemosensory perception has only been examined in a few parasites and no functional work has been completed to date. This knowledge gap underscores the need for additional studies focusing on chemosensation in parasitic nematodes. The research presented in this chapter demonstrates that infectious L3 stage *B. malayi* exhibit distinct tactic behaviors in response to a variety of chemical compounds. Using a modified chemotaxis plate assay, we determined that *B. malayi* perceives and responds to odorant and gustatory compounds.

B. malayi exhibited either no response or was actually repelled by odorants present in human sweat. These results suggest that chemosensation in parasitic nematodes may underpin transmission. *B. malayi* is transmitted by mosquitoes and thus is delivered passively to a potential host unlike, for example, the skin-penetrating parasite,

Strongyloides stercoralis, which must actively seek out an appropriate host. When infected mosquitoes take a blood meal, *B. malayi* L3s migrate out of the proboscis onto the skin of the prospective host. Once on the skin these parasites must be able to navigate away from the skin surface and penetrate the host by finding and entering the wound track left by the mosquito. In contrast to compounds found on host skin, which were repellent, compounds present within the host such as L-lactic acid and human serum were attractive to L3 stage parasites indicating that positive and negative chemotaxis coordinate to drive transmission of this parasite. The adverse response to compounds present on human skin may facilitate transmission of *B. malayi* by providing a negative stimulus to direct the parasite to the wound track left by the mosquito, while the attraction to subdermal compounds may act as signals providing further direction for the parasite. Thus these contrasting responses to host-derived compounds may function synergistically to facilitate dermal penetration and establishment of infection.

Although further studies are needed to fully characterize the role of chemosensory perception in the transmission of filarial worms, the data presented here point to a functional chemosensory system in *B. malayi* that facilitates parasite infection. It follows that perturbation of this chemosensory behavior in *B. malayi* may disrupt transmission of the parasite and could be exploited for control purposes. Chemosensation in *B. malayi* could be disrupted through the use of genetically modified mosquitoes expressing inverted repeat (IR) RNA sequences that are capable of suppressing nematode genes that are crucial for chemosensory perception. IR-RNAs forms dsRNA that would trigger RNA interference (RNAi) within the mosquito. This mechanism has already been shown to be successful in enhancing resistance to dengue type 2 viruses in transgenic *Aedes aegypti*

[27]. In addition, as shown in the Appendix of this dissertation and in Song *et al*. (2010), we have developed an *in vivo* method for suppression of *B. malayi* genes within the mosquito host and demonstrated that this method successfully suppressed genes important for molting which resulted in aberrant phenotypes that could disrupt transmission of the parasite [28]. Transgenic mosquitoes expressing proteins that bind to key chemoreceptors is another method that could be employed to disrupt chemosensory behavior in nematodes. For instance, it may be possible to engineer a transgenic mosquito using clustered regularly interspaced palindromic repeats (CRISPR) and CRISPR associated (Cas) genes to insert a gene expressing a peptide that binds to a *B. malayi* G-protein coupled receptor (GPCR) involved in chemosensory behavior. This may conceptually prevent ligand (an environmental odorant or gustatory compound) binding through competitive inhibition and thus disrupt the parasite's chemosensory response. A gene drive system could be used to rapidly spread this gene throughout the mosquito population, potentially leading to fixation. Gene drive using selfish elements like *Medea* is an ideal system to exploit for this method of control because a gene of interest (even a detrimental one) can rapidly spread (within a few generations) throughout a target population and potentially lead to fixation [29]. These types of strategies could be applied to target any gene needed for chemosensation in nematodes thus this approach could apply to a host of filaroid parasites that are vector-borne. In addition, the plasticity of this approach will allow researchers to modify their targets in the event that the nematode develops resistance. Finally, disruption of chemosensation in parasitic nematodes does not kill the parasite directly and thus targeting these genes would disrupt transmission

while minimizing any negative selection pressure exerted on the parasite, which could reduce resistance development in the parasite.

In order to explore the feasibility of novel control approaches targeting genes and proteins involved in chemosensation, we needed to gain a better understanding of the underlying mechanisms involved in chemosensation in nematodes. To this end, we conducted a pan-phylum survey of heterotrimeric G-proteins, which have been shown to be essential in sensory perception in nematodes. In Chapter 3, we explored heterotrimeric G-proteins, which are composed of α, β and γ subunits, and are fundamental components of G-protein signaling [30]. G-protein signaling pathways are a major mechanism used by eukaryotes to process and translate signals from the environment into cellular actions, including chemosensation in nematodes. Our analysis employed both bioinformatic and phylogenetic approaches using a data set that included genomes from more than 70 nematode species, representing four clades (I, III, IV and V) and both classes (Enoplea and Chromadorea) in Nematoda, and therefore is the most comprehensive analysis of heterotrimeric G-proteins in nematodes to date.

In *C. elegans*, 22 G-protein α subunits (GPAs) have been identified, of which 16 (GPA 1-3, 5-11, 13-15, 17-18 and ODR-3) have no clear homologs outside of Nematoda and are therefore considered to be "nematode-specific" [4, 5]. Using all 22 *C. elegans* GPAs to seed our homology search, we identified over 1000 putative GPA homologs.

In *C. elegans*, the overwhelming majority of nematode-specific GPAs (*gpa* 1-3, 5-6, 8-11, 13-15 and *odr*-3) are expressed either exclusively or primarily in amphid neurons, indicating that these GPAs function in signal transduction pathways related to

nematode sensory behavior [5]. Notably, our data set revealed that homologs of known sensory GPAs are restricted to nematodes in the class Chromadorea (nematodes in clades III, IV, V). This observation poses an interesting problem because these nematode-specific GPAs are thought to be integral for sensory behavior and their absence in class Enoplea (clade I) brings into question the mechanisms mediating sensory behavior in Enoplean nematodes.

Nematodes belonging to clade III are all APNs; moreover with the exception of roundworm eggs excreted in host feces, these nematodes spend their entire life within a host (i.e. they have no free-living stage). Clade III nematodes, including *B. malayi*, possess far fewer GPAs than clade V nematodes, including *C. elegans*. A more simplified GPA complement makes sense; clade III nematodes lack free-living stages and thus would only need to respond to a set of very specific host cues. By comparison, clade V nematodes all have a free-living stage, so have the need to distinguish between innumerable cues present in the environment in order to survive. Our data set was restricted to published genomes, however it would be interesting to examine *gpa* expression during different life stages of nematodes because this type of analysis would reveal stage-specific expression and perhaps subsets of GPAs that exhibit particular transcript abundance to correlate to environmental settings occupied during that stage. These data would be especially important with relation to parasite control because it would allow us identify those GPAs that function to facilitate transmission of the parasite at specific life stages.

C. elegans GPA-3 and ODR-3 mutants showed significant chemosensory defects when exposed to gustatory or olfactory compounds [5]. These results indicate that *gpa*-3

and *odr*-3 are crucial for chemosensation in this nematode. Our analysis revealed the presence of both of these genes in the *B. malayi* genome. The number of nematode-specific GPAs in *B. malayi* is significantly less than what has been observed in *C. elegans* and the conservation of GPA-3 and ODR-3 suggest an essential role for these proteins in chemosensation in all nematodes. Building on our strategies for control, disruption of these proteins could lead to aberrant chemosensory behavior, which could prevent parasite transmission from vector to vertebrate host. In support of this, chemosensory responses to both gustatory and odorant compounds are severely perturbed in *C. elegans* GPA-3 mutants [5]. GPA-3 may have similar functions in *B. malayi* and if so, disruption of *B. malayi* GPA-3 may interrupt chemosensation in this parasite. The work presented in Chapter 2 of this dissertation suggests that *B. malayi* use chemosensation to identify and invade host tissues in order to establish infection. By suppressing GPA-3 in *B. malayi* we could disrupt the chemosensory response and prevent the parasite from identifying and invading the host before the parasite desiccates and dies which would effectively prevent transmission of *B. malayi* from the mosquito vector to the human host.

We also identified a novel G-protein γ subunit (GPC-3) that was present in the majority of genomes surveyed. It was notably absent in *Caenorhabditis* species, suggesting that this γ subunit was lost prior to divergence of this genus. We have yet to interrogate the function of GPC-3, but the broad conservation of this γ subunit suggests it is generally important for nematode biology. Examination of *Ascaris suum* transcriptomic datasets revealed that *gpc*-3 expression is highest in the pharyngeal region [31]. This area of the nematode contains amphidial neurons so it is reasonable to speculate that *gpc*-3,

like *gpc-1*, is expressed at least in part in sensory neurons. Notably, more than half of the APN genomes examined included all three *gpc* genes. Why animal parasitic nematodes would have an additional sensory restricted γ subunit is unclear but it may reflect specific adaptations to a parasitic life strategy. It is possible that GPC-3 may have had a sensory function initially but the GPA lineage expansion in *Caenorhabditis* may have negated the need for GPC-3 leading to the loss of this γ subunit in *Caenorhabditis* spp. In contrast, parasitic nematodes have undergone significantly less GPA expansion; therefore GPC-3 might still have a function in these nematodes.

Chemosensation alone does not explain how parasitic nematodes successfully establish and maintain infections in their preferred hosts. In order to establish an infection, these parasites must not only be able to respond to external cues but must also have mechanisms to manipulate the external and host environment. Our understanding of the mechanisms involved in establishment and maintenance of *B. malayi* infection is limited, although one possibility is that parasites produce extracellular vesicles to mediate interactions with particular cells and tissues. To explore this possibility, we investigated exosome-like vesicles (ELVs) and their role as vehicles for the delivery of bioactive molecules such as miRNAs and proteins that are used to manipulate the host immune response in the establishment and maintenance of infection.

In Chapter 4 of this dissertation, we describe the identification and partial characterization of exosome-like vesicles (ELVs) in *B. malayi*. Exosomes are small extracellular vesicles (30-120 nm) that are secreted by a number of cell types and in bodily fluids [32]. These vesicles contain bioactive molecules including proteins and small RNAs making them potent vehicles for cell-to-cell communication [32]. A number

of parasites such as *Trichomonas vaginalis* and *Heligmosomoides polygyrus* secrete ELVs, which are important mediators of host-parasite interactions during infection with these parasites [33, 34]. We therefore sought to determine if *B. malayi* also secreted exosomes and if so, what role these vesicles play in the establishment and maintenance of infection in the human host. Using electron microscopy and nanoparticle tracking analysis, we identified ELVs released by the infectious L3 stage *B. malayi*. It was revealed that L3s release prodigious amounts of ELVs when compared to adult stages. The L3 stage is the stage which *B. malayi* is transmitted from the mosquito vector to the human host and the release of copious amounts of exosome-like vesicles at this stage suggests that ELVs may function in the establishment of infection in the human host.

We established that L3 stage *B. malayi* release ELVs and proteomics and RNA-seq revealed that these vesicles contain diverse protein and miRNA cargo. Comparisons between ELV and tissue fractions showed that predictable and considerable conservation exists between the two fractions, however there are also notable differences, indicting an underlying mechanism for the packaging of select bioactive molecules. This observation further indicates that *B. malayi* secreted exosome-like vesicles are involved in mediating infection with this parasite. For example, the miRNA Bma-let-7 is significantly enriched in *B. malayi* L3 ELVs and shares perfect sequence identity with human let-7. In vertebrates, let-7 family miRNAs target a number of genes involved in fundamental processes including cell proliferation, apoptosis, innate immunity and even cancer development [35-37]. In addition, let-7 miRNAs orchestrate host-pathogen communications for several pathogens [38-40]. Infection with a pathogen down-regulates macrophage let-7 expression, which in turn acts on Toll-like receptors including TLR4 to

stimulate production of the major immune-modulatory cytokines IL-6 and IL-10 from macrophages [38, 39, 41]. Our work here demonstrates that *B. malayi* ELVs are internalized by host macrophages and stimulate an immunological response in these cells. Macrophage activation is broadly divided into either classically activated (CAMΦ) or alternatively activated (AAMΦ) depending on the phenotype elicited. CAMΦ, which is stimulated by LPS or IFN-γ, is typically associated with a pro-inflammatory phenotype while AAMΦ, elicited by IL-4 and IL-3, is immunosuppressive or anti-inflammatory [42, 43]. Of note, *B. malayi* ELVs stimulated a classically activated phenotype in J774A.1 murine macrophages. Typically, nematode infection is associated with an AAMΦ phenotype although experiments using *B. malayi* have been shown to stimulate both CAMΦ and AAMΦ phenotypes [44-47]. It has been shown that purified exosomes from other biological systems induce CAMΦ phenotypes indicating that our observation may represent a distinct immunological reaction in response to ELVs [48-50].

Taken together these data indicate that manipulation of ELVs in *B. malayi* L3s has the potential to negatively impact the parasite, which could be exploited for control. For instance, *B. malayi* secretion of ELVs containing let-7 that is identical to human let-7 may act to allow the parasite to essentially "hide" from the host immune response. Upon infection parasite-derived let-7 may act in place of human let-7 to keep total let-7 expression high. This in turn could prevent activation of macrophages and thus the release of important host immune factors thereby allowing L3 stage parasites to migrate to the lymphatics of the host unmolested. If true, disruption of *B. malayi* ELV production or release would allow the host immune response to proceed uninhibited and thus prevent the establishment of infection with this parasite.

The association between parasite and host during the establishment and maintenance of infection is a complex and dynamic relationship. All of the knowledge gained from this dissertation provides the foundation for future work on both the function of perception physiology and behavior and host manipulation by exosome-like vesicle production in *B. malayi*. A better understanding of the mechanisms mediating chemosensation in *B. malayi* will reveal how critical chemosensation is to the establishment of infection and may lead to the development of innovative strategies of control. *B. malayi* ELVs are important in the transfer of bioactive molecules from the parasite to the host. Expanding our knowledgebase to include additional life stages will provide a clearer picture of the role ELVs have in host-parasite interactions and could identify novel targets for intervention. *B. malayi* adults can persist in the host lymphatics for years suggesting that modulation of the host immune response is crucial. Interrogating the function and cargo of ELVs in adult parasites may provide a clearer understanding of the interactions that facilitate this persistence and identify potential targets that can be exploited for treatment of these long-lived stages.

References

1. Blaxter M, Koutsovoulos G. The evolution of parasitism in Nematoda. Parasitology. 2014:1-14. doi: 10.1017/S0031182014000791. PubMed PMID: 24963797.

2. Bargmann CI. Chemosensation in *C. elegans*. WormBook. 2006:1-29. doi: 10.1895/wormbook.1.123.1. PubMed PMID: 18050433.

3. Chaisson KE, Hallem EA. Chemosensory behaviors of parasites. Trends Parasitol. 2012;28(10):427-36. doi: 10.1016/j.pt.2012.07.004. PubMed PMID: 22921895.

4. O'Halloran DM, Fitzpatrick DA, McCormack GP, McInerney JO, Burnell AM. The molecular phylogeny of a nematode-specific clade of heterotrimeric G-protein alpha-

subunit genes. J Mol Evol. 2006;63(1):87-94. doi: 10.1007/s00239-005-0215-z. PubMed PMID: 16786439.

5. Jansen G, Thijssen KL, Werner P, van der Horst M, Hazendonk E, Plasterk RH. The complete family of genes encoding G proteins of *Caenorhabditis elegans*. Nat Genet. 1999;21(4):414-9. doi: 10.1038/7753. PubMed PMID: 10192394.

6. Lans H, Rademakers S, Jansen G. A network of stimulatory and inhibitory Galpha-subunits regulates olfaction in *Caenorhabditis elegans*. Genetics. 2004;167(4):1677-87. doi: 10.1534/genetics.103.024786. PubMed PMID: 15342507; PubMed Central PMCID: PMCPMC1470997.

7. Ward S, Thomson N, White JG, Brenner S. Electron microscopical reconstruction of the anterior sensory anatomy of the nematode *Caenorhabditis elegans*. J Comp Neurol. 1975;160(3):313-37. doi: 10.1002/cne.901600305. PubMed PMID: 1112927.

8. White JG, Southgate E, Thomson JN, Brenner S. The structure of the nervous system of the nematode *Caenorhabditis elegans*. Philos Trans R Soc Lond B Biol Sci. 1986;314(1165):1-340. PubMed PMID: 22462104.

9. Perkins LA, Hedgecock EM, Thomson JN, Culotti JG. Mutant sensory cilia in the nematode *Caenorhabditis elegans*. Dev Biol. 1986;117(2):456-87. PubMed PMID: 2428682.

10. Uni S, Bain O, Agatsuma T, Harada M, Torii H, Fukuda M, et al. *Onchocerca eberhardi* n. sp. (Nematoda: Filarioidea) from sika deer in Japan; relationships between species parasitic in cervids and bovids in the Holarctic region. Parasite. 2007;14(3):199-211. PubMed PMID: 17933297.

11. Srinivasan J, Durak O, Sternberg PW. Evolution of a polymodal sensory response network. BMC Biol. 2008;6:52. doi: 10.1186/1741-7007-6-52. PubMed PMID: 19077305; PubMed Central PMCID: PMCPMC2636771.

12. Kimber MJ, Fleming CC. Neuromuscular function in plant parasitic nematodes: a target for novel control strategies? Parasitology. 2005;131 Suppl:S129-42. doi: 10.1017/S0031182005009157. PubMed PMID: 16569286.

13. Ashton FT, Schad GA. Amphids in *Strongyloides stercoralis* and other parasitic nematodes. Parasitol Today. 1996;12(5):187-94. PubMed PMID: 15275212.

14. Ashton FT, Li J, Schad GA. Chemo- and thermosensory neurons: structure and function in animal parasitic nematodes. Vet Parasitol. 1999;84(3-4):297-316. PubMed PMID: 10456420.

15. Li J, Ashton FT, Gamble HR, Schad GA. Sensory neuroanatomy of a passively ingested nematode parasite, *Haemonchus contortus*: amphidial neurons of the first stage larva. J Comp Neurol. 2000;417(3):299-314. PubMed PMID: 10683605.

16. Li J, Zhu X, Ashton FT, Gamble HR, Schad GA. Sensory neuroanatomy of a passively ingested nematode parasite, *Haemonchus contortus*: amphidial neurons of the third-stage larva. J Parasitol. 2001;87(1):65-72. doi: 10.1645/0022-3395(2001)087[0065:SNOAPI]2.0.CO;2. PubMed PMID: 11227904.

17. Hallem EA, Rengarajan M, Ciche TA, Sternberg PW. Nematodes, bacteria, and flies: a tripartite model for nematode parasitism. Curr Biol. 2007;17(10):898-904. doi: 10.1016/j.cub.2007.04.027. PubMed PMID: 17475494.

18. Ashton FT, Zhu X, Boston R, Lok JB, Schad GA. *Strongyloides stercoralis*: Amphidial neuron pair ASJ triggers significant resumption of development by infective larvae under host-mimicking in vitro conditions. Exp Parasitol. 2007;115(1):92-7. doi: 10.1016/j.exppara.2006.08.010. PubMed PMID: 17067579; PubMed Central PMCID: PMCPMC3091007.

19. Zhu H, Li J, Nolan TJ, Schad GA, Lok JB. Sensory neuroanatomy of *Parastrongyloides trichosuri*, a nematode parasite of mammals: Amphidial neurons of the first-stage larva. J Comp Neurol. 2011;519(12):2493-507. doi: 10.1002/cne.22637. PubMed PMID: 21456026; PubMed Central PMCID: PMCPMC3125480.

20. Han Z, Boas S, Schroeder NE. Unexpected Variation in Neuroanatomy among Diverse Nematode Species. Front Neuroanat. 2015;9:162. doi: 10.3389/fnana.2015.00162. PubMed PMID: 26778973; PubMed Central PMCID: PMCPMC4700257.

21. Hart AC, Chao MY. From odors to behaviors in *Caenorhabditis elegans*. In: Menini A, editor. The neurobiology of olfaction. Frontiers in Neuroscience. Boca Raton, FL: CRC Press; 2010. p. 1-33.

22. Castelletto ML, Gang SS, Okubo RP, Tselikova AA, Nolan TJ, Platzer EG, et al. Diverse host-seeking behaviors of skin-penetrating nematodes. PLoS Pathog. 2014;10(8):e1004305. doi: 10.1371/journal.ppat.1004305. PubMed PMID: 25121736; PubMed Central PMCID: PMCPMC4133384.

23. Granzer M, Haas W. Host-finding and host recognition of infective *Ancylostoma caninum* larvae. Int J Parasitol. 1991;21(4):429-40. PubMed PMID: 1917283.

24. Koga M, Tada I. *Strongyloides ratti*: chemotactic responses of third-stage larvae to selected serum proteins and albumins. J Helminthol. 2000;74(3):247-52. PubMed PMID: 10953225.

25. Vetter JC, Vingerhoed J, Schoeman E, Wauters HW. Chemotactic attraction of infective hookworm larvae of *Ancylostoma caninum* by a dog serum factor. Z Parasitenkd. 1985;71(4):539-43. PubMed PMID: 4024709.

26. Kusaba T, Fujimaki Y, Vincent AL, Aoki Y. In vitro chemotaxis of *Brugia pahangi* infective larvae to the sera and hemolymph of mammals and lower animals. Parasitol Int. 2008;57(2):179-84. doi: 10.1016/j.parint.2007.12.006. PubMed PMID: 18243775.

27. Franz AW, Sanchez-Vargas I, Adelman ZN, Blair CD, Beaty BJ, James AA, et al. Engineering RNA interference-based resistance to dengue virus type 2 in genetically modified *Aedes aegypti*. Proc Natl Acad Sci U S A. 2006;103(11):4198-203. doi: 10.1073/pnas.0600479103. PubMed PMID: 16537508; PubMed Central PMCID: PMCPMC1449670.

28. Song C, Gallup JM, Day TA, Bartholomay LC, Kimber MJ. Development of an *in vivo* RNAi protocol to investigate gene function in the filarial nematode, *Brugia malayi*. PLoS Pathog. 2010;6(12):e1001239. doi: 10.1371/journal.ppat.1001239. PubMed PMID: 21203489; PubMed Central PMCID: PMCPMC3009605.

29. Akbari OS, Chen CH, Marshall JM, Huang H, Antoshechkin I, Hay BA. Novel synthetic Medea selfish genetic elements drive population replacement in *Drosophila*; a theoretical exploration of Medea-dependent population suppression. ACS Synth Biol. 2014;3(12):915-28. doi: 10.1021/sb300079h. PubMed PMID: 23654248; PubMed Central PMCID: PMCPMC3742681.

30. Hamm HE. The many faces of G protein signaling. J Biol Chem. 1998;273(2):669-72. PubMed PMID: 9422713.

31. Rosa BA, Jasmer DP, Mitreva M. Genome-wide tissue-specific gene expression, co-expression and regulation of co-expressed genes in adult nematode *Ascaris suum*. PLoS Negl Trop Dis. 2014;8(2):e2678. doi: 10.1371/journal.pntd.0002678. PubMed PMID: 24516681; PubMed Central PMCID: PMCPMC3916258.

32. Raposo G, Stoorvogel W. Extracellular vesicles: exosomes, microvesicles, and friends. J Cell Biol. 2013;200(4):373-83. doi: 10.1083/jcb.201211138. PubMed PMID: 23420871; PubMed Central PMCID: PMCPMC3575529.

33. Buck AH, Coakley G, Simbari F, McSorley HJ, Quintana JF, Le Bihan T, et al. Exosomes secreted by nematode parasites transfer small RNAs to mammalian cells and modulate innate immunity. Nat Commun. 2014;5:5488. doi: 10.1038/ncomms6488. PubMed PMID: 25421927.

34. Twu O, de Miguel N, Lustig G, Stevens GC, Vashisht AA, Wohlschlegel JA, et al. Trichomonas vaginalis exosomes deliver cargo to host cells and mediate host：parasite interactions. PLoS Pathog. 2013;9(7):e1003482. doi: 10.1371/journal.ppat.1003482. PubMed PMID: 23853596; PubMed Central PMCID: PMCPMC3708881.

35. Roush S, Slack FJ. The let-7 family of microRNAs. Trends Cell Biol. 2008;18(10):505-16. doi: 10.1016/j.tcb.2008.07.007. PubMed PMID: 18774294.

36. Johnson SM, Grosshans H, Shingara J, Byrom M, Jarvis R, Cheng A, et al. RAS is regulated by the let-7 microRNA family. Cell. 2005;120(5):635-47. doi: 10.1016/j.cell.2005.01.014. PubMed PMID: 15766527.

37. Johnson CD, Esquela-Kerscher A, Stefani G, Byrom M, Kelnar K, Ovcharenko D, et al. The let-7 microRNA represses cell proliferation pathways in human cells. Cancer Res. 2007;67(16):7713-22. doi: 10.1158/0008-5472.CAN-07-1083. PubMed PMID: 17699775.

38. Chen XM, Splinter PL, O'Hara SP, LaRusso NF. A cellular micro-RNA, let-7i, regulates Toll-like receptor 4 expression and contributes to cholangiocyte immune responses against *Cryptosporidium parvum* infection. J Biol Chem. 2007;282(39):28929-38. doi: 10.1074/jbc.M702633200. PubMed PMID: 17660297; PubMed Central PMCID: PMCPMC2194650.

39. Schulte LN, Eulalio A, Mollenkopf HJ, Reinhardt R, Vogel J. Analysis of the host microRNA response to *Salmonella* uncovers the control of major cytokines by the let-7 family. EMBO J. 2011;30(10):1977-89. doi: 10.1038/emboj.2011.94. PubMed PMID: 21468030; PubMed Central PMCID: PMCPMC3098495.

40. Liu G, Abraham E. MicroRNAs in immune response and macrophage polarization. Arterioscler Thromb Vasc Biol. 2013;33(2):170-7. doi:

10.1161/ATVBAHA.112.300068. PubMed PMID: 23325473; PubMed Central PMCID: PMCPMC3549532.

41. Hu G, Zhou R, Liu J, Gong AY, Eischeid AN, Dittman JW, et al. MicroRNA-98 and let-7 confer cholangiocyte expression of cytokine-inducible Src homology 2-containing protein in response to microbial challenge. J Immunol. 2009;183(3):1617-24. doi: 10.4049/jimmunol.0804362. PubMed PMID: 19592657; PubMed Central PMCID: PMCPMC2906382.

42. Allen JE, Maizels RM. Diversity and dialogue in immunity to helminths. Nat Rev Immunol. 2011;11(6):375-88. doi: 10.1038/nri2992. PubMed PMID: 21610741.

43. Ginhoux F, Schultze JL, Murray PJ, Ochando J, Biswas SK. New insights into the multidimensional concept of macrophage ontogeny, activation and function. Nat Immunol. 2015;17(1):34-40. doi: 10.1038/ni.3324. PubMed PMID: 26681460.

44. Taylor MJ, Cross HF, Bilo K. Inflammatory responses induced by the filarial nematode *Brugia* malayi are mediated by lipopolysaccharide-like activity from endosymbiotic Wolbachia bacteria. J Exp Med. 2000;191(8):1429-36. PubMed PMID: 10770808; PubMed Central PMCID: PMCPMC2193140.

45. Osborne J, Hunter SJ, Devaney E. Anti-interleukin-4 modulation of the Th2 polarized response to the parasitic nematode *Brugia pahangi*. Infect Immun. 1996;64(9):3461-6. PubMed PMID: 8751885; PubMed Central PMCID: PMCPMC174249.

46. Allen JE, MacDonald AS. Profound suppression of cellular proliferation mediated by the secretions of nematodes. Parasite Immunol. 1998;20(5):241-7. PubMed PMID: 9651925.

47. Weinkopff T, Mackenzie C, Eversole R, Lammie PJ. Filarial excretory-secretory products induce human monocytes to produce lymphangiogenic mediators. PLoS Negl Trop Dis. 2014;8(7):e2893. doi: 10.1371/journal.pntd.0002893. PubMed PMID: 25010672; PubMed Central PMCID: PMCPMC4091784.

48. Atay S, Gercel-Taylor C, Taylor DD. Human trophoblast-derived exosomal fibronectin induces pro-inflammatory IL-1β production by macrophages. Am J Reprod Immunol. 2011;66(4):259-69. doi: 10.1111/j.1600-0897.2011.00995.x. PubMed PMID: 21410811.

49. Anand PK, Anand E, Bleck CK, Anes E, Griffiths G. Exosomal Hsp70 induces a pro-inflammatory response to foreign particles including mycobacteria. PLoS One. 2010;5(4):e10136. doi: 10.1371/journal.pone.0010136. PubMed PMID: 20405033; PubMed Central PMCID: PMCPMC2853569.

50. Atay S, Gercel-Taylor C, Suttles J, Mor G, Taylor DD. Trophoblast-derived exosomes mediate monocyte recruitment and differentiation. Am J Reprod Immunol. 2011;65(1):65-77. doi: 10.1111/j.1600-0897.2010.00880.x. PubMed PMID: 20560914.

APPENDIX

AN *IN VIVO* RNAi APPROACH TO DISRUPT DEVELOPMENT IN THE FILARIAL WORM, *BRUGIA MALAYI*

Lisa M. Fraser[1,2], Lyric C. Bartholomay[2]* and Michael J. Kimber[1]

[1]Department of Biomedical Sciences, Iowa State University, Ames, Iowa, United States of America, [2]Department of Entomology, Iowa State University, Ames, Iowa, United States of America, *Current Address: Department of Pathobiological Sciences, University of Wisconsin-Madison, Madison, Wisconsin, United States of America

Introduction

Lymphatic filariasis (LF) is a devastating disease caused by filarial nematodes that are transmitted from human to human by infected mosquitoes [1]. LF is a disfiguring disease characterized by damage to lymphatic vessels leading to severely disabling and chronic symptoms including lymphedema, elephantiasis and hydrocele [1]. Globally the impact of LF is immense, over 1 billion people are at risk for contracting LF while more than 120 million are infected with 40 million suffering from severe manifestations of the disease [1]. To combat LF, the Global Program for the Elimination of Lymphatic Filariasis (GPELF) was established in 2000 with the ambitious goal of eradicating LF by 2020 [1]. The strategy of GPELF is to disrupt transmission of LF through the implementation of mass drug administration (MDA) and to alleviate suffering of infected individuals [2]. MDA for prevention of LF is centered on reducing transmission through yearly administration of the anthelmintic drugs, albendazole plus either

diethylcarbamazine (DEC) or ivermectin, to all eligible individuals in endemic areas for at least five years [3]. Through the GPELF, disease prevalence has been reduced in many areas, however LF remains a significant health concern [2]. There are multiple factors that contribute to continued transmission but a significant barrier to success is the limited effectiveness of available chemotherapeutics. None of the drugs used for LF treatment are effective against the adult stages of the parasite, which is significant because the adults can live in the lymphatic system for up to 10 years [4-6]. The inefficacy against critical life stages combined with adverse side effects and the threat of resistance underscores the need for the development of novel chemotherapeutics.

A major barrier to the development of novel anthelmintic drugs is the intractability of parasitic nematodes to many common experimental protocols such as RNA interference (RNAi). RNAi is a reverse genetics technique that allows researchers to interrogate gene function by silencing gene expression [7]. Since the discovery of RNAi, it has rapidly become a standard tool to identify and validate potential new drug targets for use in rational drug discovery [8]. RNAi in parasitic nematodes of animals has had sporadic success using traditional protocols such as soaking or feeding [9-12]. One hypothesis to explain the variable effects of RNAi in parasitic nematodes is that the method of dsRNA delivery using traditional protocols is inappropriate for parasitic nematodes [13]. In support of this hypothesis, our lab developed an "*in squito*" protocol to that resulted in successful suppression of expression of cathepsin L-like cysteine protease 1 (*Bm-cpl-1*) and led to aberrant phenotypes that impacted molting and motility in infectious L3 stage *B. malayi* [14]. While our protocol was successful, it was not without caveats. For instance, establishment parasite infection within the mosquito host,

Aedes aegypti, required purification of microfilariae (mf) from host blood and intrathoracic microinjection of the mf into the mosquito host [14]. The combination of both methods was not only time consuming but required the use of specialized equipment and also resulted in a significant reduction of viable parasites available for study. These limitations severely restricted our ability to interrogate gene function in a high-throughput manner and thus led us to investigate blood feeding as an alternative method to establish *B. malayi* infection in *Ae. aegypti*.

Materials and Methods

Mosquito maintenance

Adult female *Aedes aegypti* (Black eyed Liverpool strain, LVP), previously selected for susceptibility to infection with *B. malayi* [15], were fed a diet of 10% sucrose and maintained in controlled conditions (27°C ± 1°C and 75% ± 5% relative humidity) with a 16:8 photoperiod.

Establishment of *Brugia malayi* infection

B. malayi - infected cat blood was obtained from the University of Georgia NIH/NIAID Filariasis Research Reagent Resource Center (FR3). Blood containing the parasites was diluted with defibrinated sheep blood (Hemostat Laboratories, CA, USA) to achieve a concentration of 80-100 mf per 20 µl. To establish infection, three- to five-day-old female *Ae. aegypti* (LVP) were allowed to feed for one hour on a water-warmed water-jacketed glass membrane feeder through a Parafilm membrane. Mosquitoes were sucrose-starved for 24 hrs prior to blood feeding and those that did not take a blood meal were removed from the experiment.

RT-PCR/Time course experiments

In order to determine transcript patterns of cathepsin genes in *B. malayi*, 10 infected adult female *Ae. aegypti* were collected 1-14 days post infection (dpi). In addition, 10 uninfected adult female *Ae. aegypti* were collected at 14 dpi to demonstrate that cathepsin primers do not amplify mosquito genes. Total RNA was extracted from all mosquito pools (1-14 dpi and uninfected) using RNAqueous Total RNA Isolation Kit (Thermo Fisher Scientific, Waltham, MA, USA) and DNase treated using TURBO DNA-Free Kit (Thermo Fisher Scientific, Waltham, MA, USA). This RNA was used as template for cDNA synthesis using ImProm-II Reverse Transcription System (Promega, Madison, WI, USA). The oligonucleotide primers used for each gene are shown in Table 1. PCR reactions (25 µL) were carried out for each gene using the PCR conditions: 94°C for five minutes, 35 cycles of 94°C for 30 seconds, 55°C for 30 seconds, 72°C for one minute followed by one cycle of 72°C for 15 minutes. All reactions were visualized on a 1% agarose gel containing ethidium bromide.

dsRNA generation and injection protocol

dsRNA triggers were generated in house using a T7 transcription-based approach. Transcription templates were PCR amplified from *B. malayi* cDNA using gene specific oligonucleotides designed to incorporate a T7 promoter sequence (TAATACGACTCACTATAGGGTACT) at both 5' and 3' ends of the amplicon. The corresponding location of the *Bm-cpl-1* dsRNA duplex was chosen because this region shares little homology with other cathepsin genes and thus increasing specificity of this

dsRNA trigger. To generate template for dsRNA synthesis targeted to *Bm-cpl-1* oligonucleotide sequences were: L1T7dsRNA-F 5' TAATACGACTCACTATAGGGTACTACGCTTACCAAGTTC 3' and L1T7dsRNA-R 5' TAATACGACTCACTATAGCCTACTCGACAACAACAGGTC 3'. *Bm-cpl-4* and *Bm-cpl-5* share 94% sequence identity [16] and we were unable to identify and region of the genes that lacked homology for spans of 19 nucleotides thus it was assumed that *Bm-cpl-4* dsRNA and *Bm-cpl-5* dsRNA will cross target each other (*Bm-cpl-4/5*). To enhance our chances for successful suppression, two *Bm-cpl*-4/5 dsRNA triggers were generated: one to target the 5' end of the genes and the other to target the 3' end of the gene. To generate template for dsRNA synthesis targeted to *Bm-cpl-4/5* oligonucleotide sequences were: T7CPL4-F1 5' TAATACGACTCACTATAGGGTACTATCCTAGCCGATTTTGCTGTC 3', T7CPL4-R1 5' TAATACGACTCACTATAGGGTACTCCTTGGGTCATACCTATAAAACCT 3', T7CPL4-F2 5' TAATACGACTCACTATAGGGTACTGCATCAAGATATGGAATAGCAATGG 3' and T7CPL4-R2 5' TAATACGACTCACTATAGGGTACTTCAAATCGGAAATGAAGCAGCG 3'. To confirm that our results were specific and not due to exogenous dsRNA, we generated dsRNA targeting LacZ as a random exogenous RNA. To generate template for dsRNA synthesis targeted to *Bm-tph-1* oligonucleotide sequences were: LacZ400-F 5' TAATACGACTCACTATAGGGCGTAATCATGGTCATAGCTGTTTCC 3' and LacZ400-R 5' TAATACGACTCACTATAGGGCTTTTGCTGGCCTTTTGCTC 3'. dsRNA duplexes were generated using the MEGAscript RNAi kit (Thermo Fisher

Scientific, Waltham, MA, USA) according to manufacturer's protocols. dsRNA was quantified using NanoDrop 2000 (Thermo Fisher Scientific, Waltham, MA, USA) prior to use. Timing of dsRNA injection was determined based on target gene expression (Figure 1) and parasite stage of interest: *Bm-cpl-1* dsRNA was injected 10 dpi to target the L3 stage of the parasite while *Bm-cpl-4/5* dsRNA was injected 5 dpi to target the L2 stage of the parasite [17]. Throughout the study mosquitoes to be injected were cold anesthetized and immobilized on a vacuum saddle for intrathoracic microinjection at the base of the head using a pulled borosilicate glass pipette attached to a manual syringe [14]. The mosquitoes were collected and processed 48 hrs post dsRNA injection to confirm target gene suppression and assess resulting phenotypes.

Relative Semi-quantitative multiplex RT-PCR

B. malayi infected, RNA-treated and control mosquitoes were cold anesthetized on ice. Total RNA was extracted from individual mosquitoes using TRIzol (Thermo Fisher Scientific, Waltham, MA, USA), DNase treated using TURBO DNA-free kit and quantified using NanoDrop 2000 prior to use. The resulting RNA served as a template for relative semi-quantitative multiplex RT-PCR using the SuperScript III one-step RT-PCR system with Platinum Taq DNA polymerase (Thermo Fisher Scientific, Waltham, MA, USA). The principle behind this reaction is to PCR amplify a target gene and compare its intensity to a multiplexed internal control during the linear phase of the reaction. Tumor protein homolog (*Bm-tph*-1, accession number U80971) was chosen as the internal control for this reaction because it is expressed throughout the life of the parasite and it had previously shown it to be an appropriate internal control [18]. The oligonucleotide primers used for each gene are shown in Table 2. PCR reactions (25 µL) were carried out

for each gene using the PCR conditions: cDNA synthesis at 50°C for 30 minutes, initial denaturation at 94°C for five minutes, 35 cycles of 94°C for 30 seconds, 55°C for 30 seconds, 72°C for one minute followed by a final extension phase of 72°C for 15 minutes. Reactions were visualized on a 1% agarose gel containing ethidium bromide.

Phenotype analysis

Parasite prevalence, location and motility were observed to identify any aberrant effects that occurred as a result of target gene suppression. At 14 dpi, RNAi treated and control L3 stage *B. malayi* were harvested for phenotype analysis. To harvest L3 stage parasites, infected adult female *Ae. aegypti* were cold-anesthetized on ice and dissected into three sections (head and proboscis, thorax and abdomen) in separate drops of room temperature *Aedes* physiological saline [19], and parasites were allowed to migrate out of the mosquito into the saline solution. Digital images of RNAi treated and control parasites were captured using a Nikon Eclipse 50i compound fluorescent microscope (Nikon, Japan).

Statistical analysis

One-way ANOVA with Tukey's post-tests were used to analyze the effects of RNAi treatment on gene expression in semi quantitative RT-PCR experiments. In all tests, P values ≤ 0.05 were considered significant. All statistical analyses were performed using Prism 6 for Mac (GraphPad).

Results and Discussion

B. malayi cathepsin cysteine proteases are differentially expressed throughout the mosquito stages of the parasite life cycle.

Cathepsin cysteine proteases have been shown to be integral components in the molting pathway of parasitic nematodes [16, 20-23]. Inhibition of these proteins resulted in significant impairment of the L3 to L4 molt in filarial worms making them attractive targets for the development of novel chemotherapeutics [21-23]. While cathepsin cysteine proteases have been shown to be important in molting the specific role of each cathepsin in molting remains unknown. We were previously able to successfully suppress cathepsin L-like cysteine protease 1 (*Bm-cpl-1*) expression and elicit aberrant phenotypes that disrupted molting and development [14] thus we chose to focus on suppression of cathepsin cysteine proteases using our modified protocol. To date, eight cathepsin L-like genes, one cathepsin F and one cathepsin Z gene have been identified in *B. malayi* [22]. Using RT-PCR, we determined that each *B. malayi* cathepsin gene had a different transcriptional profile suggesting that these genes have differential functions throughout the mosquito stages of the parasite life cycle (Figure 1). Transcription of *Bm-cpl-1* was observed only during the L3 stage of the parasite (Figure 1) while *Bm-cpl-5* transcription spanned both the L2 and L3 stages of *B. malayi* (Figure 1). *Bm-cpl-4* transcription was restricted to L2 and early L3 stage parasites (Figure1). Cathepsin L-like cysteine protease 8 and cathepsin Z was transcribed throughout the parasite's development within the mosquito (Figure 1). Transcription of cathepsin F was observed in all life stages analyzed with the exception of the L1 stage (Figure 1).

Our modified *in squito* approach results in robust *Bm-cpl-1* gene suppression

In order for our modified protocol to be successful, we not only needed to establish infection but we also needed to be able to successfully suppress genes of interest using RNAi. Our previous success suppressing *Bm-cpl-1* using our *in squito* protocol led us to use this gene to test our modified *in squito* protocol. We have previously shown that we could achieve significant suppression of *Bm-cpl-1* using as little as 150 ng of the dsRNA trigger [14]. In support of our previous results, injection of 150 ng *Bm-cpl-1* dsRNA potently and specifically suppressed *Bm-cpl-1* transcript abundance (Figure 2). Injection with 150 ng *Bm-cpl-1* dsRNA resulted in complete suppression of *Bm-cpl-1* in 80% of the treated samples tested (P-value ≤ 0.001) (Figure 2A, B). However, parasite prevalence was unaffected (Figure 2C) as was mosquito survival (data not shown). This contrasts with our previous results which demonstrated that the prevalence of L3 stage *B. malayi* was reduced when compared to controls [14]. Overall, we saw an increase in parasite prevalence and mosquito survival when compared to our previous results, which may be due to a decrease in virulence of the parasites that were used for the experiments. Suppression of *Bm-cpl-1* expression also produced kinking phenotypes that are likely to inhibit or even prevent parasite transmission from the mosquito to the human host (Figure 3). We observed kinking at both ends of parasites exposed to *Bm-cpl-1* dsRNA (Figure 3). This phenotype was only observed in parasites exposed to *Bm-cpl-1* leading us to the conclusion that this phenotype was a result of *Bm-cpl-1* suppression. Additionally, this phenotype was observed previously in *Bm-cpl-1* dsRNA exposed parasites using our original protocol [14]. Parasites that exhibited this phenotype were virtually non-motile which illustrates that suppression of *Bm-cpl-1* in L3 stage *B. malayi* could inhibit or

disrupt transmission because parasites with this phenotype would not be able to migrate out of the mosquito to infect the human host. We repeated these experiments using 150 ng dsRNA targeting *LacZ* as a random exogenous RNA to confirm that our results were specific and not due to exogenous dsRNA suppressing *Bm-cpl*-1 expression or impairment of parasite motility (Figure 2 and 3). These experiments were nearly identical to our saline injected and uninjected controls confirming the specificity of the results we observed in our *Bm-cpl-1* suppressed parasites (Figure 2 and 3).

Bm-cpl-4/5 gene expression is not suppressed using our modified _in squito_ approach

Bm-cpl-4 and *Bm-cpl-5* share 94% sequence identity [16]. The high percent of shared sequence identity between the two genes makes it unlikely that we would be able to target one gene without cross-targeting the other therefore we assumed that we were targeting both genes simultaneously (*Bm-cpl-4/5*) using our RNAi triggers. While we were able to achieve consistent suppression of *Bm-cpl-1* expression using our modified *in squito* approach we were not able to suppress *Bm-cpl-4/5* expression (Figure 4). There are a number of possible reasons for the lack of suppression observed. We were not able to target *Bm-cpl-4* or *Bm-cpl-5* individually using dsRNA as our RNAi trigger, which may have been the cause of our inability to suppress the genes *in squito* as our trigger was likely targeting both genes however we tested using both 500 ng and 1 µg of our RNAi triggers in order to compensate for this possibility (Figure 4). It is also possible that the regions we targeted were not amenable to suppression using RNAi. To avoid this possibility, we designed RNAi triggers that targeted both the 5' and 3' end, however neither trigger was successful (Figure 4). The regions that we can target that may result in specific suppression are extremely limited due to the high shared sequence identity

between *Bm-cpl-4* and *Bm-cpl-5*; therefore if repeating this experiment it would be ideal to use siRNA as an RNAi trigger. Specifically, we could repeat our experiments using siRNA targeting the 3' untranslated region of each gene to specifically target each gene, but we have not validated the use of siRNA in gene suppression in the *in squito* model. Finally, the timing of dsRNA injection may also have led to our failure to see suppression. We injected our RNAi trigger 5 dpi which is during the L2 stage of the parasite because *Bm-cpl-4* expression appears to be highest during the L2 to L3 molt, which may not be a *B. malayi* stage that is amenable to suppression.

To date, there are no studies available that have targeted developmental stages prior to L3 and shown successful suppression. If we were to repeat this experiment it would be interesting to see if we could achieve *Bm-cpl-4/5* suppression by injecting the RNA trigger at a later time point. Suppression of *Bm-cpl-1* could be achieved as early as 7 dpi and because both *Bm-cpl-4* and *Bm-cpl-5* are expressed at 7 dpi it would be worthwhile to inject *Bm-cpl-4/5* dsRNA at this time point to determine if we could successfully suppress these genes. In addition, we could specifically target *Bm-cpl-5* at a later time point by injecting our RNAi trigger later (at 10 dpi for example).

In conclusion, while we demonstrated that our modified *in squito* protocol can be used to specifically suppress *Bm-cpl-1* in a more convenient and high-throughput manner, we failed to show suppression of *Bm-cpl-4/5* suggesting that our protocol will need further optimization specific to each gene of interest.

Author Contributions

Conceived and designed the experiments: LMF, LCB, MJK. Performed the experiments: LMF. Analyzed the data: LMF, LCB, MJK. Wrote the paper: LMF, LCB, MJK.

Acknowledgements

The authors would like to thank Brendan Dunphy and Mara Schulze for technical assistance with mosquito rearing and maintenance. The authors would also like to thank Dr. Andrew Moorhead, Erica Burkman and the NIH-NIAID Filariasis Research Reagent Resource Center (FR3) for providing parasite material.

References

1. Global programme to eliminate lymphatic filariasis: progress report, 2014. Wkly Epidemiol Rec. 2015;90(38):489-504. PubMed PMID: 26387149.

2. Ramaiah KD, Ottesen EA. Progress and impact of 13 years of the global programme to eliminate lymphatic filariasis on reducing the burden of filarial disease. PLoS Negl Trop Dis. 2014;8(11):e3319. doi: 10.1371/journal.pntd.0003319. PubMed PMID: 25412180; PubMed Central PMCID: PMCPMC4239120.

3. Ichimori K, King JD, Engels D, Yajima A, Mikhailov A, Lammie P, et al. Global programme to eliminate lymphatic filariasis: the processes underlying programme success. PLoS Negl Trop Dis. 2014;8(12):e3328. doi: 10.1371/journal.pntd.0003328. PubMed PMID: 25502758; PubMed Central PMCID: PMCPMC4263400.

4. Bennett JL, Williams JF, Dave V. Pharmacology of ivermectin. Parasitol Today. 1988;4(8):226-8. PubMed PMID: 15463103.

5. Pax RA, Williams JF, Guderian RH. In vitro motility of isolated adults and segments of *Onchocerca volvulus*, *Brugia pahangi* and *Acanthocheilonema viteae*. Trop Med Parasitol. 1988;39 Suppl 4:450-5. PubMed PMID: 2852396.

6. Norões J, Dreyer G, Santos A, Mendes VG, Medeiros Z, Addiss D. Assessment of the efficacy of diethylcarbamazine on adult *Wuchereria bancrofti in vivo*. Trans R Soc Trop Med Hyg. 1997;91(1):78-81. PubMed PMID: 9093637.

7. Dalzell JJ, McVeigh P, Warnock ND, Mitreva M, Bird DM, Abad P, et al. RNAi effector diversity in nematodes. PLoS Negl Trop Dis. 2011;5(6):e1176. doi: 10.1371/journal.pntd.0001176. PubMed PMID: 21666793; PubMed Central PMCID: PMCPMC3110158.

8. Mohr SE, Smith JA, Shamu CE, Neumüller RA, Perrimon N. RNAi screening comes of age: improved techniques and complementary approaches. Nat Rev Mol Cell Biol. 2014;15(9):591-600. doi: 10.1038/nrm3860. PubMed PMID: 25145850; PubMed Central PMCID: PMCPMC4204798.

9. Visser A, Geldhof P, de Maere V, Knox DP, Vercruysse J, Claerebout E. Efficacy and specificity of RNA interference in larval life-stages of *Ostertagia ostertagi*. Parasitology. 2006;133(Pt 6):777-83. doi: 10.1017/S0031182006001004. PubMed PMID: 16879764.

10. Geldhof P, Murray L, Couthier A, Gilleard JS, McLauchlan G, Knox DP, et al. Testing the efficacy of RNA interference in *Haemonchus contortus*. Int J Parasitol. 2006;36(7):801-10. doi: 10.1016/j.ijpara.2005.12.004. PubMed PMID: 16469321.

11. Geldhof P, Visser A, Clark D, Saunders G, Britton C, Gilleard J, et al. RNA interference in parasitic helminths: current situation, potential pitfalls and future prospects. Parasitology. 2007;134(Pt 5):609-19. doi: 10.1017/S0031182006002071. PubMed PMID: 17201997.

12. Lendner M, Doligalska M, Lucius R, Hartmann S. Attempts to establish RNA interference in the parasitic nematode *Heligmosomoides polygyrus*. Mol Biochem Parasitol. 2008;161(1):21-31. doi: 10.1016/j.molbiopara.2008.06.003. PubMed PMID: 18606194.

13. Viney ME, Thompson FJ. Two hypotheses to explain why RNA interference does not work in animal parasitic nematodes. Int J Parasitol. 2008;38(1):43-7. doi: 10.1016/j.ijpara.2007.08.006. PubMed PMID: 18028931.

14. Song C, Gallup JM, Day TA, Bartholomay LC, Kimber MJ. Development of an *in vivo* RNAi protocol to investigate gene function in the filarial nematode, *Brugia malayi*. PLoS Pathog. 2010;6(12):e1001239. doi: 10.1371/journal.ppat.1001239. PubMed PMID: 21203489; PubMed Central PMCID: PMCPMC3009605.

15. MacDonald WW. The selection of a strain of *Aedes aegypti* susceptible to infection with semi-periodic *Brugia malayi.* Annals of Tropical Medicine and Parasitology. 1962;56:368-72.

16. Ford L, Zhang J, Liu J, Hashmi S, Fuhrman JA, Oksov Y, et al. Functional analysis of the cathepsin-like cysteine protease genes in adult *Brugia malayi* using RNA interference. PLoS Negl Trop Dis. 2009;3(2):e377. doi: 10.1371/journal.pntd.0000377. PubMed PMID: 19190745; PubMed Central PMCID: PMCPMC2634747.

17. Erickson SM, Xi Z, Mayhew GF, Ramirez JL, Aliota MT, Christensen BM, et al. Mosquito infection responses to developing filarial worms. PLoS Negl Trop Dis. 2009;3(10):e529. doi: 10.1371/journal.pntd.0000529. PubMed PMID: 19823571; PubMed Central PMCID: PMCPMC2752998.

18. Laney SJ, Buttaro CJ, Visconti S, Pilotte N, Ramzy RM, Weil GJ, et al. A reverse transcriptase-PCR assay for detecting filarial infective larvae in mosquitoes. PLoS Negl Trop Dis. 2008;2(6):e251. doi: 10.1371/journal.pntd.0000251. PubMed PMID: 18560545; PubMed Central PMCID: PMCPMC2413423.

19. Hayes RO. Determination of a Physiological Saline Solution for *Aedes aegypti* (L.). Journal of Economic Entomology. 1953;46(4):624-7.

20. Richer JK, Hunt WG, Sakanari JA, Grieve RB. *Dirofilaria immitis*: effect of fluoromethyl ketone cysteine protease inhibitors on the third- to fourth-stage molt. Exp Parasitol. 1993;76(3):221-31. doi: 10.1006/expr.1993.1027. PubMed PMID: 8500582.

21. Lustigman S, McKerrow JH, Shah K, Lui J, Huima T, Hough M, et al. Cloning of a cysteine protease required for the molting of *Onchocerca volvulus* third stage larvae. J Biol Chem. 1996;271(47):30181-9. PubMed PMID: 8939969.

22. Guiliano DB, Hong X, McKerrow JH, Blaxter ML, Oksov Y, Liu J, et al. A gene family of cathepsin L-like proteases of filarial nematodes are associated with larval molting and cuticle and eggshell remodeling. Mol Biochem Parasitol. 2004;136(2):227-42. PubMed PMID: 15478801.

23. Lustigman S, Zhang J, Liu J, Oksov Y, Hashmi S. RNA interference targeting cathepsin L and Z-like cysteine proteases of *Onchocerca volvulus* confirmed their essential function during L3 molting. Mol Biochem Parasitol. 2004;138(2):165-70. doi: 10.1016/j.molbiopara.2004.08.003. PubMed PMID: 15555728.

Table 1. Oligonucleotides used to amplify cathepsin genes from *B. malayi*.

Target	Oligonucleotide sequence (5' to 3')	Amplicon size (Bp)
Cathepsin L1	Forward: ACGCTTACCAAGTTC Reverse: CGACAACAACAGGTC	410
Cathepsin L2/L3/L7	Forward: CGGAACCAATTCGATTACT Reverse: CCACTACAATCCATTACATCCT	397
Cathepsin L4	Forward: GGCAGGCTAATAGGTTTTATAGG Reverse: CATTGTCTGTAACAACAGCGATA	369
Cathepsin L5	Forward: CAGACTTCTGAATTTTATAGGTATGAT Reverse: CATTATCCTTGGCAACAGC	361
Cathepsin L8	Forward: GGAACATCGTCGATTTATGACA Reverse: CCAACAGCAAGTAAAGCATGG	720
Cathepsin F	Forward: ATGTTCTGATTATGTTCCATCG Reverse: CCAAAGACTTTCAATATTACCG	511
Cathepsin Z	Forward: GGATTGTAACGTAAATGG Reverse: GCGATTGGACCATGATGATAA	438
Tumor Protein Homolog	Forward: CTTGCGTCGGACTCGTTC Reverse: CACCTCACCATCTTCTTCATCTC	463

Table 2. Oligonucleotides used to assess suppression of *B. malayi* cathepsin genes.

Target	Primer sequence (5' to 3')	Amplicon size (Bp)
Cathepsin L1	Forward: ACGCTTACCAAGTTC Reverse: CGACAACAACAGGTC	410
Cathepsin L4/L5 5' end	Forward: ATCCTAGCCGATTTTGCTGTC Reverse: CCTTGGGTCATACCTATAAAACCT	498
Cathepsin L4/L5 3' end	Forward: GCATCAAGATATGGAATAGCAATGG Reverse: TCAAATCGGAAATGAAGCAGCG	417
Tumor Protein Homolog	Forward: ATGAACAAGTGAAGTGTGCTTGC Reverse: GAAGGGAATACGGCTGATGC	605

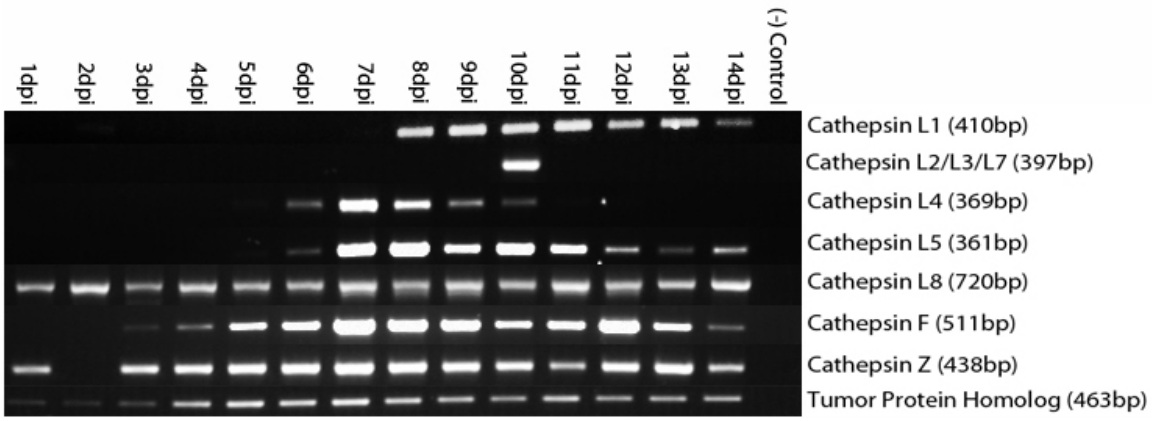

Figure 1. *B. malayi* cathepsin genes are differentially expressed throughout the mosquito stages of the life cycle. Amplification of *B. malayi* cathepsin genes from infected adult female *Ae. aegypti* (LVP) total RNA collected 1-14 day post infection (dpi). Amplification using gene-specific primers of all cathepsin genes was visualized in the expected sizes. Tumor protein homolog is a nematode specific gene that is expressed throughout the life of the parasite and was used as an internal control to confirm parasite infection within adult female *Ae. aegypti* (LVP). Total RNA from uninfected adult female *Ae. aegypti* (14 dpi) was used as a negative (-) control to validate amplification of nematode specific genes.

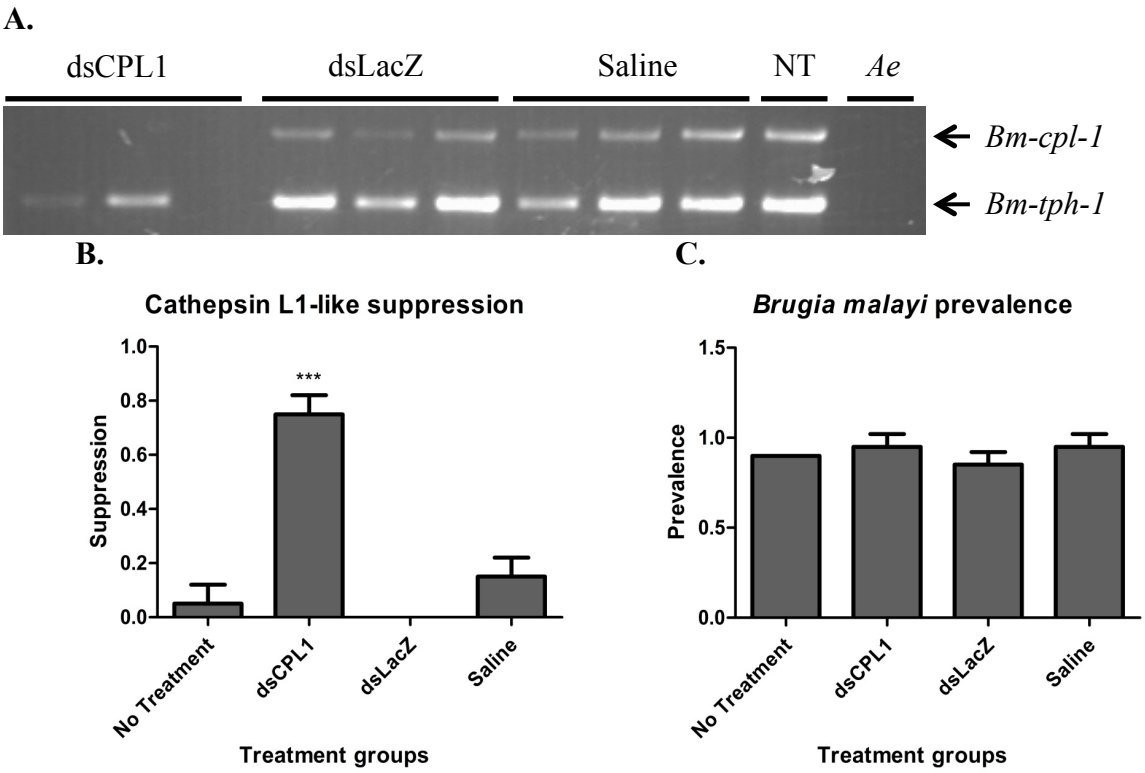

Figure 2. 150 ng of *Bm-cpl-1* dsRNA potently and specifically suppresses *Bm-cpl-1* transcript abundance. (A) Micrograph shows ethidium bromide stained 1% agarose gel of semi quantitative RT-PCR of individual *B. malayi* infected *Ae. aegypti* 48 hrs post injection of RNAi trigger at 10 dpi. Injection with 150 ng *Bm-cpl-1* resulted in complete suppression of *Bm-cpl-1* in 80% of the samples tested (B) but had no impact on parasite prevalence (C). Tumor protein homolog (*Bm-tph-1*) is a nematode specific gene that is expressed throughout the life of the parasite and was used as an internal control to confirm parasite infection within adult female *Ae. aegypti* (LVP). dsCPL1 = 150 ng *Bm-cpl-1*, dsRNA injected, dsLacZ = 150 ng LacZ dsRNA injected, Saline = saline injected, NT = infected uninjected *Ae. aegypti*, *Ae* = uninfected *Ae. aegypti*. Statistical analysis: One-way ANOVA with Tukey's post-test. ***, P-value ≤ 0.001 relative to control (NT). N = 3.

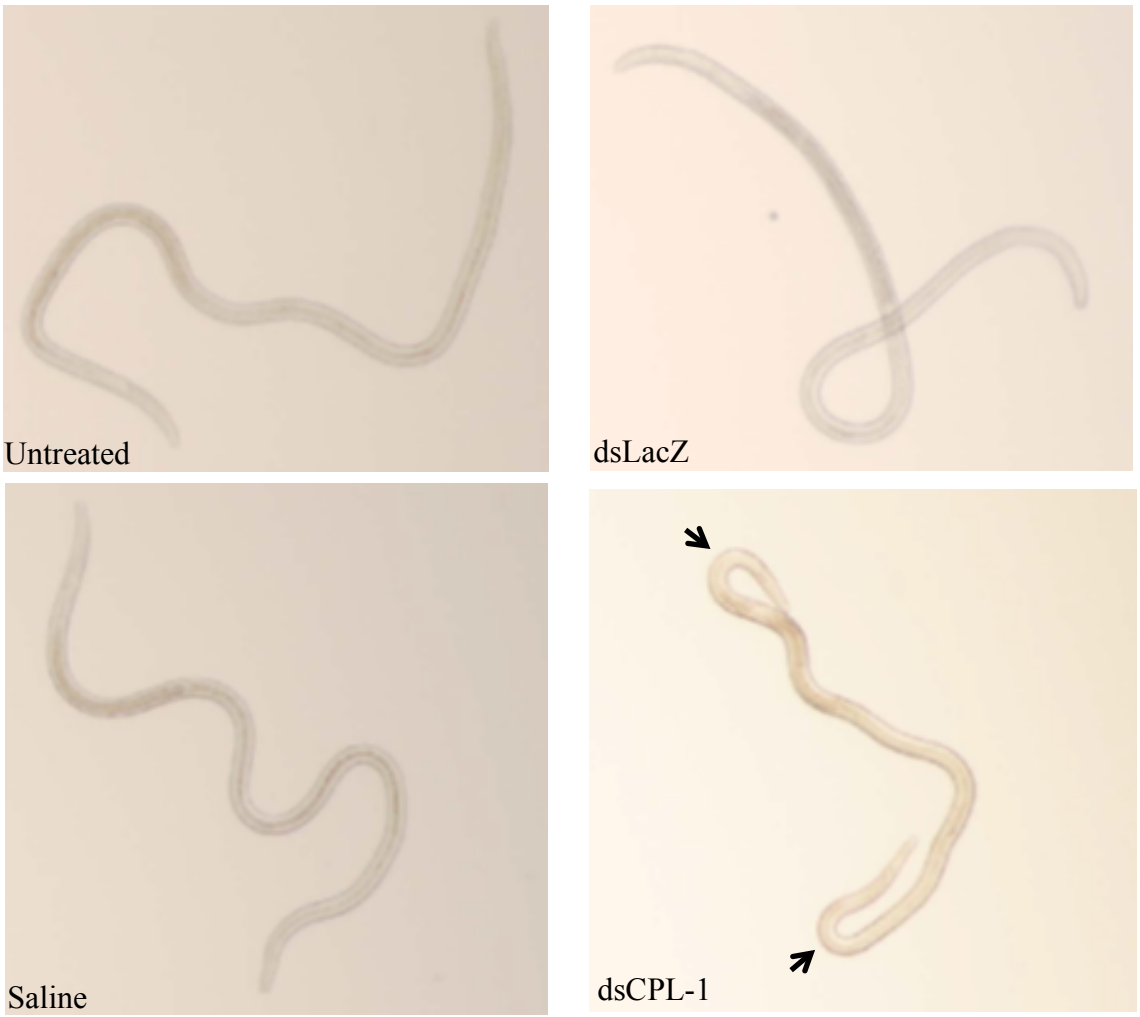

Figure 3. Suppression of *Bm-cpl-1* leads to aberrant phenotypes. Representative images of *B. malayi* L3 stage parasites collected from adult female *Ae. aegypti* (LVP) four days post injection (14 dpi) with RNAi trigger or controls. Images show kinked phenotype that was only observed in *Bm-cpl-1* dsRNA injected individuals (arrows). Untreated = infected uninjected *Ae. aegypti*, dsLacZ = 150 ng LacZ dsRNA injected, Saline = saline injected, dsCPL1 = 150 ng *Bm-cpl-1* dsRNA injected.

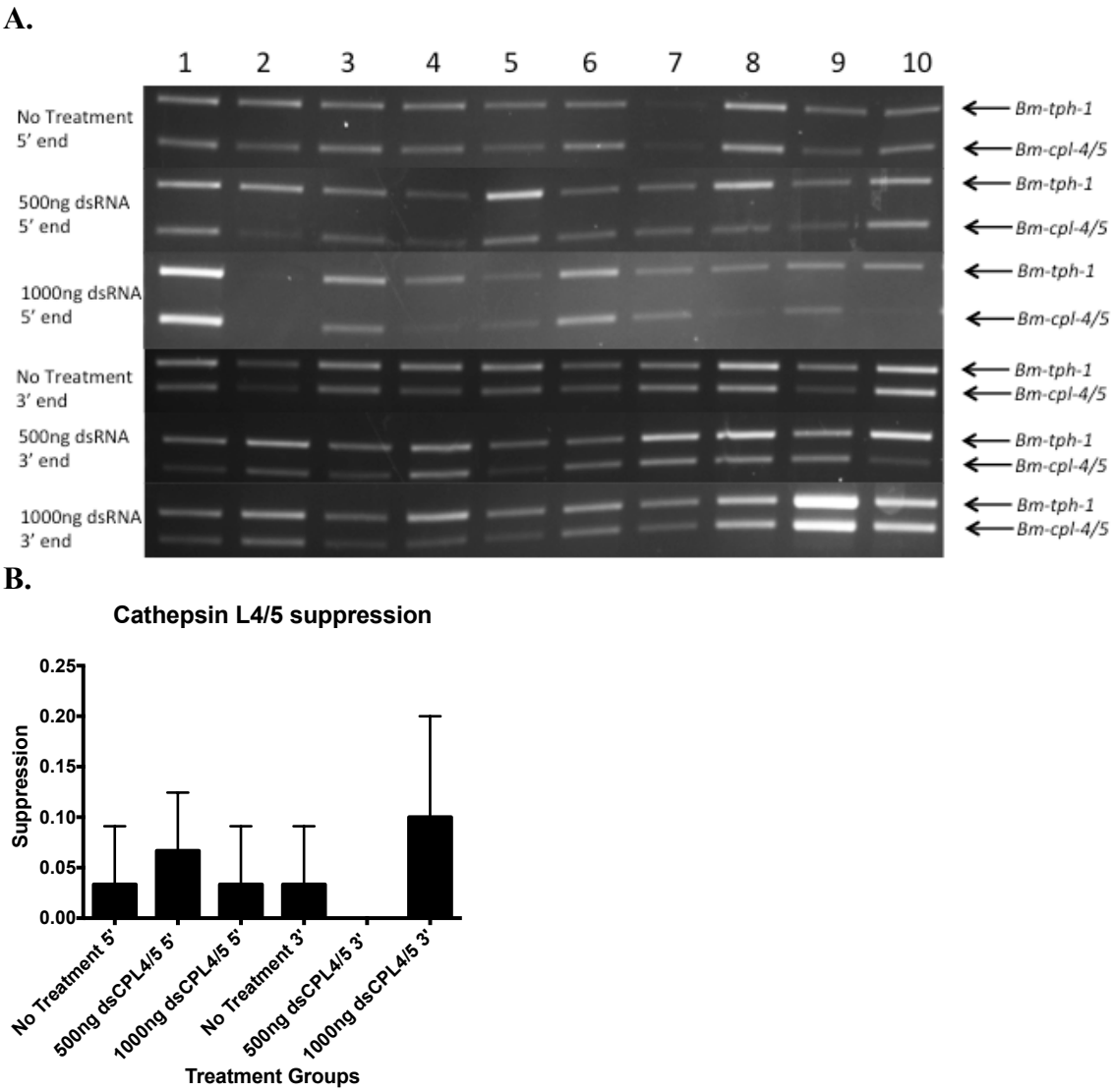

Figure 4. *Bm-cpl-4/5* is not suppressed using our modified *in squito* protocol. (A) Representative micrograph of three trials shows ethidium bromide stained 1% agarose gel of semi quantitative RT-PCR of individual *B. malayi* infected *Ae. aegypti* 48 hrs post injection of RNAi trigger at 5 dpi. 1-10 represents individual adult female *Ae. aegypti* that have been injected with 500 ng or 1000 ng dsRNA targeting either the 5' or 3' end of *Bm-cpl-4/5* or uninjected controls (No Treatment). (B) RNAi triggers targeting *Bm-cpl-4/5* (dsCPL4/5) did not suppress *Bm-cpl-4/5* expression regardless of region targeted (5' or 3' end). Statistical analysis: One-way ANOVA with Tukey's post-test. N = 3.

ACKNOWLEDGEMENTS

I would like to thank my major professors, Dr. Michael Kimber and Dr. Lyric Bartholomay for their mentoring, encouragement and understanding through my journey in graduate school. They offered invaluable support and guidance throughout my graduate career.

I would also like to thank my committee members, Dr. Bryony Bonning, Dr. Tim Day and Dr. Thomas Baum for providing guidance on different aspects of my dissertation work. Thank you to current and past members of the Bartholomay and Kimber labs who have been an important part of my graduate school life providing both practical help and moral support. A very special thank you to my co-authors Dr. Mostafa Zamanian, Isai Madriz and Nic Wheeler for providing suggestions and guidance for my research projects.

Most importantly, I would like to thank my dad and my best friend Dave who always gave me support and motivation when I needed it.